FACULTY OF ENGINEERING AND BUILT ENVIRONMENT

Department of Civil Engineering

Experimental Study of Shear Behaviour of High Density Polyethylene Reinforced Sand Under Triaxial Compression

Geotechnical Engineering Group

Author:	**Paul Wanyama**
Supervisor:	**Dr Denis Kalumba**
Co-Supervisor:	**Faridah Chebet**

A dissertation submitted in partial fulfilment of the requirement for award of the degree of Master of Science in Civil Engineering specialising in Geotechnical Engineering at the University of Cape Town

November 2016

DECLARATION

1. I know the meaning of plagiarism and declare that all the work in the document, save for that which is properly acknowledged, is my own. This dissertation has been submitted to the Turnitin module (or equivalent similarity and originality checking software) and I confirm that my supervisor has seen my report and any concerns revealed by such have been resolved with my supervisor.
2. I have used the UCT Author-date-referencing-guide 2016 based on the Harvard convention for citation and referencing. Each significant contribution to and quotation in this dissertation from the work or works of the other people has been attributed and has been cited and referenced.
3. This dissertation is my own work.
4. I have not allowed and will not allow anyone to copy my work with the intention of passing it as his or her own.

Name: Paul Wanyama **Student no:** WNYPAU001

Signature: signature removed **Date:** 04/11/2016

ABSTRACT

Soil reinforcement is an ancient technique which involves the addition of tensile elements like plastics in the soil to increase its engineering properties like shear strength, settlement, cohesion and bearing capacity. In consideration of this, a series of triaxial tests were undertaken to investigate the reinforcing effect of High-Density Polyethylene (HDPE) plastic material in Cape Flats sand, predominant in the Western Cape region of South Africa.

Plastic strips of various lengths were randomly included to the soil at different concentrations to form a homogenous soil-plastic composite specimen prepared at varying compactive effort. Using a split mould, cylindrical specimens of 50 mm diameter and 100 mm height were prepared using the dry tamping technique. The test specimens were compacted to achieve target average dry densities of the composite sample. The plastic strip reinforcement parameters comprised of 7.5 mm to 30 mm lengths, and concentrations of 0.1 % to 0.3 % by weight of dry sand. Triaxial compression tests were performed using confining pressures of 50 kPa, 100 kPa, 200 kPa, 300 kPa and 400 kPa at a shear rate of 0.075 %/min, and to a maximum strain of 10 %.

Laboratory results favourably suggest that there is an improvement in the soil shear strength properties due to these inclusions. The friction angle increased up to a peak value on varying plastic strip length and concentration, beyond which further addition of plastic material led to a reduction in the friction angle. The greatest friction angle was reported at plastic strip length and content of 15 mm and 0.2 % respectively. Additionally, the results indicate that a higher compactive effort leads to a greater increase in friction angle of the soil.

The existence of a critical confining stress was observed from triaxial test results on soil-plastic composites. This threshold limit was influenced significantly by the plastic inclusions, and the range of confining stresses. Consequently, a bilinear failure envelope was reported in reinforced samples while unreinforced specimens realised a linear relationship. The Mohr-Coulomb failure line above the critical confining pressure almost paralleled the unreinforced linear relationship.

An embankment model was developed using Slide Modeler software and the factor of safety of slope was analysed with unreinforced and reinforced backfill subjected to static and dynamic loading. It was observed that the safety factor increased due to polyethylene strip inclusions. Therefore, the proposed technique will find potential practical applicability in low-cost embankment or road construction.

ACKNOWLEDGEMENTS

First, I thank the Almighty God for his protection and the gift of knowledge from the start to the completion of this work.

My appreciation goes to Dr Denis Kalumba for his guidance, mentorship, immense knowledge, encouragement and excellent supervision throughout this research. A special thank you to the co-supervisor, Ms Faridah Chebet, for her constructive critique of my work.

My sincere gratitude to the Commonwealth Scholarship in low and middle income countries for the generous financial support towards funding my Master's studies. I thank Linda Harrison and Terry Jacques for the timely processing of my tuition fees and stipend that enabled me to concentrate on my studies and complete the programme within the stipulated timelines.

Mr Noor Hansen, the laboratory manager and all technical staff of the geotechnical engineering laboratory, especially Mr Tahir Mukaddam and Mr Elvino Witbooi are acknowledged for their contribution that partly made this study a success. I am indebted to Mr Charles Nicholas and Mr John Coetzee for the assistance offered in the fabrication of the steel hand tamper and laser cutting of plastics respectively.

My friends and proofreaders, Aurelie Tabart and David Barasa. I appreciate your valuable input and for making my stay in Cape Town much more fun.

I also thank my colleagues in the Geotechnical Engineering Research Group for their invaluable contribution to my studies – Dennis, Vincent, Byron, Sam, Jjuuko, Angella, Sane, Vuvu, Lita, Joan, Laxmee, Motheo, Mark, Tracey, Paul, Steve and Sheila.

Finally, I am grateful to my family for the support and encouragement throughout the years – Dan, Rasmo, Phelista, Teddy, dad, mum, aunt Julia and uncle Nicholas. I am eternally grateful to my fiancée, Dyna Gakii for the love, patience and moral support during the two years. Thank you for the visits and many Skype calls. No amount of words can express my gratitude to you.

DEDICATION

To my late **MOTHER**, Roselyne Auma Nanzala.

TABLE OF CONTENTS

LIST OF TABLES

LIST OF FIGURES

NOTATIONS

Symbols	Description	Units
G_s	Specific gravity	Mg/m^3
ρ	Density	kg/m^3
ρ_d	Target dry density	kg/m^3
$\rho_{d(\max)}$	Maximum (densest) dry density	kg/m^3
$\rho_{d(\min)}$	Minimum (loosest) dry density	kg/m^3
γ	Unit weight of soil	kN/m^3
D_r	Relative density	%
V	Volume	cm^3
W	Weight of compacted soil	kg
w	Moisture content	%
σ_v	Total vertical stress	kPa
σ'_v	Effective vertical stress	kPa
σ_h	Total horizontal stress	kPa
σ'_h	Effective horizontal stress	kPa
σ'_1	Effective major principal stress at failure	kPa
σ'_3	Effective minor principal stress at failure	kPa
$\Delta\sigma_D$	Deviator (axial) stress, σ_1 - σ_3,	kPa
c'	Drained cohesion	kPa
c_u	Undrained cohesion	kPa
τ_f	Shear stress at failure	kPa
σ_f	Normal stress at failure	kPa
G_s	Specific gravity	---
D_{50}	Mean soil grain size	mm

C_u	Coefficient of uniformity	---
C_c	Coefficient of curvature	---
$\emptyset'$	Drained angle of internal friction	°
u	Pore water pressure force	kN/m
σ_N	Normal confining stress	kPa
X_i	Plastic strip content	%
W_i	Plastic strip width	mm
L_i	Plastic strip length	mm
W_p	Mass of plastic strips	kg
W_s	Mass of dry sand	kg
B	Slice width	m
W	Self-weight of the slice	kN/m

Abbreviations	**Description**
AASHTO	American Association of State Highway and Transportation Officials
AR	Aspect Ratio
ASTM	American Standard Test Method
BS	British Standard
CBR	California Bearing Ratio
CD	Consolidated Drained triaxial test
CU	Consolidated Undrained triaxial test
DEAT	Department of Environmental Affairs and Tourism
E	Compactive Effort/Energy
LE	Low Compactive Effort
HE	High Compactive Effort
SS	Sand-Sand samples

PS	Sand-Plastic Samples
MSE	Mechanically Stabilized Earth
MDD	Maximum Dry Density
m	Metre
mm	Millimetre
OMC	Optimum Moisture Content
SD	Standard Deviation
SPI	Society of the Plastics Industry
UCS	Unconfined Compressive Strength
UCT	University of Cape Town
USA	United States of America
USCS	Unified Soil Classification System

1 INTRODUCTION

1.1 Background to the Study

Reinforcement of soil is an ancient technique which involves the addition of tensile elements to stabilise the soil and improve its engineering properties such as shear strength, settlement, and bearing capacity. In the past, natural materials such as reeds, straws, sisal, jute, bamboo, palm and root fibres were added to soil resulting in stronger more stable earth structures. However, the modern concept and scientific principles of soil reinforcement emerged in the 1960s with Henri Vidal's patented idea of reinforced earth® for the construction of mechanically stabilized earth (MSE) retaining walls. New reinforcing elements have since been developed for geotechnical engineering purposes. Some of which include steel, geosynthetics, and plastic materials (Mitchell & Villet, 1987).

In recent years, the use of geosynthetics as a reinforcement medium has gained prominence due to the growth of the plastics industry and also the corrosive nature of steel reinforcement. However, they are expensive and constitute a large proportion of project costs. Therefore, the suitability of alternative materials such as recycled tyre wastes, carpet wastes, and plastic wastes has been explored for soil reinforcement especially in developing countries (Foose et al., 1996; Ghiassian et al., 2004; Mishra et al., 2013).

In most developing countries such as South Africa, these materials particularly plastic waste, contribute to a large quantity of the total volume destined to landfills whose capacity is steadily declining leading to environmental challenges of solid waste generated from widespread use. Plastic waste such as grocery bags are abundant, low-priced, easily accessible, and are non-biodegradable with properties that can be reused for other applications requiring large quantities of materials. In consideration of this, new innovative and sustainable solutions have been proposed by numerous researchers who have studied the potential use of plastics as a soil reinforcement material (Benson & Khire, 1994; Dutta & Rao, 2007; Choudhary et al., 2010; Chebet & Kalumba, 2014).

Experimental studies on the shear behaviour of soils reinforced with plastic inclusions used laboratory tests such as direct shear, triaxial compression, and California Bearing Ratio (CBR). The studies reported increased peak strength and a reduction in the post-peak strength loss (Gray & Ohashi, 1983; Maher & Gray, 1990; Benson & Khire, 1994). However, contradicting results are reported on the influence of confining pressure on the shear behaviour of soil-plastic

inclusions. For this reason, the current study investigated the shear behaviour of sand soil reinforced with polyethylene bags of varying concentrations and lengths over a wide range of confining pressure. Furthermore, the effect of compactive effort was investigated which was not covered by previous studies. Triaxial compression tests were selected for the study due to the fact it is a superior test compared to direct shear and CBR tests. Dry soil samples were used in the study in order to remove the variation of the shear behaviour of the soil if water were added to the samples. The addition of water to soil leads to complexity in investigations in the shear behaviour of the soil.

1.2 Justification of the Study

This study investigates the shear behaviour of soil reinforced with strips of plastic bag material. The application of this abundant waste medium in geotechnics is intended to provide an economic and readily available soil reinforcement material as an alternative soil improvement technique and also provide ways of reusing abundant plastic material destined for disposal in landfills. The plastic material can find potential practical geotechnical application in slope stabilisation, and as lightweight backfill materials in foundations and embankments. It is envisaged that the results from the study will contribute to faster adoption of the use of plastic shopping bags as a soil reinforcement material in the construction industry in developing countries such as South Africa.

1.3 Research Objectives

The objective of the study was to undertake an experimental investigation on the effect of including high-density polyethylene (HDPE) material on the shear behaviour of sand under triaxial compression. The specific objectives were:

i. To investigate the effect of plastic strip length and content in the sand,
ii. To determine the effect of compactive effort and,
iii. To investigate the effect of confining pressure on the shear behaviour of sand.

1.4 Scope of the Study

The study focused on the evaluation of the engineering strength of Cape Flats sand reinforced with strips of HDPE plastic bag material by means of an automated triaxial machine. A comprehensive laboratory testing programme was undertaken on unreinforced and reinforced sand samples at different plastic strip lengths and concentrations, compactive efforts, and

confining pressures. Dry soil samples were used to eliminate moisture content effects in the tests conducted for better understanding of the shear behaviour of the soil. The width of the plastic strips was kept constant throughout the experimental programme.

1.5 Research Overview

Chapter 2 covers literature review on soil reinforcement, and previous research on the topics pertinent to the study. The research materials, equipment, and testing procedures are discussed in Chapter 3. The results of laboratory tests and their discussions are presented in Chapter 4. Practical applications in a design problem using results of this experimental study are also discussed in Chapter 4. Finally, a summary of findings, conclusions, and recommendations for further research are discussed in Chapter 5.

2 LITERATURE REVIEW

2.1 Introduction

In this chapter, a review of the literature on plastics, soil reinforcement techniques and previous research work is presented and discussed in order to provide a theoretical background in the current research on the potential use of polyethylene plastic bags for ground improvement in civil engineering construction. The different types of plastics, their properties, and common uses are presented. The theory, benefits and classification of soil reinforcement methods are then discussed and finally a comprehensive review of previous research pertinent to the current study is presented.

2.2 Plastics

According to the United States Environmental Protection Agency, EPA (1990), *plastics are resins or polymers that have been synthesised from petroleum or natural gas derivatives. The term "plastics" encompasses a wide variety of resins each offering unique properties and functions. In addition, the properties of each resin can be modified by additives.*

EPA (1990) argues that plastic production and consumption increased due to the many favourable characteristics plastics offer over other conventional traditional materials. A few of the desirable intrinsic properties that make it possible for the use of plastics in the geotechnical field include (EPA, 1990):

iv. Design flexibility – plastics can be modified for a wide variety of end uses,
v. High resistance to corrosion,
vi. Durability,
vii. Low weight, and
viii. Shatter resistance.

2.2.1 Types of plastics

The plastic family is diverse and in the modern world, specific plastics are used for different applications. The various plastic materials are manufactured from different polymers and industrial processes which give rise to varied physical and chemical properties for each plastic type. Thus, in 1988 the Society of the Plastics Industry (SPI) developed a coding system for guidance on classification of plastics which was adopted by the Plastics Federation of South Africa. The code categorises plastic material types based on the different polymers, properties,

and uses. Table 2.1 presents the Plastic Identification Code for the different types of plastics according to Plastics SA.

Table 2.1: The plastic identification code (Plastics SA., 2011)

The Plastic Identification Code				
Symbol	**Type of Plastics**	**Properties**	**Common Uses**	**Recycled into:**
1 PET	**PET** Polyethylene Terephthalate	Clear, tough solvent resistant, barrier to gas and moisture, softens at 80˚C	Soft drink and water bottles, salad domes, biscuit trays, salad dressing and containers.	Pillow and sleeping bag filling, clothing, soft drink bottles, carpeting, building insulation.
2 HDPE	**HDPE** High-Density Polyethylene	Hard to semi-flexible, resistant to chemicals and moisture, waxy surface, opaque, softens at 70˚C, easily coloured, processed and formed.	Shopping bags, freezer bags, milk bottles, ice cream containers, juice bottles, shampoo, chemical and detergent bottles, buckets, rigid architectural pipe, crates.	Recycling bins, compost bins, buckets, detergent containers, posts, fencing, pipes, plastic timber.
3 PVC	**PVC** Unplasticised Polyvinyl Chloride PVC-U Plasticised Polyvinyl Chloride PVC-P	Strong, tough, can be clear, can be solvent welded, softens at 80˚C. Flexible, clear, elastic, can be solvent welded.	Cosmetic containers, electrical conduit, plumbing pipes and fittings, blister packs, wall cladding, roof sheets, bottles. Garden hose, shoe soles, cable sheathing, blood bags and tubing.	Flooring, film and sheets, cables, speed bumps, packaging, binders, mud flaps, and mats, new gumboots and shoes.
4 LDPE	**LDPE** Low-Density Polyethylene	Soft, flexible, waxy surface, translucent, softens at 70˚C, scratches easily.	Cling wrap, garbage bags, squeeze bottles, irrigation tubing, mulch film, refuse bags.	Bin liners, pallet sheets.
5 PP	**PP** Polypropylene	Hard but still flexible, waxy surface softens at 140˚C, translucent, withstands solvents, versatile.	Bottles and ice cream tubs, potato chip bags, straws, microwave dishes, kettles, garden furniture, lunch boxes, packaging tape.	Pegs, bins, pipes, pallet sheets, oil funnels, car battery cases, trays.
6 PS	**PS** Polystyrene PS-E Expanded Polystyrene	Clear, glassy, rigid, opaque, semi-tough, softens at 95˚C. Affected by fat, acids and solvents, but resistant to alkalis, salt solutions. Low water absorption, when not	CD cases, plastic cutlery, imitation glassware, low-cost brittle toys, video cases\ Foamed polystyrene cups, takeaway clamshells, foamed meat trays, protective packaging	Coat hangers, coasters, white ware components, stationery trays and accessories, picture frames, seed trays, building products.

Table 2.1 (continued)

The Plastic Identification Code				
Symbol	**Type of Plastics**	**Properties**	**Common Uses**	**Recycled into:**
		pigmented is clear, odour and taste free. Special types of PS are available for special applications.	and building and food insulation.	
1 PET	**PET** Polyethylene Terephthalate	Clear, tough solvent resistant, barrier to gas and moisture, softens at 80˚C	Soft drink and water bottles, salad domes, biscuit trays, salad dressing and containers.	Pillow and sleeping bag filling, clothing, soft drink bottles, carpeting, building insulation.

2.2.2 Waste management in South Africa

The use of resources and waste management in South Africa is based on the internationally accepted concept of waste hierarchy with waste disposal at the end of the chain. Figure 2.1 shows the waste management hierachy adopted in South Africa with preferred options higher in the chain (Karani & Jewasikiewitz, 2007). The main focus of the integrated resource and waste management hierarchy is on waste reduction, re-use, recycling, and recovery into energy. After these options are fully implemented, the waste is either incinerated or destined to landfills (Azapagic et al., 2003). However, due to the lower cost of dumping, waste disposal is still the most common method. Nevertheless, the comparison between disposal to landfill and the benefits associated with recycling indicate that disposal to landfill is the most expensive option in terms of overall social costs (Nahman, 2010).

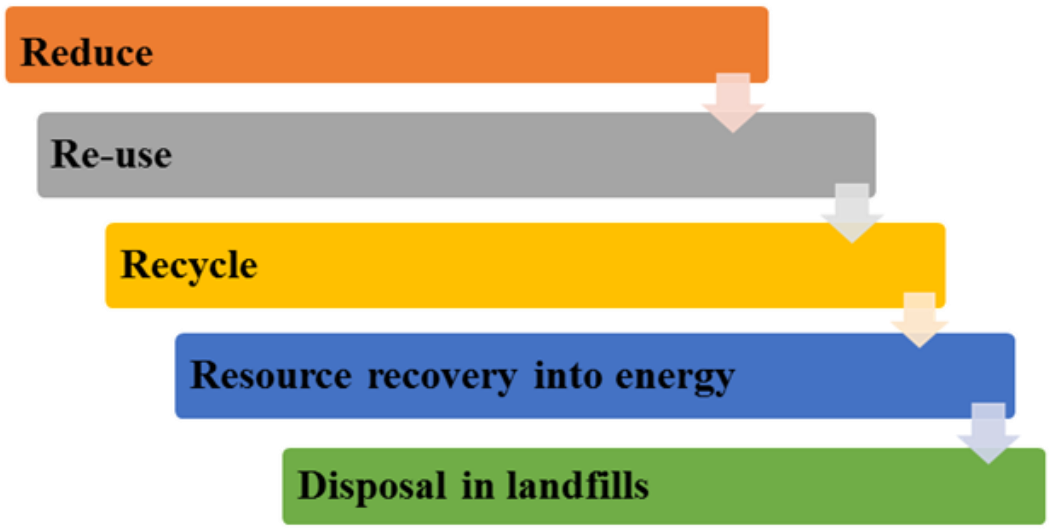

Figure 2.1: Waste management hierarchy in decreasing order of priority (Karani & Jewasikiewitz, 2007)

2.2.3 Legislative and regulatory framework

The current legislation on waste management in South Africa is governed by *Act No. 26 of 2014: National Environmental Management: Waste Amendment Act, 2014* (South Africa., 2014). The purpose of the act was to reform the laws regulating waste management, by providing a detailed legal framework. The main objectives of the act were:

i. To protect health, well-being, and the environment by providing reasonable measures for:
   - Minimising the consumption of natural resources,
   - Avoiding and minimising the generation of waste,
   - Reducing, re-using, recycling and recovering waste,
   - and preventing pollution and ecological degradation.

ii. To ensure that people are aware of the impact of waste on their health, well-being and the environment.

Another legislation prohibiting the manufacture, sale and commercial distribution of plastic bags including HDPE grocery bags of less than a certain thickness came into effect in May 2003. According to the Department of Environmental Affairs and Tourism (DEAT), the new law aimed to protect the environment by minimising waste and promoting the recycling of plastic bags. Plastic waste is non-biodegradable and the predominant waste material in the environment, thus the need to manage the problem (SouthAfrica.info., 2003).

The legislation that was passed prohibited the use of thin-film plastic bags and encouraged the use of the thicker, more durable and recyclable bags with retailers across the country required to comply. Consumers, on their part, were granted the option of re-using the thicker plastic bags; using their own carrier bags or doing without bags altogether. The regulations stipulated the required thickness of the bags to be in the order of 30 microns in order to enable ease of the recycling process. The DEAT argued that the move would strengthen recycling, preserve existing jobs as well as create new ones (SouthAfrica.info., 2003).

Contrary to the goals set out by the DEAT in 2003, studies by Dikgang et al. (2012) and Nahman (2010) revealed that the regulations failed in creating a practicable industry for the recycling of plastic shopping bags. A survey conducted by one of the major retailers in South Africa revealed that most consumers did not reuse their plastic bags for shopping due to the inconvenience of transporting the bags to the shops; instead, the bags were commonly reused by households for the containment of waste (Dikgang et al., 2012). Therefore, the need to find alternative uses for

the plastic material is underscored as the reuse and recycle components in the waste hierarchy chain seemed not to have achieved the targeted outcome.

2.3 Soil Reinforcement

In an ideal world, civil engineering projects require sites with desirable in-situ material properties. However, the growth in the global population has put a strain on land resources, therefore availability of land with suitable material properties and underlying geology is limited. Additionally, due to the location of certain project sites, the soil may fail to meet the minimum required engineering properties. Geotechnical engineers are therefore required to devise ways of improving the engineering properties of the soil for the safety and reliability of civil engineering structures. One method is the inclusion of tensile elements in the soil to reinforce its strength properties as is the case for reinforcement of concrete. The term 'soil' refers to clay, silt, sand, and gravel of different sizes formed by weathering of rocks. 'Reinforcement' refers to natural or synthetic elements with low or high modulus and can withstand tensile stresses. Various methods have been used to reinforce soils which range from polymeric materials of low modulus to stiff metallic inclusions, and are of different forms, that is, strips, bars, grids, sheets fibres, woven and non-woven fabrics (Gray & Ohashi, 1983; Gray & Al-Refeai, 1986; Consoli et al., 2002).

The inclusion of these reinforcing elements seeks to improve engineering parameters of soil such as the shear strength, permeability, density, compressibility (Hejazi et al., 2012), tensile strength, rigidity (Maher & Gray, 1990), material strength and ductility (Consoli et al., 2007). The technique of soil reinforcement is widely used today in geotechnical applications such as earth retaining walls, embankment slope and subgrade stabilisation in road construction (Gray & Ohashi, 1983).

2.3.1 Historical development

Ground improvement by reinforcement of soil through the insertion of tensile elements in the soil can be dated back 3000 years to the ancient Ziggurats found in Iraq as well as to Roman architecture and construction (Fluet, 1985). The reinforced fill construction of The Great Wall of China used tamarisk branches to strengthen a mixture of clay and gravel (Manceau et al., 2012). Furthermore, naturally occurring plant roots have been reported to improve the stability of slopes (Waldron, 1977; Gray & Ohashi, 1983). The modern concept of soil reinforcement was developed in the 1960s by Henri Vidal who patented the idea of Reinforced Earth® where

self-supporting earth retaining walls were reinforced with metal strips (Vidal, 1969). This is illustrated using the schematic of the reinforced earth wall in Figure 2.2.

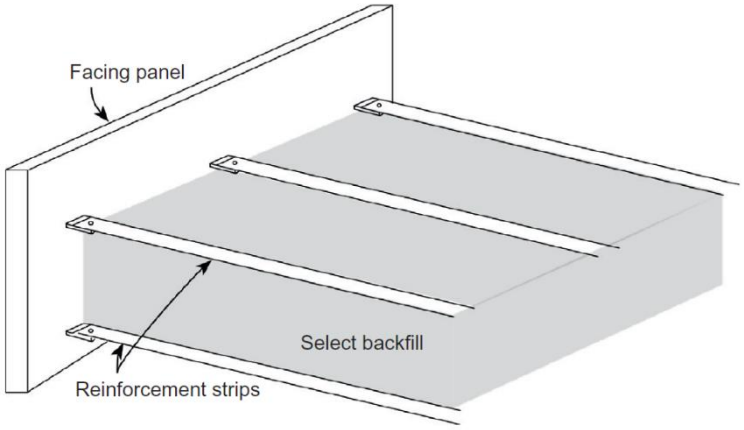

Figure 2.2: Schematic diagram of reinforced earth wall (Nicholson, 2015)

In the 1980s, geosynthetics were introduced for use in various geotechnical applications (Nicholson, 2015). Geosynthetics are widely used in the world as reinforcing materials. More recently however, new reinforcing materials have continually been investigated which include waste materials as they are cheap, accessible, readily available and destined to the landfill. Some of the materials that have been studied for purposes of soil reinforcement include recycled tyre wastes (Miraftab & Lickfold, 2008), carpet wastes (Freilich et al., 2010), fibres (Gray & Ohashi, 1983), plastic materials (Gray & Al-Refeai, 1986; Benson & Khire, 1994; Choudhary et al., 2010). The corrosiveness of steel has also contributed to the increased attention towards plastic material for reinforcement.

2.3.2 Reinforcement mechanism in soil

Soil provides resistance to compression and shear, while the reinforcement provides the tensile resistance. In the composite, soil will therefore withstand higher tensile forces in addition to compression and shear (Nicholson, 2015). The use of reinforcements stabilises the soil mass structure by providing additional tensile strength to the composite thereby increasing its shearing properties. This is achieved through the transfer of lateral stresses from the soil to the reinforcement at their interface, adhesion of the materials, and through the interface friction between the soil and reinforcement (Gray & Ohashi, 1983; Pokharel, 1995; Craig & Knappett, 2012; Nicholson, 2015). The efficiency of the reinforcement is dependent on how well the soil adheres or interacts with the reinforcement surface (Vidal, 1969). In cohesionless soils like sand,

the reinforcement causes the composite to exhibit a cohesion value due to the friction between the reinforcement elements and the soil. The friction generated at the interface allows the soil mass to behave as a cohesive composite and increases its resistance to stress (Vidal, 1969).

As a result of the extensive study into randomly distributed tensile materials, predictive models have been proposed by several researchers to demonstrate the engineering behaviour of soils reinforced with natural and synthetic fibres. These include mechanistic models (Gray & Ohashi, 1983; Maher & Gray, 1990), a statistical model (Ranjan et al., 1996), an energy-based limit equilibrium analysis model (Michalowski & Zhao, 1996), and a discrete framework model (Zornberg, 2002).

Gray & Ohashi (1983) used a fibre-sand reinforcement theoretical model for predicting the mechanism of reinforcement and soil which can be extended to soil-plastic composites. The reinforcement element was either oriented perpendicular to the shear zone of the direct shear box, Figure 2.3 (a), or inclined at an angle, Figure 2.3 (b). During shear, the reinforcement deforms as shown in Figure 2.3. The reinforcement was reported to contribute to increased vertical confining stress on the failure surface due to tension thus resulting in increased shear stresses. It also directly improved the shear stress of the sand (Gray & Ohashi, 1983).

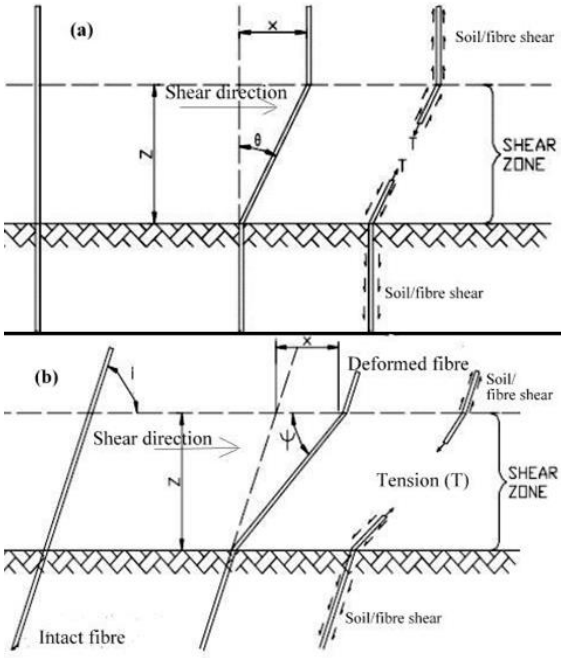

Figure 2.3: Soil reinforcement mechanism a) Tensile element perpendicular to failure plane b) Tensile element inclined at an angle to the failure plane (Gray & Ohashi, 1983)

Waldron (1977) proposed a model based on Coulomb's theory, to quantify the shear strength increase in soil due to fibre inclusions given by:

$$\boldsymbol{\tau = c + \sigma \tan \emptyset + \Delta S} \qquad \textbf{Equation 2.1}$$

Where; $\boldsymbol{\tau}$ = Shear strength,

$\boldsymbol{c}$ = Cohesive strength,

$\boldsymbol{\phi}$ = Internal friction angle, and

$\boldsymbol{\Delta S}$ = Shear strength increase due to the fibre reinforcement.

Gray & Ohashi (1983) adapted the above model to estimate the strength increase, ΔS, in the sandy soil due to fibre inclusions oriented at different angles.

For fibres oriented perpendicular to the shear zone;

$$\boldsymbol{\Delta S = \sigma_t (\sin \theta + \cos\theta \tan \theta)} \qquad \textbf{Equation 2.2}$$

For fibres inclined at angle to the shear zone;

$$\boldsymbol{\Delta S = \sigma_t [\sin (90 - \psi) + \cos (90 - \psi) \tan \theta)]} \qquad \textbf{Equation 2.3}$$

Where; $\boldsymbol{\sigma_t}$ = Mobilised tensile strength of the reinforcement per unit area of soil,

$\boldsymbol{\psi = \tan^{-1}\left[\frac{1}{\left(\frac{x}{z}\right) + (\tan^{-1} i)^{-1}}\right]}$,

$\boldsymbol{\phi}$ = Internal friction angle **of** sand,

$\boldsymbol{\theta}$ = Angle of shear distortion,

$\boldsymbol{i}$ = Initial orientation of fibre with respect to shear plane,

x = Horizontal shear displacement,

z = Thickness of shear zone, and

$\frac{\boldsymbol{x}}{\boldsymbol{z}}$ = The shear distortion ratio.

The mobilised tensile strength per unit area of soil, σ_t , is given by:

$$\boldsymbol{\sigma_t = \left(\frac{A_r}{A}\right)\sigma_f} \qquad \textbf{Equation 2.4}$$

Where; $\frac{A_f}{A}$ = Fibre concentration or area ratio,

A_f = Area of the fibre in shear,

A = Total area of soil in shear, and

σ_f = Tensile stress in a single fibre.

Maher & Gray (1990) improved the force-equilibrium model proposed by Gray & Ohashi (1983) and used statistical concepts to explain the behaviour of randomly distributed discrete fibre-reinforced sand. The probabilistic approach was based on the following conditions;

1. The fibres were deposited in the composite mass independent of each other.
2. The fibres had an equal probability of occurrence in any portion of the composite mass.
3. The fibres had an equal probability of making all possible angles with any arbitrarily chosen fixed axis (random orientation).

Using this approach, the average number of fibres per unit area, N_s, intersecting the shear plane was given as:

$$N_s = \frac{2V_f}{\pi d^2} \qquad \textbf{Equation 2.5}$$

Where; V_f = Volumetric fibre concentration, and

d = Diameter of the fibres.

The fibre area ratio was computed as:

$$\frac{A_f}{A} = N_s\left(\frac{\pi d^2}{4}\right) \qquad \textbf{Equation 2.6}$$

The tensile strength in the fibres, σ_t, was represented as:

$$\sigma_t = \left[2(\sigma_3 \tan\delta)\frac{l}{d}\right], \quad \text{for } 0 < \sigma_3 < \sigma_{crit} \qquad \textbf{Equation 2.7}$$

$$\sigma_t = \left[2(\sigma_{crit} \tan\delta)\frac{l}{d}\right], \quad \text{for } \sigma_3 > \sigma_{crit} \qquad \textbf{Equation 2.8}$$

The following equations were proposed for the estimation of increase in shear strength, ΔS, due to inclusion of randomly distributed discrete fibres in the soil:

$$\Delta S = N_s\left(\frac{\pi d^2}{4}\right)\left[2(\sigma_3 \tan\delta)\frac{l}{d}\right](\sin\theta + \cos\theta \tan\theta)(\xi), \text{ for } 0 < \sigma_3 < \sigma_{crit} \quad \textbf{Equation 2.9}$$

$$\Delta S = N_s\left(\frac{\pi d^2}{4}\right)\left[2(\sigma_{crit} \tan\delta)\frac{l}{d}\right](\sin\theta + \cos\theta \tan\theta)(\xi), \text{ for } \sigma_3 > \sigma_{crit} \quad \textbf{Equation 2.10}$$

Where; σ_3 = Average triaxial cell confining pressure acting on the fibres,

δ = Fibre skin frictional angle,

l = Length of the fibre,

σ_{crit} = Critical confining pressure at which a break in the failure envelope develops, It is determined empirically from triaxial shear test results, and

ξ = Empirical coefficient dependent upon sand and fibre properties.

Ranjan et al. (1996) pointed out that the mechanistic model proposed by Gray & Ohashi (1983) and Maher & Gray (1990) require the estimation of the thickness of the shear zone which is difficult to quantify from laboratory testing. Consequently, Ranjan et al. (1996) proposed a regression model to quantify the improvement in the shear strength of fibre reinforced soil from a series of triaxial tests. The effect of fibre properties, soil properties, and confining pressure were factored in the equations below used in the statistical analysis:

$$\sigma_{1f} = 12.3(\omega_f)^{0.4}\left(\frac{l}{d}\right)^{0.28}(f^*)^{0.27}(f)^{1.1}\sigma_3, \text{ for } \sigma_3 > \sigma_{crit} \quad \textbf{Equation 2.11}$$

Coefficient of determination (R^2) = 0.903, degree of freedom = 176

$$\sigma_{1f} = 12.3(\omega_f)^{0.4}\left(\frac{l}{d}\right)^{0.28}(f^*)^{0.27}(f)^{1.1}\sigma_3, \text{ for } \sigma_3 > \sigma_{crit} \quad \textbf{Equation 2.12}$$

Coefficient of determination (R^2) = 0.930, degree of freedom = 220

Where; σ_{1f} = Shear strength/major principal stress at failure in fibre reinforced soil,

ω_f = Fibre content (%),

$\frac{l}{d}$ = Fibre aspect ratio i.e. length over diameter of fibres,

$f^* = \frac{c_a}{\sigma_N} + \tan\delta$, where f^* = surface friction coefficient, c_a = the adhesion intercept, σ_N = vertical stress, and δ = Fibre skin friction angle of skin.

$f = \frac{c}{\sigma_N} + \tan\delta$, where f = coefficient of friction, c = cohesion, and δ = Fibre skin friction angle.

σ_3 = Confining stress, and

σ_{crit} = Critical confining stress.

The predictive models showed that fibre reinforced soils exhibited either a bilinear (Gray & Ohashi, 1983; Maher & Gray, 1990) or curvilinear (Ranjan et al., 1996) failure envelope. There existed a critical confining stress beyond which the stress-strain curve ceased to exhibit a linear relationship. Moreover, the regression model proposed by Ranjan et al. (1996) relied on laboratory test results implying the accuracy of the results depends on operator technique.

Michalowski & Zhao (1996) proposed an energy-based mathematical model to calculate the macroscopic stress of fibre-reinforced sand at failure. It was assumed slippage occurs on both ends of the fibres and tensile rupture takes place in the middle of the fibres, Figure 2.4.

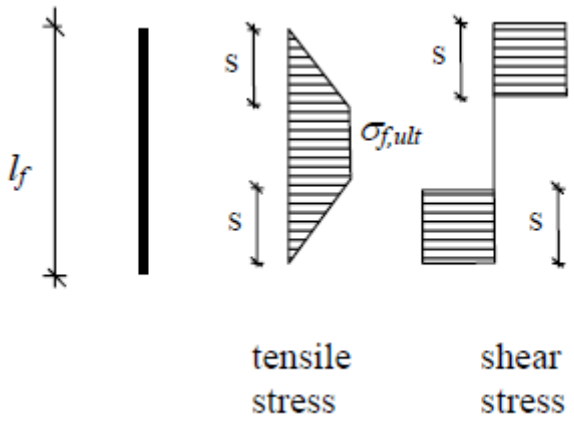

Figure 2.4: Shear stress and axial stress of a deformed fibre reinforced soil (Michalowski & Zhao, 1996)

The researchers further developed the mechanistic and regression predictive models discussed earlier by proposing a homogenization technique. The equation below was derived to account for the energy dissipation rate, *d*, due to fibre slippage and rupture:

$$d = \pi d_f s^2 \sigma_N \tan\delta \langle\dot{\varepsilon}_\theta\rangle + \frac{1}{4}\pi {d_f}^2 (1 - 2s)\, \sigma_{f,ult} \langle\dot{\varepsilon}_\theta\rangle \qquad \textbf{Equation 2.13}$$

Where; d_f = Diameter of fibres,

σ_N = Vertical stress,

$\boldsymbol{\delta}$ = Fibre skin friction angle,

$\dot{\boldsymbol{\varepsilon}}_{\boldsymbol{\theta}}$ = Strain rate in the direction of the fibre, $\boldsymbol{\theta}$,

$\boldsymbol{s}$ = Length over which fibre slippage occurs (see Figure 2.4), and

$\boldsymbol{\sigma_{f,ult}}$ = Yield stress of the fibres.

The total energy dissipation per volume of the soil, *D*, is the integral of the above equation over the volume of fibre reinforced soil mass. This is represented by the equation below:

$$\boldsymbol{D = \frac{V_f \sigma_{f,ult}}{3} M \left(1 - \frac{1}{4\eta} \frac{\sigma_{f,ult}}{p \tan \delta}\right) \varepsilon_1} \qquad \textbf{Equation 2.14}$$

Where; $\boldsymbol{V_f}$ = Volumetric fibre content,

$\boldsymbol{\eta}$ = Fibre aspect ratio,

$\boldsymbol{p}$ = Average of the confining stresses of the reinforced soil, = $\frac{\sigma_1 + \sigma_3}{2}$,

$\boldsymbol{\varepsilon_1}$ = Strain, and

$$\boldsymbol{M = \left(\frac{1}{2} + \frac{\phi}{\pi} + \frac{1}{\pi} \cos \phi\right) \tan^2 \left(\frac{\pi}{4} + \frac{\phi}{2}\right) - \frac{1}{2} - \frac{\phi}{\pi} + \frac{1}{\pi} \cos \phi}$$

A failure criterion was derived as shown below:

$$\boldsymbol{\frac{R}{V_f \sigma_{f,ult}} = \frac{p}{V_f \sigma_{f,ult}} \sin \phi + \frac{1}{3} N \left(1 - \frac{1}{4\eta V_f} \frac{\cot \delta}{\frac{p}{V_f \sigma_{f,ult}}}\right)} \qquad \textbf{Equation 2.15}$$

Where; $\boldsymbol{R}$ = Radius of the Mohr's circle, and

$$\boldsymbol{N = \frac{1}{\pi} \cos \phi + \left(\frac{1}{2} + \frac{\phi}{\pi}\right) \sin \phi}$$

All the above models use a composite approach to quantify the equivalent shear strength of fibre reinforced soils. Conversely, Zornberg (2002) proposed a discrete approach for the design of fibre reinforced soil slopes. The contribution of soil and fibre samples to the equivalent shear strength was estimated independently.

The fibre induced tensile strength, $\boldsymbol{t_p}$, is expressed by the equation below:

$$\boldsymbol{t_p = V_f \eta \left(c_{i,c}\, c + c_{i,\phi} \tan \phi\, \sigma_{N,ave}\right)} \qquad \textbf{Equation 2.16}$$

Where; $\boldsymbol{V_f}$ = Volumetric fibre content,

$\boldsymbol{\eta}$ = Fibre aspect ratio,

$\boldsymbol{c_{i,c}} = \frac{a}{c}$, where; a = adhesive component of fibre reinforced soil, and c = cohesive component of soil strength.

$\boldsymbol{c_{i,\phi}} = \frac{\tan \delta}{\tan \phi}$, where; δ = fibre skin friction, and ϕ = angle of internal friction of the soil,

$\boldsymbol{\sigma_{N,ave}}$ = Average normal stress acting on the fibres.

The equivalent shear strength of fibre-reinforced specimens, τ_{eq}, was defined as a function of the fibre-induced distributed tension, t, and the shear strength of the unreinforced soil, τ:

$$\boldsymbol{\tau_{eq} = \tau + \alpha t = c + \sigma_N \tan \phi + \alpha t} \qquad \textbf{Equation 2.17}$$

Where; $\boldsymbol{\alpha}$ = an empirical coefficient accounting for fibre orientation and is equal to 1 for fibre reinforced soils.

2.3.3 Benefits of soil reinforcement

Soil reinforcement has various advantages. The major ones include:

i. Improvement in the shear resistance of the soil thereby improving its structural capability and stability (Nicholson, 2015),
ii. The potential construction on difficult soils (Christopher et al., 1990; Nicholson, 2015):
    - Compressible/soft soils to limit settlement and increase the shear strength,
    - Loose granular soils to limit settlement and improve shear strength,
    - Mitigate liquefiable soils,
    - Limit shrinkage and swelling in expansive soils,
    - Remediate contaminated soils,
    - Improve workability of frost-susceptible soils,
iii. Land acquisition can be kept to a minimum because reinforced structures can be made steeper than would otherwise be possible (Christopher et al., 1990; Mirafi, 2010),
iv. Reduction in project costs and ease of construction (Christopher et al., 1990; Mirafi, 2010; Nicholson, 2015),
v. Accelerated settlement and soil shear strength gain (Nicholson, 2015),
vi. Construction time can be reduced (Mirafi, 2010),
vii. Savings in total volume and haulage of fill material required for construction.

viii. Relatively cost effective compared to conventional methods (Christopher et al., 1990; Mirafi, 2010).

2.4 Classification of Soil Reinforcement Materials

Soil reinforcement techniques can be classified based on the material properties, method of placement or inclusion in the soil, type of material and waste inclusions. Table 2.2. presents a summary of the classification criteria including types of reinforcing inclusions and examples. Most of the reinforcing elements will lie in more than one classification criteria.

Table 2.2: Classification of reinforcing materials

Classification based on:	Type	Example(s)
Material properties	Ideally extensible inclusions	Polymeric materials etc.
	Ideally inextensible inclusions	Soil nails, metallic strips etc.
Method of placement	Continuous oriented inclusions	Geosynthetics
	Randomly distributed discrete inclusions	Plastic fibres, glass fibres etc.
Type of material	Natural fibres	Palm, sisal, bamboo etc.
	Synthetic materials/fibres	Plastic strips, geosynthetics etc.
Waste materials	Various waste inclusions	Carpet wastes, tyre wastes, plastic wastes etc.

2.4.1 Material properties

Soil reinforcement materials are generally classified into two categories namely; ideally extensible and ideally inextensible reinforcements (McGown et al., 1978). Furthermore, Gray & Ohashi (1983) expounded that ideally extensible materials such as natural or synthetic inclusions have a relatively low modulus while ideally inextensible inclusions such as metal strips or bars have a high modulus and are stiff. The differences between the two are illustrated in Table 2.3.

An inextensible reinforcement causes a structure to be brittle, such as is the case with steel, while extensible reinforcements cause the soil to be more ductile such as the case of geosynthetics (Gurung, 2001). This can be attributed to the high modulus of the former, and comparatively low modulus of the latter thus making it more flexible (Gray & Ohashi, 1983). The extensibility of soils can also be illustrated by the axial load–axial strain behaviour of soil with the different types of inclusions, Figure 2.5, (McGown et al., 1978).

Table 2.3: Comparative behaviour of earth reinforcement (adapted from McGown et al., 1978; Gray & Ohashi, 1983)

Type of reinforced soil	Classification	Shear stress–strain behaviour of reinforcement	Significance
Reinforced Earth® (Vidal, 1969)	Ideally extensible inclusions e.g. polymeric materials, etc. $^{a}E_R/E_S > 3000$	Extensible reinforcements have tensile strains greater than unreinforced soil i.e. these inclusions cannot rupture irrespective of the imposed loads.	Strengthens the soil leading to greater extensibility (ductility) and a smaller loss of post-peak stress of the reinforced soil.
"Ply-Soil" (McGown et al., 1978)	Ideally inextensible inclusions e.g. metallic materials, etc. $E_R/E_S < 3{,}000$	Extensible reinforcements have tensile strains less than unreinforced soils i.e. these inclusions may or may not rupture.	Strengthens soil (increases apparent shear resistance) and inhibits both internal and boundary deformations. Catastrophic failure and the collapse of soil can occur due to breakage of reinforcement.
$^{a}E_R/E_S$ is the ratio of reinforcement modulus (longitudinal stiffness to the average sand modulus).			

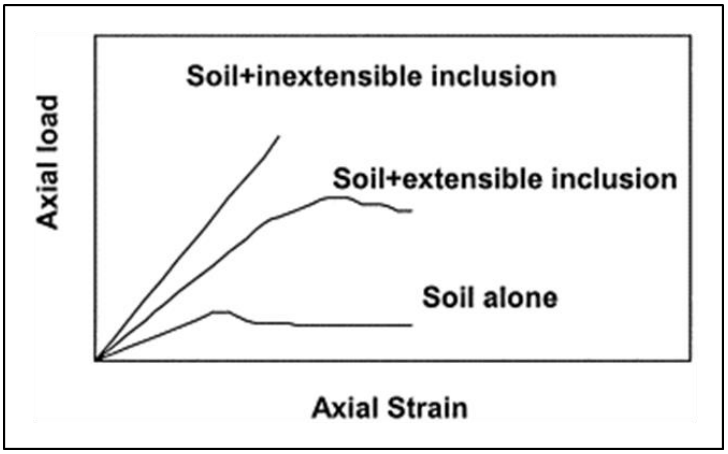

Figure 2.5: Extensibility of reinforcements (McGown et al., 1978)

2.4.2 Placement method

Reinforced soils may be classified based on the method of inclusion by either incorporating continuous reinforcement like bars, strips or sheets within a soil mass in a specific pattern, referred to as systematically reinforced soils or randomly mixing discrete elements like fibres in the soil (Yetimoglu et al., 2005).

Geosynthetics are typical examples of continuous oriented (planar or systematic) inclusions in which the geosynthetics are placed between lifts of engineered fill and each layer compacted. In contrast, randomly distributed discrete fibres are mixed in soil to form a composite in the same way as traditional soil stabilisation using cement, fly ash, etc. The main advantage of

randomly distributed fibres over planar inclusions is the maintenance of isotropy in strength and absence of potential planes of weakness at soil-reinforcement interfaces (Maher & Gray, 1990; Freilich et al., 2010). Randomly distributed fibre inclusions in soil may either be synthetic or natural. Further characteristics of the different placement methods based on properties such as failure mode, the stiffness of the materials and the general effect of the inclusions in soil are presented in Table 2.4.

Table 2.4: Differences in constitutive behaviour (after Maher & Gray, 1990)

Property	Planar/continuous fabrics	Randomly distributed discrete fibres
Failure mode	Bulging between compacted lifts	Planar failure
Stiffness	Reduces at low strains	Increases at the both high and low strains
Effect of orientation of inclusions	Horizontal fabric layers oriented parallel to the failure plane reported the highest strength.	Random fibre inclusions reported similar results to fibres oriented perpendicular to the failure plane

2.4.3 Material type

Based on the type of material, reinforcement inclusions are broadly categorised into man-made/synthetic and natural materials.

Natural fibres

Natural materials have the advantage of being cheaper and environmentally friendly however, most of these materials tend to be biodegradable resulting in loss of soil strength in the long term. Some examples include bamboo, coir, sisal and palm, and fibres.

Bamboo fibre obtained from bamboo plant has been identified as a cost-effective and abundant material with high tensile and compressive strength. It is the largest member of the grass family and is naturally anti-bacterial thus does not require insecticides during growth. Research into the use of bamboo fibres for soil reinforcement has reported increased unconfined compressive strength (UCS) of the composite soil mass by the inclusion of the bamboo (Mustapha, 2008), as illustrated in Figure 2.6.

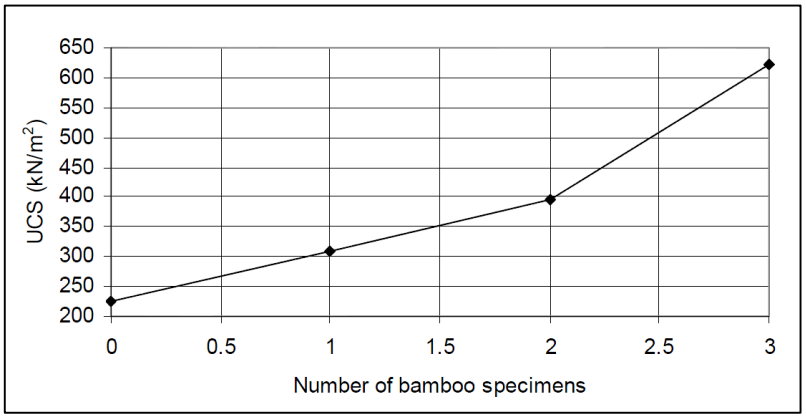

Figure 2.6: Variation of UCS with number of bamboo specimens (Mustapha, 2008)

Extracted from palm trees, palm fibres are a readily available resource material in many Asian, African and North American countries. Marandi et al. (2008) investigated the resultant strength and ductility behaviour of silty sand soils reinforced with randomly distributed palm fibres and revealed a significant improvement in the maximum strength of the reinforced specimens, Figure 2.7.

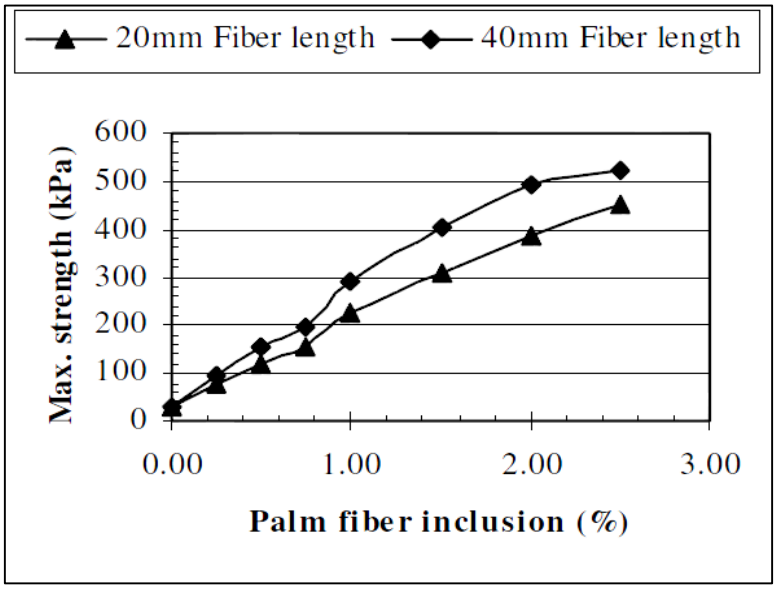

Figure 2.7: Variation of maximum strength with palm fibre inclusion (Marandi et al., 2008)

Despite the abundance, local availability and low cost of natural materials, the issue of biological degradation raises durability concerns, therefore synthetic materials which are non-biodegradable are generally preferred in the construction industry for longer design life.

Synthetic materials

Synthetic materials are manufactured from the various polymer types such as polyethylene, polypropylene, polyester etc., have been employed in the design of reinforced structures due to their favourable tensile properties. These materials can be categorised into oriented fabrics such as geosynthetics, and randomly distributed fibres. Geosynthetics are the most commonly used synthetic materials for various engineering applications and are discussed briefly.

According to ASTM D4439, a geosynthetic can be defined as "*a planar product manufactured from polymeric material used with soil, rock, earth, or other geotechnical engineering related material as an integral part of a human-made project, structure, or system*." The different types of geosynthetics are discussed below:

Geotextiles are manufactured into sheets of nonwoven, woven, stitched, or knitted fibres. They may be made of natural or polymeric fibres. They are principally used to provide separation, reinforcement, filtration, and limited drainage in soil (Nicholson, 2015).

Geogrids are polymeric products with open apertures between intersecting elements known as ribs. They are categorized into uniaxial, biaxial and triaxial geogrids based on the manufactured geometry. They are primarily used as reinforcement inclusions (Nicholson, 2015).

Geocells are three-dimension sheets of HDPE membranes (or geogrids) that are mainly used for soil and rock confinement in addition to other load supporting functions (Nicholson, 2015).

Geofoam or expanded polystyrene (EPS) is defined according to ASTM D4439 as a *block or planar rigid cellular foamed polymeric material used in geotechnical engineering applications.* It is used as lightweight fills for the construction of embankments and other structures over soft or loose soils (Nicholson, 2015).

Geonets are formed by interconnected relatively thick, parallel, polyethylene ribs intersecting at the same acute angle, forming a diamond-shaped network. They are solely used for drainage purposes (Nicholson, 2015).

Geomembranes are manufactured from polyethylene, polyvinyl chloride, and polypropylene and provide a barrier a low permeability for leakage or seepage control (Nicholson, 2015). They are widely used in landfills and tailings dams for waste containment.

Geocomposites are combinations of two or more geosynthetics to perform composite functions e.g. drainage or barrier and geotextile filters to prevent blockage of the drainage system (Nicholson, 2015).

Geosynthetic Clay Liners (GCLs) are manufactured by *bonding, needle-punching, or stitching very low permeability material (i.e., natural sodium bentonite clay) to geosynthetic materials (usually textiles) to create an economical, long-term solution where hydraulic barriers are required* (Nicholson, 2015).

Different types of geosynthetics are categorised based on the method of manufacture and the function as shown in Figure 2.8, while Table 2.5 presents a summary of the functions of geosynthetics.

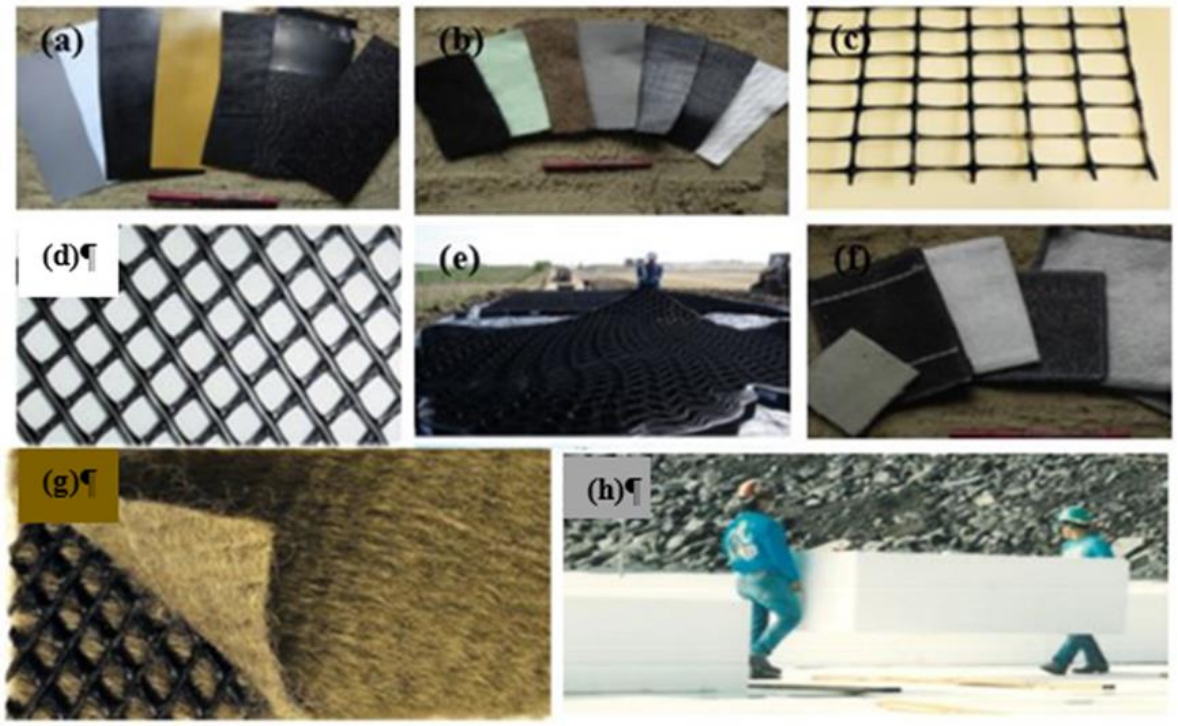

Figure 2.8: Types of geosynthetics: a) Geomembrane, b) Geotextile, c) Geogrid, d) Geonet, e) Geocell, f) Geosynthetic clay liners, g) Geocomposite, and h) Geofoam (Nicholson, 2014)

Table 2.5: Functions of the different types of geosynthetics (Koerner, 2012)

Main function	**Geosynthetics**
Reinforcement	Geotextile, geogrid, geocomposite.
Separation	Geotextile, geocomposite, geofoam.
Filtration	Geotextile, geocomposite.
Drainage	Geotextile, geonet, geocomposite.
Containment	Geomembrane, Geosynthetic clay liners, geocomposite.

The use of geosynthetics for soil reinforcement using is well documented in literature (Ingold & Miller, 1983; Gray & Al-Refeai, 1986; Sarsby, 2007; Nguyen et al., 2013). Studies have reported higher soil shear strength by increasing the number of fabric layers or reducing the distance between reinforcements. The inclusions improved the tensile and shear resistance of the soil through a combination of interface friction and adhesion between materials (Nicholson, 2015).

The high cost of geosynthetics has led to research into the potential use of other synthetic fibres for construction applications. The different synthetic fibres include polypropylene, plastic, nylon, glass, asbestos, metallic fibres etc. Extensive studies have been conducted on the prospect of fibre reinforcement in soil (Gray & Ohashi, 1983; Gray & Al-Refeai, 1986; Maher & Gray, 1990; Zornberg, 2002; Michalowski & Cermák, 2003; Ibraim & Fourmont, 2007; Consoli et al., 2007; Falorca & Pinto, 2011). Test results show that fibre inclusion increased the peak shear strength and reduced post-peak strength loss in the soil composite.

2.4.4 Waste materials for soil reinforcement

The increased demand for sustainable construction techniques has contributed to exploring the reuse of waste materials for ground improvement. Studies have been conducted into the use of alternative materials such as carpet waste for geotechnical applications (Miraftab & Lickfold, 2008), the recycling of shredded waste tyres as engineered fill (Yoon et al., 2004; Hataf & Rahimi, 2006), and the use of plastic waste as a soil reinforcement material (Consoli et al., 2002; Babu & Chouksey, 2011).

Miraftab & Lickford (2008) investigated the effect of including nylon pile carpet waste fibres in a clayey soil. Triaxial compression tests were conducted at three confining pressures on five samples with different concentrations. Test results indicated that the strength of the soil improved as the fibre content was increased. It was also demonstrated that for soil reinforced with up to a maximum of 10 % fibre content, an improvement in the internal friction angle, cohesion and shear strength. Furthermore, the compressive strength and load bearing capacity of the soil was enhanced.

Hataf & Rahimi (2006) conducted a series of laboratory tests on the model of a shallow footing resting on sand reinforced with tyre shreds of varying width, aspect ratio and concentration. It was observed that increasing the tyre shred content increased the bearing capacity ratio (BCR)

of the soil. Nonetheless, a peak value existed beyond which an increase in the shred content led to a decrease in the BCR.

Yoon et al. (2006) constructed a test embankment using an equal proportion of sand and tyre shreds by volume. Instrumentation was installed to monitor and determine total and differential settlements after the road was opened to traffic over a period of one year. The findings in the investigation revealed that tyre-shred sand mixtures had lower compressibility and high shear strength. Therefore, based on test results, the researchers proposed that tyre shreds should be promoted for use as lightweight fill materials for embankment construction.

Consoli et al. (2002) investigated the engineering behaviour of sand reinforced with randomly distributed polyethylene terephthalate (PET) plastic waste. Waste fibres of varying lengths and contents, as well as rapid hardening Portland cement at different contents was mixed randomly in the soil. Unconfined compression tests, splitting tensile tests, saturated drained triaxial compression tests were conducted to evaluate the reinforcing effect of fibres and admixture. Test results showed that PET fibre reinforcement improved the peak and ultimate strength of both cemented and uncemented soil, and reduced the brittleness of the cemented sand.

Babu & Chouksey (2011) carried out a study on the stress-strain response of a clayey and sandy soil reinforced with plastic waste. Plastic parameters such as length, width and concentration were varied in the research. Unconfined compression tests, consolidated undrained triaxial compression tests, and one-dimensional compression tests were performed on the fibre-soil composite to determine their stress-strain relationships. Laboratory results reported increased shear strength and reduction in the compressibility of the soil. Consequently, it was envisaged that the inclusion of plastic waste can find practical application in the improvement of bearing capacity and limiting of settlements in the design of shallow foundations.

2.5 Review of Previous Research on Soil-Plastic Composites

Experimental studies on the shear behaviour of soils reinforced with synthetic materials are based on laboratory tests such as direct shear, triaxial shear, and California Bearing Ratio (CBR) on composite samples. For this reason, the choice of test for design purposes has remained a matter of debate in the civil engineering field because the various types of tests give different findings due to the variances in test conditions.

Several studies have been conducted utilising man-made fibres as reinforcing elements in soil. The various reinforcement elements are manufactured from the different plastic polymers as

presented in section 2.2.1. Most used the concept of random inclusion of the tensile fibres or strips into soil specimens and, CBR, direct shear or triaxial compression tests carried out to investigate the effect of the tensile elements on the soil stress-strain response and strength properties.

A majority of studies conducted using randomly distributed discrete fibres or plastic strips have been performed on granular soils such as sands and silty sands since most engineered backfills are made of cohesionless soils. Moreover, the choice of soil type is due to the ease of compaction of such soils to achieve a target density when compared to cohesive soils such as clay.

The research conducted will be reviewed for each test whereby California Bearing Ratio tests are discussed in section 2.5.1, Direct shear strength tests in section 2.5.2, and Triaxial compression tests in section 2.6.

2.5.1 California Bearing Ratio Tests of Soil-Plastic Composites

California Bearing Ratio (CBR) is an index test used to determine the strength and stability of soil subgrade, subbase, base course materials, including recycled wastes. The tests are widely used for the design of roads, pavements, and runways.

Researchers have shown that high-density polyethylene (HDPE) plastics can be used to improve the strength and load bearing capacity of subgrade soils (Benson & Khire, 1994; Rao & Dutta, 2004; Choudhary et al., 2010). Generally, results indicated that inclusion of waste HDPE strips at optimum percentages and lengths improved the shear strength and deformation behaviour of soils. A summary of the research discussed in this section is presented in Table 2.6.

A study into the feasibility of reinforcing soil with HDPE strips reclaimed from waste milk jugs was undertaken by Benson & Khire (1994). Strips of thickness 0.6 mm, width 6 mm and aspect ratios (length/width); 4, 8, and 12 (lengths of 24 mm, 48 mm, and 72 mm) were added at strip contents of 1 %, 2 %, 3 %, and 4 % to a dry sand; with a coefficient of uniformity of 1, coefficient of curvature of 1, and classified as a uniformly graded, SP, according to the Unified Soil Classification System (USCS). The minimum and maximum dry unit weights of the sand were 15.2 kN/m^3 and 17.8 kN/m^3 respectively.

Choudhary et al. (2010) investigated the CBR behaviour of soil reinforced with plastic strip wastes. HDPE strips with a width and thickness of 12 mm and 0.40 mm respectively were utilised. Other plastic parameters varied included length; 12 mm [Aspect Ratio (AR) = 1], 24

mm (AR = 2) and 36 mm (AR = 3), and strip content; 0.25 %, 0.50 %, 1.0 %, 2.0 % and 4.0 %. Dry sand with the following material properties was used; specific gravity of 2.62, mean particle diameter (D_{50}) of 0.55 mm, coefficient of uniformity (C_u) of 2.40 and coefficient of curvature (C_c) of 1.67. It was classified as, SP, in the USCS, and had a maximum and minimum dry unit weight 16.5 kN/m^3 and 14.6 kN/m^3 respectively.

Effect of strip content

Test results by Benson & Khire (1994), Figure 2.9 (a), indicated that inclusion of HDPE strips to sand increased its CBR. The highest increase occurred for strip contents of 4 %. The recorded CBR value was increased fivefold. The secant modulus of the subgrade soil also improved. The optimum value of the secant modulus in the reinforced sand was recorded at a plastic concentration of 3 % beyond which it decreased. The strips provided frictional resistance to deformation as the soil sheared during penetration which resulted in the increase in CBR as evidenced by clear impressions of sand particles on the reinforcing element.

Choudhary et al. (2010) observed similar results, Figure 2.9 (b), and reported a threefold increase in the CBR. A dimensionless parameter was devised that represented the CBR value of reinforced soil (CBR_r) to the CBR value of unreinforced soil (CBR_u) and referred to as the California bearing ratio index (CBRI). The results show the CBRI improved significantly and the maximum value recorded at 4 % polyethylene content.

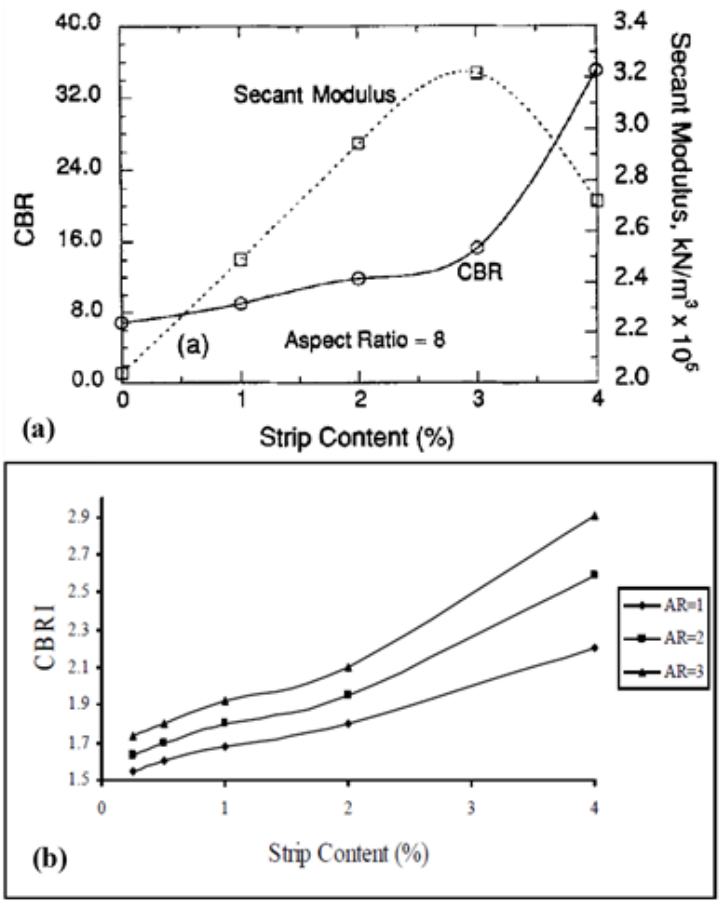

Figure 2.9: Variation of CBR with strip content; a) After Benson & Khire (1994), and b) After Choudhary et al. (2010)

Effect of length or aspect ratio

Figure 2.10 depicts that all tests conducted at a constant strip content of 4 %, and aspect ratios of 4 to 12, reported a maximum CBR at aspect ratio 8 (Benson & Khire, 1994; Choudhary et al., 2010). A similar trend of increase in CBR was observed with increasing length from 12 mm to 36 mm for the concentrations of 0 % to 4 % (Choudhary et al., 2010).

Results by Benson & Khire (1994), Figure 2.10 (a), show a non-linear relationship with a peak value observed in reinforced soil with an aspect ratio of 8 (48 mm length). They attributed the low CBR at 24 mm length to the short strips which could not develop sufficient frictional resistance thus reinforced soil could only withstand low tensile forces.

Choudhary et al. (2010) concur that the increase in CBR is due to the resisting action of the reinforcements. On the contrary, it is clear that the trend curve, Figure 2.10 (b), was linear. Varying length from 12 mm to 36 mm resulted in a considerable increase in the CBR, 41.65 % to 54.89 %. This is due to an increase in the contact area between the sand and HDPE strips.

Besides, the CBR of the reinforced sand at 5.0 mm penetration was greater than at 2.5 mm penetration. It was deduced that that at higher deformation the strengthening element provided greater resistance to penetration thereby improving the strength of sand.

Based results of these studies the technique may be applied in the civil engineering field in highways and other light-duty geotechnical applications. Nevertheless, further research is required to determine the optimum size and content (Benson & Khire, 1994; Choudhary et al., 2010).

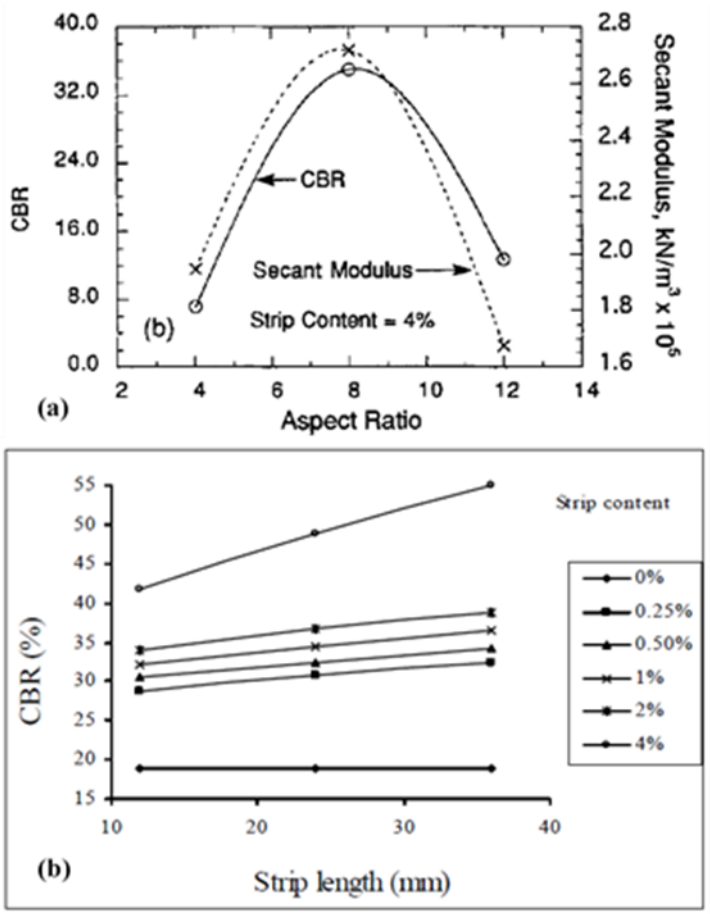

Figure 2.10: Variation of CBR with strip length: a) After Benson & Khire (1994), and b) After Choudhary et al. (2010)

2.5.2 Direct Shear Strength Testing of Soil-Plastic Composites

The direct shear test is one of the oldest and simplest strength tests for soils (Das & Sobhan, 2013). The apparatus used to conduct this test consists of a square or circular metal box split into two halves across its middle. The size of soil specimens used is normally 100 mm × 100 mm, or 300 mm × 300 mm, for small and large direct shear tests respectively. During testing, a

normal force is applied to the specimen from the top box. A shear force causes relative displacement between the top and bottom halves of the box until failure of the soil sample. The test is widely used to determine internal friction angles and cohesion parameters for granular materials for the design of foundations, retaining structures, bridges etc.

Direct shear tests have been conducted to study the effect of randomly distributed fibres (RDFS) and plastic strips on shear strength behaviour of sand (Gray & Ohashi, 1983; Benson & Khire, 1994; Yetimoglu & Salbas, 2003; Chebet & Kalumba, 2014). The experimental studies reported a considerable increase in the shear strength of the soils used. Table 2.6 summarises the research discussed in this section.

Gray & Ohashi (1983) investigated mechanics of fibre reinforcement in sand using direct shear tests on dry sand reinforced with synthetic polyvinyl chloride (PVC) plastics. The effect of fibre orientation, fibre content, fibre area ratio, and fibre stiffness on the shear strength behaviour was investigated. The variables used included diameters; 1 mm–2 mm, lengths; 20 mm–250 mm, and concentrations 0.25 %–0.5 %. The sand tested had minimum and maximum void ratios of 0.50 and 0.73 respectively. The samples were compacted to loose (D_r = 20 %) and densest (D_r = 100 %) state and tests run at normal stresses up to 144 kN/m^2. The maximum horizontal displacement and strain rate specified were 5 mm and 8 % respectively.

Benson & Khire (1994) conducted direct shear tests on soil reinforced with HDPE strips reclaimed from milk jugs. The soil and plastic properties were the same as those used in CBR test presented in section 2.5.1.

Yetimoglu & Salbas (2003) used a direct shear test to study the effect of randomly distributed discrete fibres on the shear strength of sand. with as inclusions. The properties of polypropylene fibres that were varied include: concentrations of 0.10 %, 0.25 %, 0.50 % and 1.00 %, while the diameter and length were kept constant at 0.05 mm and 20 mm respectively. The dry sand used had a specific gravity of 2.64; maximum and minimum void ratio of 0.77 and 0.51 respectively; coefficient of uniformity of 1.65; coefficient of curvature of 1.02. The minimum and maximum dry unit weights of the sand were 14.92 kN/m^3 and 17.48 kN/m^3 respectively. Reinforced and unreinforced sand samples were prepared at a relative density, D_r, of 70 % (equivalent to dense state), and tests performed at normal pressures of 100 kPa, 200 kPa, and 300 kPa. The loading rate and horizontal displacement used were 0.002 mm/s and 16 mm respectively

Falorca & Pinto (2011) studied the effect of randomly distributed polypropylene fibres on the shear strength behaviour of a clayey soil and sandy soil. The fibre properties varied include:

Fibre contents of 0 % to 1.0 %; lengths of 25 mm to 100 mm. The sand used had a specific gravity of 2.65; dry unit weight of 16.5 kN/m^3; and D_{50} of 0.567 mm; C_u and C_c of 3.45 and 0.77 respectively. The soil was classified as poorly graded, SP, according to the USCS. The clay soil used had a specific gravity of 2.72; dry unit weight of 17.5 kN/m^3; percent finer than no. 200 sieve of 53 %; D_{50} of 0.067 mm; liquid limit of 23 %; and plasticity index of 7 %. The soil was classified as a low plasticity clay, CL. The tests were performed at normal stresses in the range of 8 kPa to 350 kPa at a constant displacement rate of 0.005 mm/min.

Chebet & Kalumba (2014) conducted a series of direct shear tests on Klipheuwel and Cape Flats sands reinforced with polyethylene (plastic) bag waste material. Strips of plastic material were used as tensile inclusions at concentrations of 0.1 % to 0.3 % by weight of dry soil; strip lengths of 15 mm to 45 mm, strip widths from 6 mm to 18 mm, and perforation diameters of 1 mm and 2 mm. Klipheuwel sand had the following characteristics: Specific gravity of 2.64; natural moisture content of 2.72 %; optimum moisture content of 6.7 %; maximum dry density of 1985 kg/m^3, particle size range of 0.075 mm-2.36 mm; angle of friction of 41.6° and cohesion of 4.8 kN/m^2. Cape Flats sand used had a specific gravity of 2.66; natural moisture content of 2.20 %; optimum moisture content of 15.0 %; maximum dry density of 1710 kg/m^3, particle size range of 0.075 mm-1.18 mm; angle of friction of 38.5° and cohesion of 8.4 kN/m^2. Both sands contained little or no fines and were classified as poorly graded, SP, using USCS. Klipheuwel sand exhibited better grading with a greater range of particles than Cape Flats sand which had particles with more uniform grading. The tests were run at normal pressures of 25 kPa, 50 kPa, and 100 kPa at a strain rate of 1.2 mm/min.

Shear stress-displacement behaviour of the soil-plastic composite

Gray & Ohashi (1983), Yetimoglu & Salbas (2003), and Chebet & Kalumba (2014) reported that reinforcements increased the peak shear strength of the soil. Furthermore, the resisting elements increased the residual shear strength and reduced the post-peak shear strength loss in the reinforced soil (Gray & Ohashi, 1983; Benson & Khire, 1994; Yetimoglu & Salbas, 2003). In contrast, Falorca & Pinto (2011) showed that the fibre reinforced soil shear stress increased up to the specified maximum displacement for both reinforced clay and sand, as illustrated in Figure 2.11.

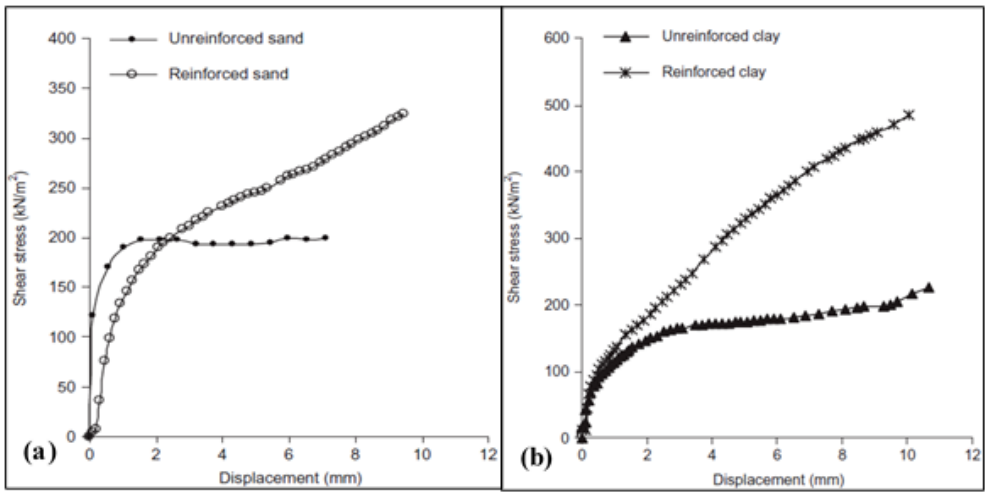

Figure 2.11: Stress-strain curves for the unreinforced and reinforced soil specimens: a) Sand soil, and b) Clay soil (Falorca & Pinto, 2011)

Varying concentration of plastic in the composite

Test results indicated that the variation of plastic content affected the value of the angle of friction. Subsequently, the shear strength (as illustrated in Figure 2.12) was observed to increase to a peak value with increase in the plastic content beyond which further increase had no effect (Gray & Ohashi, 1983; Benson & Khire, 1994; Yetimoglu & Salbas, 2003; Chebet & Kalumba, 2014). However, Falorca & Pinto (2011) reported no peak stress from test results and found that the initial stiffness of the reinforced sand decreased with increase in fibre content whereas for reinforced clay, there was no significant change.

Chebet & Kalumba (2014) presented results that indicated an increase in the friction angle on the addition of the solid strips and perforated strips of varied concentrations for both Cape Flats and Klipheuwel sands. Varying the diameter of perforations in strips resulted in greater values of friction angle, with average increases of 2° for every 1 mm in perforation diameter as compared to results obtained using specimens prepared with solid strips. Plastics with perforations of 2 mm diameter reported the greatest improvement in shear strength.

For HDPE material, the optimum concentration was found to be 0.1 % (Chebet & Kalumba, 2014), and 1 % (Benson & Khire, 1994) as shown in Figure 2.12. The difference may be attributed to the soil and plastic properties utilised in the studies

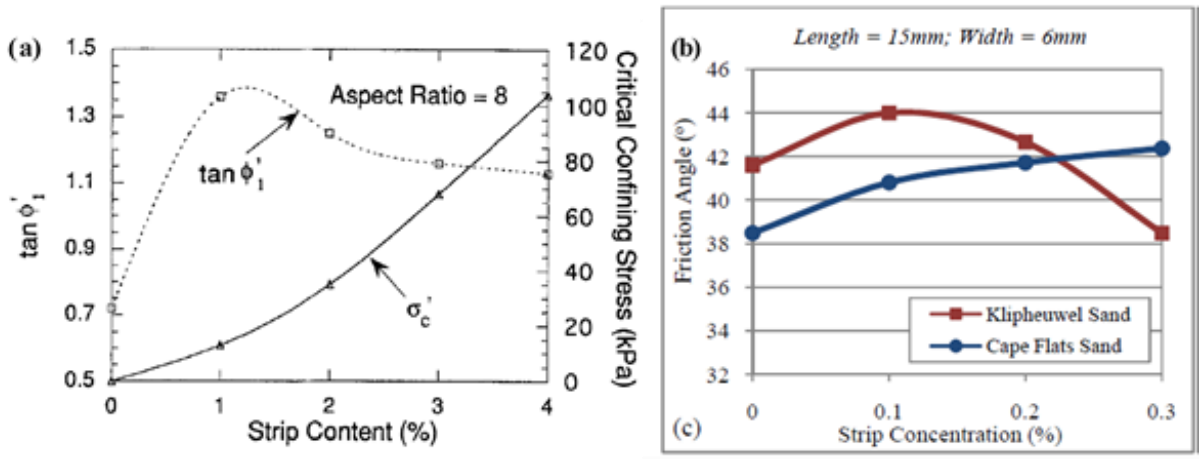

Figure 2.12: Variation of strip content and friction angle: a) After Benson & Khire (1994), and b) After Chebet & Kalumba (2014)

Variation of the strip length or aspect ratio of the composite sample

Test results indicate that varying the lengths of reinforcements significantly affects the soil friction angle (Gray & Ohashi, 1983; Benson & Khire, 1994; Yetimoglu & Salbas, 2003; Falorca & Pinto, 2011; Chebet & Kalumba, 2014). Further, increasing the length of reinforcements increased the shear strength of the reinforced soil up to a limiting value beyond which any further increase had no substantial influence (Gray & Ohashi, 1983; Benson & Khire, 1994; Yetimoglu & Salbas, 2003; Chebet & Kalumba, 2014). This is illustrated in Figure 2.13. Conversely, laboratory results by Falorca & Pinto (2011) stated no peak length.

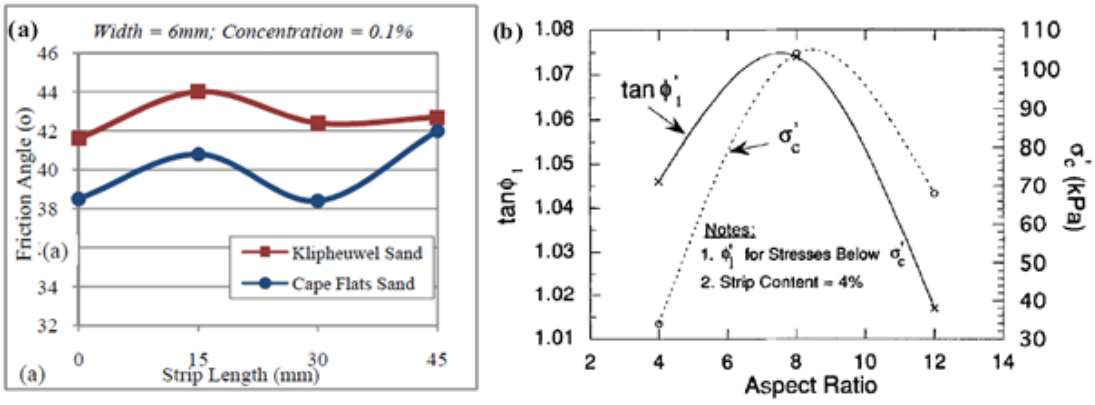

Figure 2.13: Variation of strip length and friction angle: a) After Chebet & Kalumba (2014), and b) After Benson & Khire (1994)

From Figure 2.13, Benson & Khire (1994) obtained the greatest improvement in friction angle at 48 mm length (aspect ratio 8), while Chebet & Kalumba (2014) reported maximum increase at 15 mm length for Klipheuwel sand and at 45 mm length for Cape Flats sand. It is probable

there exists a threshold plastic strip length for the different sand-plastic composites beyond which further increase in length results in a reduction in the friction angle. Additionally, the difference in results in the Cape Flats and Klipheuwel could also be due to the gradation of the soils. Klipheuwel sand is composed of angular shaped grains and has a better grading compared to poorly graded Cape Flats sand which has got round shaped grains.

Shear stress versus normal stress behaviour

The effect of applied normal stress was investigated by plotting Mohr-Coulomb failure envelopes which were observed to be bilinear, or curvilinear (Gray & Ohashi, 1983; Benson & Khire, 1994; Falorca & Pinto, 2011). The shear strength envelopes clearly indicated the existence of a critical or threshold confining stress below which failure was governed by plastic slippage or pull-out. Above this threshold stress, the envelopes deviated from the linear trend and failure was governed by plastic breakage or rupture, Figure 2.14. The envelope at normal stresses greater than the critical stress tended to be parallel to the envelope for unreinforced sand, Figure 2.14 (b), suggesting the tensile inclusions do not affect the frictional characteristics of the sand. Below the critical confining pressure, the reinforced soil revealed a higher friction angle than in the unreinforced soil (Gray & Ohashi, 1983) and a linear relationship was observed (Yetimoglu & Salbas, 2003; Chebet & Kalumba, 2014).

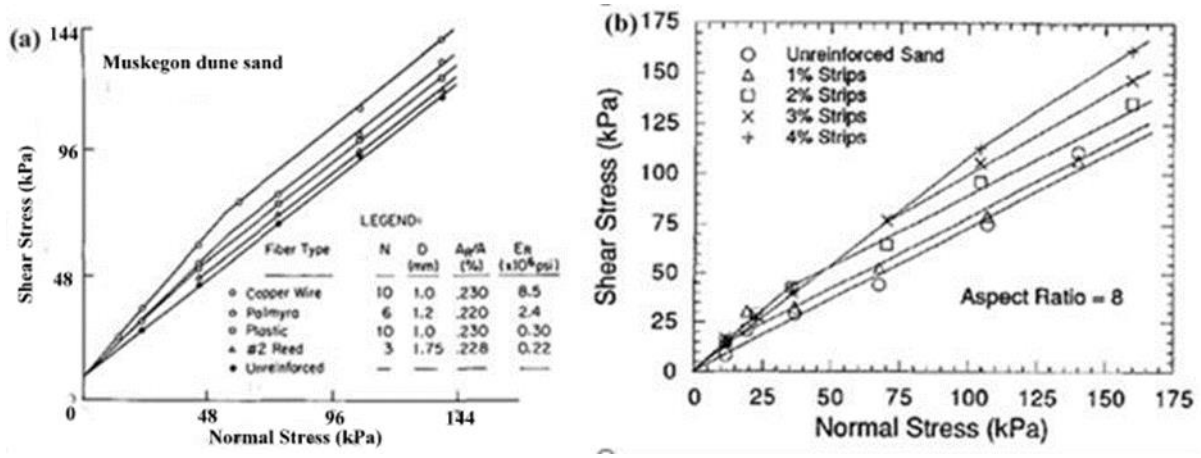

Figure 2.14: Bilinear failure envelope: a) After Gray & Ohashi (1983), and b) After Benson & Khire (1994)

The threshold confining stress was found to be in the range of 47 kPa to 200 kPa, and the value was found to be higher with increasing concentration of the reinforcing elements, Figure 2.14 (b) (Gray & Ohashi, 1983; Benson & Khire, 1994; Falorca & Pinto, 2011).

2.6 Triaxial Testing of Soil-Plastic Composite

The triaxial test is one of the commonly used methods for research and conventional testing of the strength behaviour of soils (Das & Sobhan, 2013). Soil specimens of approximately 35 mm to 100 mm in diameter, and 70 mm to 200 mm in height respectively are generally used. The specimen is encased in a rubber membrane and placed in a triaxial cell that is usually filled with water or air. The sample is subjected to isotropic confining pressure by compression of the fluid in the cell. A deviator or axial stress is applied to cause shear failure of the specimen. A schematic diagram of a typical triaxial test equipment is shown in Figure 2.15.

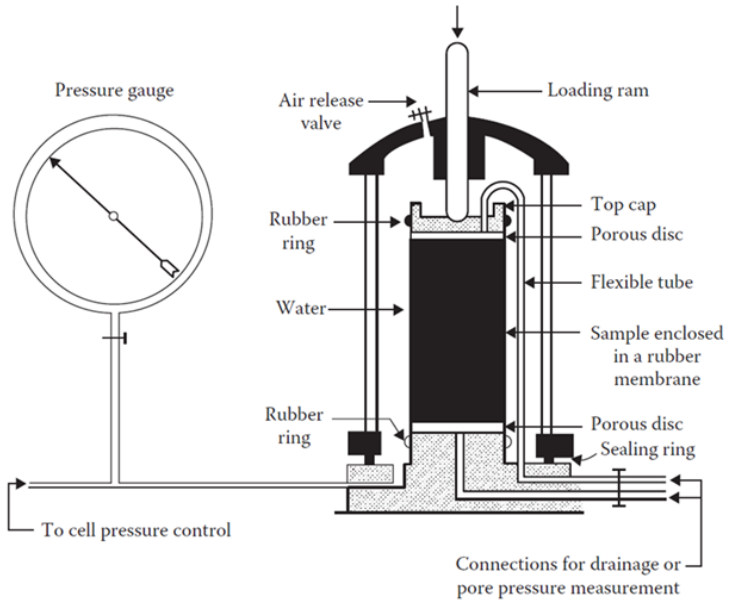

Figure 2.15: Triaxial test equipment (after Bishop & Bjerrum, 1960)

The triaxial method has numerous advantages in comparison with the direct shear box method;

i. Specimens are sheared at the weakest plane as opposed to a predetermined shear plane,
ii. Strains and stresses applied on the test samples are approximately uniform,
iii. A comprehensive stress-deformation response of soils can be performed,
iv. Pore water pressures and volumetric strains can be measured,
v. Different test variations of cell pressure and deviator stress can be conducted,
vi. Tests can be conducted in drained and undrained conditions.

Conventional triaxial tests have largely been used to investigate the behaviour of saturated soils with different types of triaxial tests being used to simulate field conditions of unsaturated soils. These tests include; consolidated drained (CD), constant water content (CW), consolidated undrained (CU), and unconfined compression (UC). A number of researchers using triaxial tests have studied the shear behaviour of unsaturated soils reinforced with synthetic materials (Gray & Al-Refeai, 1986; Maher & Gray, 1990; Dutta & Rao, 2007) reporting increases in the shear strength and stiffness of the soil as a result of the inclusions. Previous research reviewed in this section is presented in Table 2.6.

Gray & Al-Refeai (1986) compared the stress-strain behaviour of dry sand reinforced with continuous, oriented fabric layers as opposed to randomly distributed discrete fibres. The effect of content and aspect ratio of reinforcement, confining stress, and compactive effort were investigated using both natural and synthetic fibres. Glass fibres of 0.3 mm in diameter, concentrations of up to 6 % and lengths of 13 mm to 38 mm were added to clean, uniform, medium-grained sand, with the following material properties; specific gravity of 2.65, mean grain diameter (D_{50}) of 0.41 mm, maximum and minimum void ratios of 0.78 and 0.50 respectively. Triaxial compression tests were performed on the sand- glass fibre composite using specimens with a diameter of 38 mm and height of 80 mm, and 71 mm diameter and 180 mm height for longer fibres, at strain rates of 0.03 %/min to 1.56 %/min under confining stresses of up to 400 kPa.

Maher & Gray (1990) conducted laboratory triaxial compression tests to investigate the engineering response of sands reinforced with randomly distributed fibres. Several course grained sands with no fines were used to examine the influence of soil properties i.e. grain size, shape, and gradation. Glass-reinforced plastic fibres with a diameter of 0.3 mm, aspect ratio (length/diameter) of 60, 80 and 125, were added to the sand at concentrations of up to 6 % and tested over a range of confining stresses to determine the stress-strain behaviour of the reinforced soil at low and high stresses (up to approximately 500 kPa).

More recently, Dutta & Rao (2007) presented regression models for predicting the behaviour of dry sand reinforced with waste plastic by conducting drained triaxial compression tests. Packaging strips made of HDPE of width 12 mm, and thickness 0.45 mm, were cut into lengths of 12 mm (AR = 1) and 24 mm (AR = 2), and added to the soil at strip contents in the range of 0 % to 2 %. A uniform, medium-grained sand having sub-angular particles was used. It had a specific gravity of 2.66, mean particle diameter (D_{50}) of 0.42 mm, coefficient of uniformity (C_u)

of 2.11 and coefficient of curvature (C_c) of 0.96. The sand was classified as SP-SW according to the USCS and had minimum and maximum void ratios of 0.56 and 1.12 respectively while the corresponding dry unit weights were 16.70 kN/m^3 and 12.30 kN/m^3 respectively. Samples of 100 mm diameter and 200 mm height were compacted to a density of 14.88 ± 0.42 kN/m^3, and tests carried out at a strain rate of 1.016 mm/min under confining stresses in the range of 69 kPa to 276 kPa.

2.6.1 Varying concentration and aspect ratio

Laboratory results indicate that the behaviour of reinforced soil is influenced significantly by the concentration and aspect ratio of the inclusions. Shear strength increased linearly to the amount of reinforcement up to a limiting content (Gray & Al-Refeai, 1986; Maher & Gray, 1990; Dutta & Rao, 2007). The optimal content and aspect ratio (AR)/length were found to be approximately 6 % and 84 respectively (Gray & Al-Refeai, 1986), 6 % and 80 respectively (Maher & Gray, 1990), and 0.15 % and 2 (24mm) respectively (Dutta & Rao, 2007). The strength increase eventually reached an optimal upper value at high plastic contents and confining stress (Maher & Gray, 1990). Besides, multiple regression analysis by Dutta & Rao (2007) showed that increase in HDPE strip content and aspect ratio increased both the cohesion and internal friction angle.

On the contrary, Gray & Al-Refeai (1986) observed that the increase in strength of the sand was proportional to the concentrations at high confining pressures or lengths, but approached a peak value at lower values of the two variables. Additionally, the resisting elements increased the stiffness of the reinforced sand (Gray & Al-Refeai, 1986; Dutta & Rao, 2007).

2.6.2 Effect of varying confining pressure

Review of previous research shows that the failure mechanism of the reinforced soil is dependent on the confining stress. It is reported that there exists a critical confining pressure where the failure envelope sharply deviates from a linear relationship. At stresses below this threshold value, failure is governed by frictional slippage of the fibre or plastic. At stresses greater than the critical stress, failure is governed by the tensile strength of the inclusion. A bilinear or curvilinear relationship is observed on plotting Mohr-Coulomb failure envelopes (Gray & Al-Refeai, 1986; Maher & Gray, 1990), as illustrated in Figure 2.16. The critical confining stress was found to be influenced by the fibre aspect ratio, texture, and content (Gray & Al-Refeai, 1986; Maher & Gray, 1990), as shown in Figure 2.16. Gray & Al-Refeai (1986)

reported a critical confining pressure of 98 kPa for fabrics and 392 kPa for smooth textured fibreglass and the value decreased with increasing aspect ratio, Figure 2.16 (a). On the contrary, Maher & Gray (1990) reported a threshold confining pressure of between 98 kPa and 300 kPa and it improved with increasing fibre aspect ratio, Figure 2.16 (b).

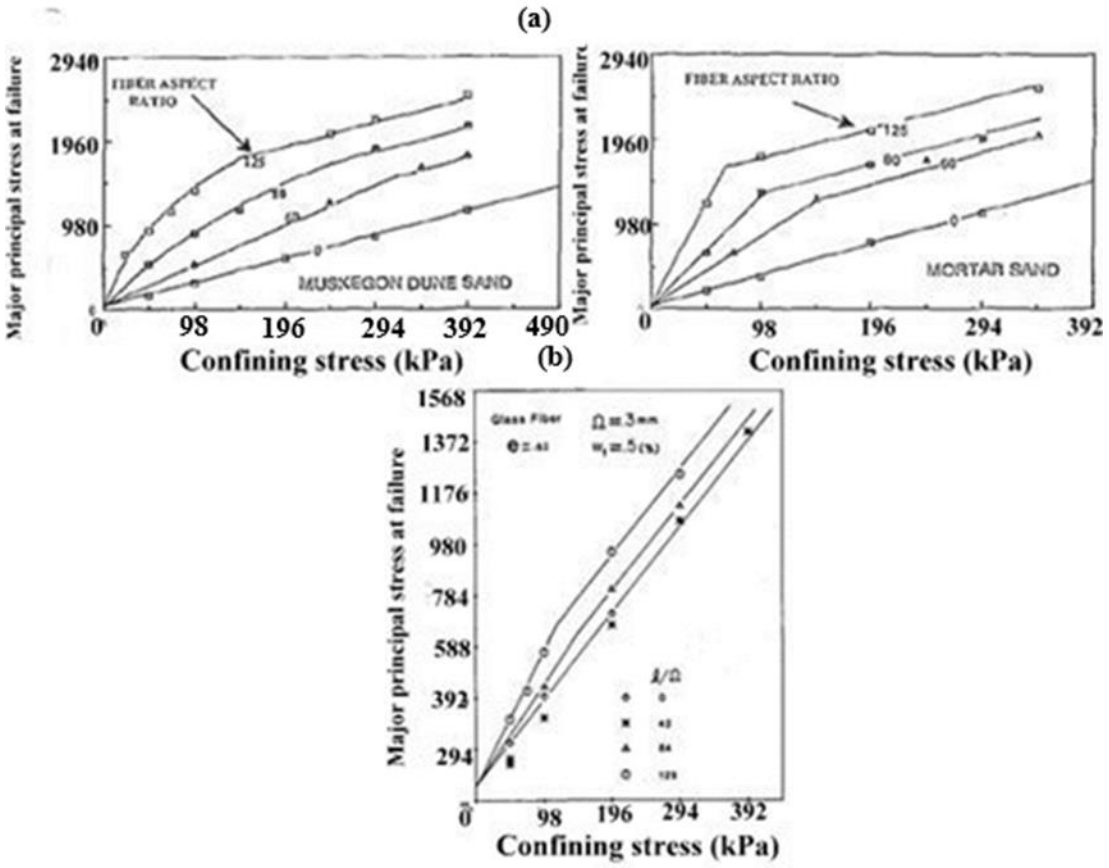

Figure 2.16: Failure envelopes from triaxial compression tests on reinforced sand: a) After Maher & Gray (1990), and b) After Gray & Al-Refeai (1986)

Maher & Gray (1990) further noted that well-graded or angular sands exhibited a bilinear behaviour while uniform, rounded sands exhibited a curvilinear behaviour. They also observed that the failure plane was planar and oriented at an oblique angle or as predicted by the Mohr-Coulomb criterion i.e. $(45^{\circ} + \frac{\varphi}{2})$.

2.6.3 Stress-deformation behaviour

It was found that the presence of tensile inclusions altered the stress-strain behaviour of the soil. The addition of synthetic materials occasioned an increase in the peak strength and stiffness of the reinforced soil (Gray & Al-Refeai, 1986; Maher & Gray, 1990; Dutta & Rao, 2007). This

lead to a loss in compressive stiffness at low strains for continuous, oriented fabrics (Gray & Al-Refeai, 1986). Likewise, significant improvements in the axial strain at failure and reduction in the post-peak loss of strength was reported (Gray & Al-Refeai, 1986; Maher & Gray, 1990).

2.6.4 Effect of soil properties

Maher & Gray (1990) observed that soil properties had an effect on the behaviour of the reinforced soil. An increase in the size of the sand particles, D_{50}, lowered the fibre contribution to strength but had no effect on the critical confining stress, Figure 2.17 (a). A better soil gradation or an increase in coefficient of uniformity resulted in lower critical confining pressure and higher fibre influence on the strength, Figure 2.17 (b). An increase in particle sphericity also led to a higher critical vertical confining pressure and lower fibre influence on strength, Figure 2.17 (c).

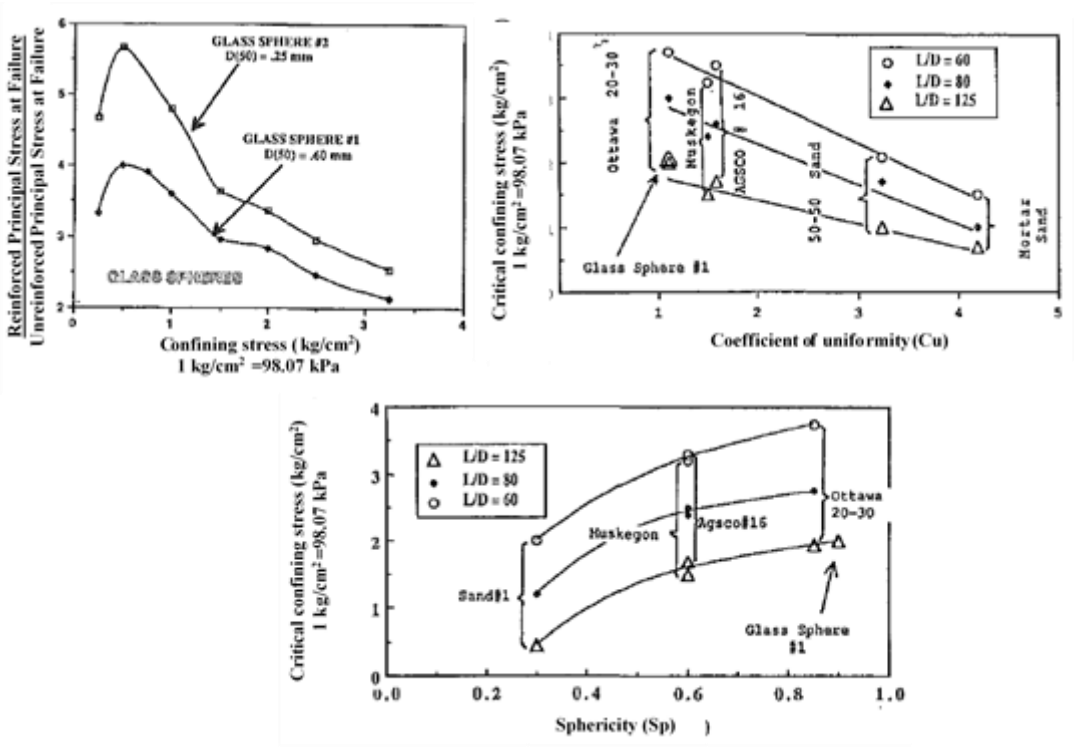

Figure 2.17: Influence of soil properties on behaviour of reinforced sand: a) Soil grain size, b) Coefficient of uniformity, and c) Sphericity index (after Maher & Gray, 1990)

2.7 Summary of the Literature Review

The synthesis of literature on the shear behaviour of soils reinforced with randomly distributed discrete soil-plastic composites has shown that research has been undertaken mainly based on CBR, direct shear and triaxial tests. A summary of previous research is presented in Table 2.6 which shows a wide range of reinforcement lengths and contents investigated in the published works. Most studies were conducted using granular soils probably due to the fact they are widely used as engineered fills and the ease of densifying processes of these soils.

In general, the synthesis of previous research has shown that, even when different tests are conducted and reinforcing materials added to soil, the shear strength behaviour of a composite soil mass is governed by the soil and fibre or plastic properties. It was observed that addition of HDPE reinforced soils exhibited similar behaviour to fibre reinforced soils. Several researchers reported common findings of enhanced shear strength, stiffness and a reduction in the post-peak strength loss due to the inclusions. Emphasis was placed on the effect of concentration and aspect ratio or length of the plastic material.

Only a few of the experimental studies investigated the influence of confining stress over a wide range. However, it was reported that there existed a critical confining stress beyond which the failure envelope deviated from the linear relationship resulting in a curved-linear or bilinear relationship. The behaviour of the reinforced soil above and below this stress was due to the pull-out or breakage of the plastic inclusions. The value of the critical confining stress was found to be in the range of approximately 100 kPa to 400 kPa. Additionally, previous research reported contradicting findings on whether this value reduced or increased with varying fibre properties. Consequently, this prompted an investigation into the effect of plastic strip length and content on the value of the critical confining stress.

The literature review showed that a limited number of laboratory investigations using triaxial tests had been conducted to evaluate the potential use of HDPE plastic bag material in the geotechnical engineering field. The findings of the studies reported contradictions on the shear behaviour of the soil-plastic composites upon varying plastic parameters and confining stress. This encouraged further research to better understand the shear behaviour of the soil-plastic composites on varying plastic strip length, concentration, and confining stress. The influence of compactive effort on the soil-plastic interaction was also investigated in the current study.

Table 2.6: Summary of previous research on synthetic materials for soil reinforcement

Authors	Soil	Inclusion	Test type (s)	Test variables	Findings
Gray & Ohashi (1983)	Sand	Fibre (plastic PVC)	Direct shear	Fibre content: 0.25-0.5 % Length: 20-250 mm	Shear strength increase to a peak value Bilinear failure envelope
Gray & Al-Refeai (1986)	Sand	Fibre (glass-reinforced plastic)	Triaxial compression	Concentration: 0-6 % Length: 13-38 mm	Shear strength increase to a peak value Stress-strain behaviour of sand affected significantly Bilinear failure envelope
Maher & Gray (1990)	Sands of different gradation	Fibre (glass-reinforced plastic)	Triaxial compression	Concentration: 0-6 % Aspect ratio: 60, 80 and 125	Shear strength increase & stiffness to a peak value Bilinear failure envelope
Benson & Khire (1994)	Poorly graded and	HDPE strips from milk jugs	Direct shear & CBR	Length: 24, 48 and 72 mm Concentration: 1-4 %	Increased the CBR & secant modulus Shear strength increase - peak value. Bilinear failure envelope
Consoli et al. (2002)	Sand	PET fibres recycled from plastic waste bottles	UCS, split tensile tests, saturated drained triaxial compression	Plastic content: 0-0.9 % Length: 12-36 mm Cement content: 3-7 %	Improvement of strength of both cemented and uncemented sand Reduction in brittleness of cemented sand. No change in stiffness of sand
Yetimoglu & Salbas (2003)	Sand	Fibre (polypropylene)	Direct shear	Content: 0.1-1 %	Shear strength increase to a peak value Linear failure envelope

Table 2.6 (continued)

Authors	Soil	Inclusion	Test type (s)	Test variables	Findings
Dutta & Rao (2007)	Sand	LDPE & HDPE packaging strips	Triaxial compression	Strip length: 12-24 mm Strip content: 0-2 %	Deviator stress improved with increased aspect ratio, content & confining pressure
Babu et al (2010)	Silty clay	PET strips from waste plastic water bottles	Triaxial compression One-dimensional consolidation	Plastic content: 0-1%	Improvement in strength of soil
Falorca & Pinto (2011)	Low plasticity clay Poorly graded sand	Fibre (polypropylene)	Direct shear	Length: 25-100 mm Content: 0-1 %	Shear stress increase to maximum deformation Curvilinear failure envelope
Neopaney et al. (2012)	Inorganic silt of high plasticity Organic clay of high plasticity	HDPE strips from shopping plastic bags	CBR	Strip length: 10-40 mm Strip concentration: 0-1 %	Improved CBR Optimum results: Aspect ratio and plastic content of 3 and 0.5 % respectively
Chebet & Kalumba (2014)	Dry sand	HDPE strips	Direct shear	Length: 15-45 mm Strip content: 0.1-0.3 % Strip width: 6-18 mm	Shear strength increase to an optimum content (0.1 %) and length (15 mm) Linear failure envelope

3 RESEARCH MATERIALS AND METHODOLOGY

3.1 Introduction

This chapter discusses the materials, apparatus, specimen preparation and experimental procedures adopted in the triaxial testing investigation. The major research materials used were Cape Flats sand soil and HDPE plastic bag. Classification tests and experimental procedures were carried out in accordance with American Standard Test Method (ASTM) standards. Triaxial compression tests were carried out using a computerized automated triaxial testing apparatus.

3.2 Research Materials and Apparatus

3.2.1 Cape Flats sand

The soil used in the experiments was Cape Flats sand sourced from Afrimat quarry (34º 02'42.42" S,18º 33' 02.34" E) – Olieboom Road, Philippi in the Western Cape Province, South Africa. It was selected because it was readily available, clean, easily controllable and consistent which ensured reproducibility of the test results. Additionally, the choice of soil was because reinforced soil structures are mainly constructed with granular engineered fills.

Cape Flats sand can be described as a medium dense, light grey, clean quartz sand (Kalumba, 1998). Photomicrographs of the sand were obtained using a Nova NanoSEM 230 scanning electron microscope to examine the physical structure of the soil which has an influence on the mechanical properties of the soil (Das & Sobhan, 2013). The magnification of the microscope was set to include as many grain particles as possible and make sure that the finest sand particles were visible. The sand was observed to have neary uniformly sized grains with the larger grains elongated and subrounded while medium sized grains were sub-angular in shape, Figure 3.1. It was anticipated that the use of sand with sub-rounded to sub-angular particular sizes would provide better soil-plastic interaction and improve the engineering properties of the soil.

Standard soil tests were conducted according to the testing standards listed in Table 3.1 to determine the mechanical and physical properties of the sand material.

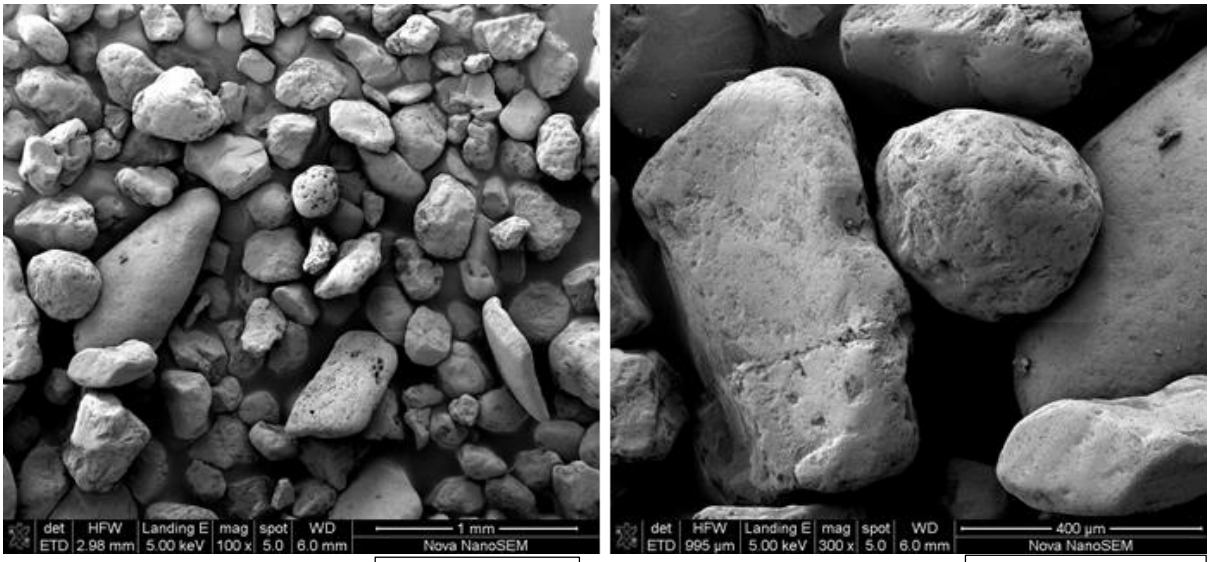

Figure 3.1: Photomicrographs of Cape Flats sand particles under different levels of magnification

Table 3.1: Laboratory soil classification tests

Property	**Method**	**Test standard**
Specific gravity	Small pycnometer	ASTM D854-14
Moisture content	Oven drying	ASTM D2216-10
Maximum index density	Vibratory table	ASTM D4253-16
Minimum index density	Method A; funnel & mould	ASTM D4254-16
Particle size distribution	Particle size analysis	ASTM D6913-04
Shear strength	Triaxial shear method	ASTM D7181-11

The grading curve from sieve analysis tests on the sand shows that the soil consisted of 99.96 % sand, and 0.04 % fines (passing 0.075 mm sieve size), Figure 3.2. The sand with grading characteristics; coefficient of uniformity 1.42 and the coefficient of curvature 1.10 was classified according to the Unified Soil Classification System (USCS) as poorly graded sand (SP). Table 3.2 gives a summary of the physical properties of the sand soil. The detailed data is presented in Appendix A.

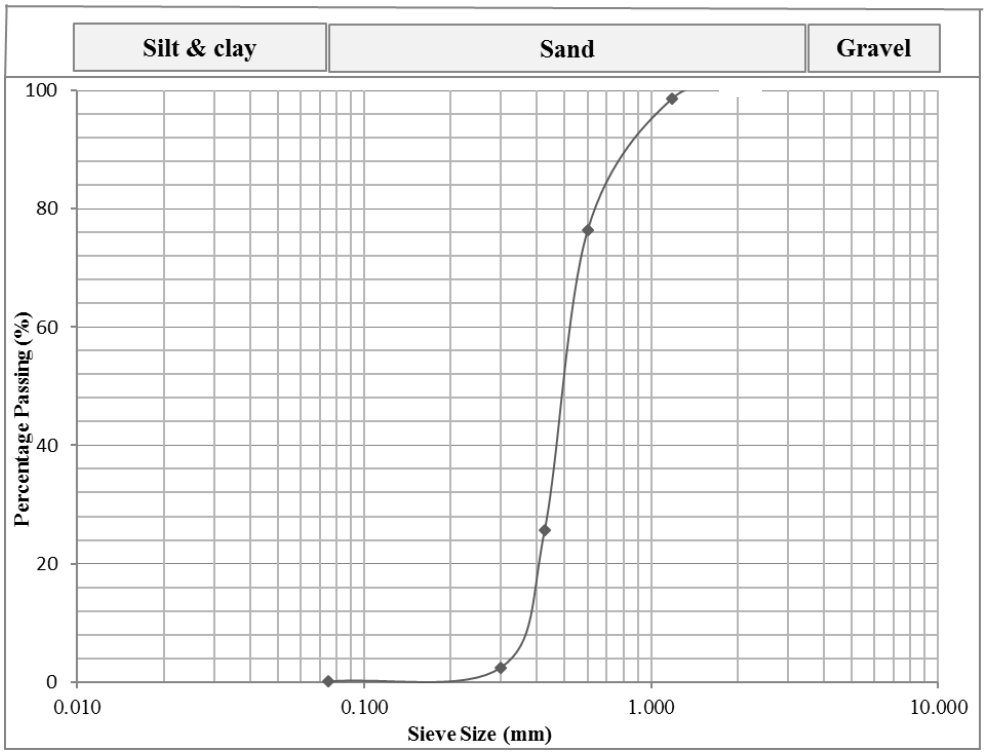

Figure 3.2: Grading curve for Cape Flats sand

Table 3.2: Summary of physical properties of Cape Flats sand

Property	**Unit**	**Value**
Specific gravity, G_s	Mg/m^3	2.64
Average densest (maximum) dry density	kg/m^3	1803
Average loosest (minimum) dry density	kg/m^3	1552
Mean grain size, D_{50}	mm	0.50
Coefficient of uniformity, C_u	-	1.42
Coefficient of curvature, C_c	-	1.10
Particle size	mm	0.075–1.200
Unified soil classification	-	SP
Angle of internal friction, φ' (Peak), D_r = 52 %,	º	29
Angle of internal friction, φ' (Peak), D_r = 57 %,	º	30

3.2.2 Plastic material

The plastic bags used were 24-litre grocery shopping bags sourced from the local Pick ‘n Pay supermarket in Cape Town, South Africa. The bags were manufactured from high-density polyethylene (HDPE) polymers by Transpaco Limited in Johannesburg, South Africa, using a process known as Blown film extrusion (Mughtar, 2009). The plastic bags were white in colour, with red and blue prints on the front side. Each bag was labelled high-density polyethylene (PE-HD) with a recycling number 2 (Figure 3.3) classified in accordance with the SPI polymer identification code. The shopping bags were selected from one brand name for consistency and repeatability purposes.

Figure 3.3: Plastic bag shopping material used in the study

Williamson (2012) conducted tests using the Zwick Universal Tensile and Compression Machine to determine engineering properties of the plastic bags. Table 3.3 shows a summary of the plastic material properties.

Table 3.3: Material properties of Pick 'n Pay polyethylene shopping bag (Williamson, 2012)

Property	Unit	Value
Average thickness	mm	0.02
Longitudinal tensile strength	MPa	17
Longitudinal strain	%	62.81
Transverse tensile strength	MPa	17
Transverse strain	%	7.55
Average density	kg/m^3	1265

3.2.3 Triaxial Test apparatus

The triaxial tests were conducted in accordance with ASTM D7181-11 – "Standard Test Method for Consolidated Drained Triaxial Compression Test for Soils." A standard fully automated LoadTrac-II/FlowTrac-II triaxial system (Figure 3.4) manufactured and supplied by Geocomp Corporation was used to run the tests.

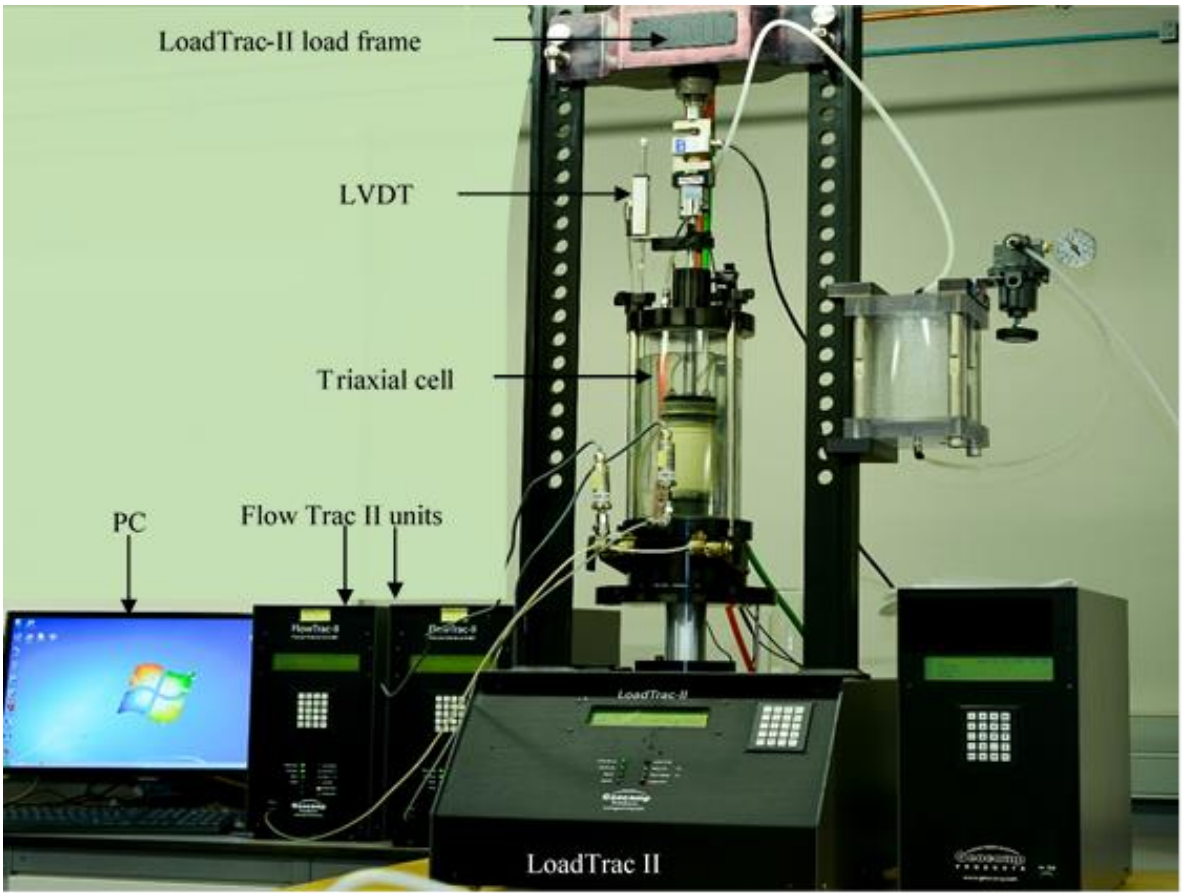

Figure 3.4: Triaxial test apparatus

The system comprised of hardware and software components whose functions are as described below:

Triaxial cell: The chamber in which the sample to be tested is placed and included a load cell/piston coupling and a modified base/platen for triaxial testing.

Two FlowTrac-II units: The units had two computer-controlled flow pumps used to control chamber pressure and back pressure, and to measure volume changes.

LoadTrac-II load frame: The unit had a platen that is computer-controlled for static loading on a sample.

Linear Variable Differential Transducers (LVDT): Sensors used to measure force, displacement, sample and cell pressures.

Computer: Desktop computer to log test data and controlling the test. Editing and reporting were built into the test and control software program.

Software:

The LoadTrac II/FlowTrac II is a menu driven triaxial system with the Windows®-based software allowing the user to define the conditions for running the test, logging test data and reporting results. The software was used to specify values for controlling the initialisation, saturation, consolidation and shearing of the test specimen. Calibration was carried out before the commencement of the testing regime. The calibration data in Appendix B provided by the manufacturer was used to calibrate the equipment.

Current data and system status information was displayed on the computer monitor during testing and collected data were written to a file on the system's hard drive. The reporting software permitted the user a variety of options in graphing and generating test data which were then exported to Excel for analysis.

3.3 Methodology

3.3.1 Plastic strips preparation

The "Laser Pro Spirit GX" machine with a bed size of 965 mm x 610 mm and a laser cartridge of 40 W, (Figure 3.5) was used to cut plastics into strips to the required dimensions. The use of the machine ensured accurate dimensions and the required quantities of plastic strips were achieved in a timely manner.

Figure 3.5: Laser Pro Spirit GX used to cut plastics

The size of strips required was drawn in AutoCAD and the drawing scaled. Before cutting, the handles and bottom of the plastic bags were removed to form a 380 mm by 300 mm plastic sheet. A stack of plastic bags was placed in the working area of the machine and a SmartPIN Auto Focus probe focused the laser at the correct height, guaranteeing the precision required for optimum, quality cutting. AutoCAD drawings were then sent through to the machine while speed and power settings were then adjusted to ensure production of specimens with smooth edges. The control panel at the front of the machine was used to initiate the cutting operations. The process was followed by the manual separation and sorting of the cut plastic strips as a quality assurance measure in order to obtain uniform and comparable samples. The process illustrated in Figure 3.6 was repeated for the different dimensions to ensure production of uniform strip lengths and widths.

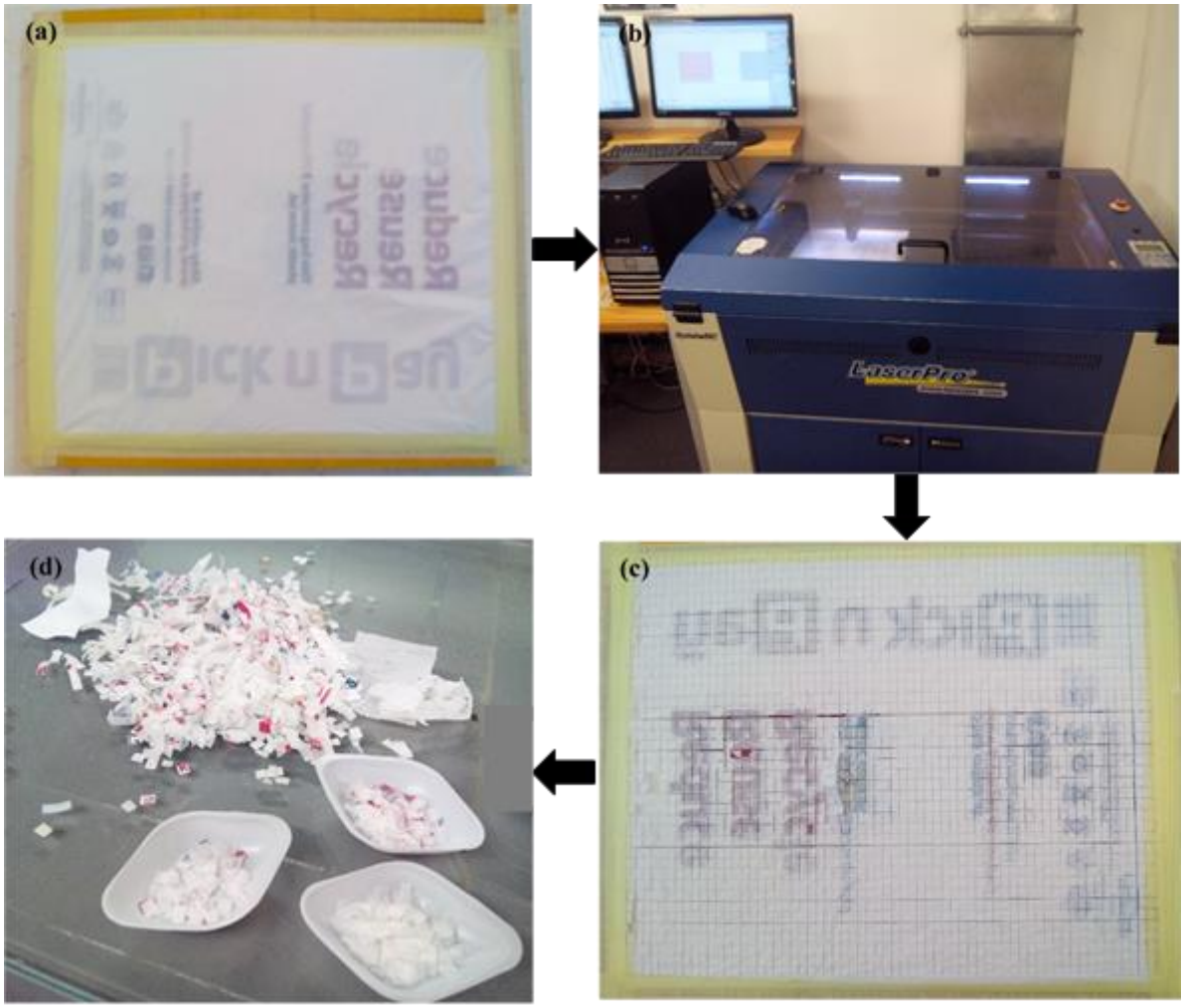

Figure 3.6: a) Stack of plastic bags ready for cutting, b) Plastic bags placed in the working area of the machine, c) After cutting and d) Sorting prepared specimens

3.3.2 Soil preparation

Cape Flats sand was dried using a laboratory thermostatically controlled oven, following ASTM D2216-10 - "Standard Test Methods for Laboratory Determination of Water (Moisture) Content of Soil and Rock by Mass." to eliminate the effects of moisture changes during testing. The soil was placed in the oven at 105 ^{0}C temperature for 12 hours after which it was removed from the oven, allowed to cool and the dried soil stored in sealed plastic bags.

3.3.3 Test specimen preparation

The composite specimens were prepared according to the dry tamping technique recommended in ASTM D7181-11 – "Standard Test Method for Consolidated Drained Triaxial Compression Test for Soils." For each experiment, 360 g of oven-dried Cape Flats sand was used. This was determined through volume calculations and laboratory trials before addition of any plastic

reinforcement. The requisite amount of plastic strips to mix with the sand was determined as a percentage by dry weight of the sand. The equation below was used to compute the different concentrations of plastic strips to be weighed for each test:

$$W_p = W_s \times \frac{X}{100} \qquad \textbf{Equation 3.1}$$

Where W_p = Mass of plastic strips,

W_s = Mass of dry sand, and

X = Concentration of plastic strips

Lengths were varied from 7.5 mm to 30 mm while the width was kept constant at 6 mm, Figure 3.7. The plastic content was also varied from 0.1 % to 0.3 % by weight of dry sand. These plastic parameters used in the experiments were selected based on previous studies (Consoli et al., 2002; Rao & Dutta, 2004; Choudhary et al., 2010; Chebet & Kalumba, 2014). The selection of the parameters was based on the range of values used by the researchers.

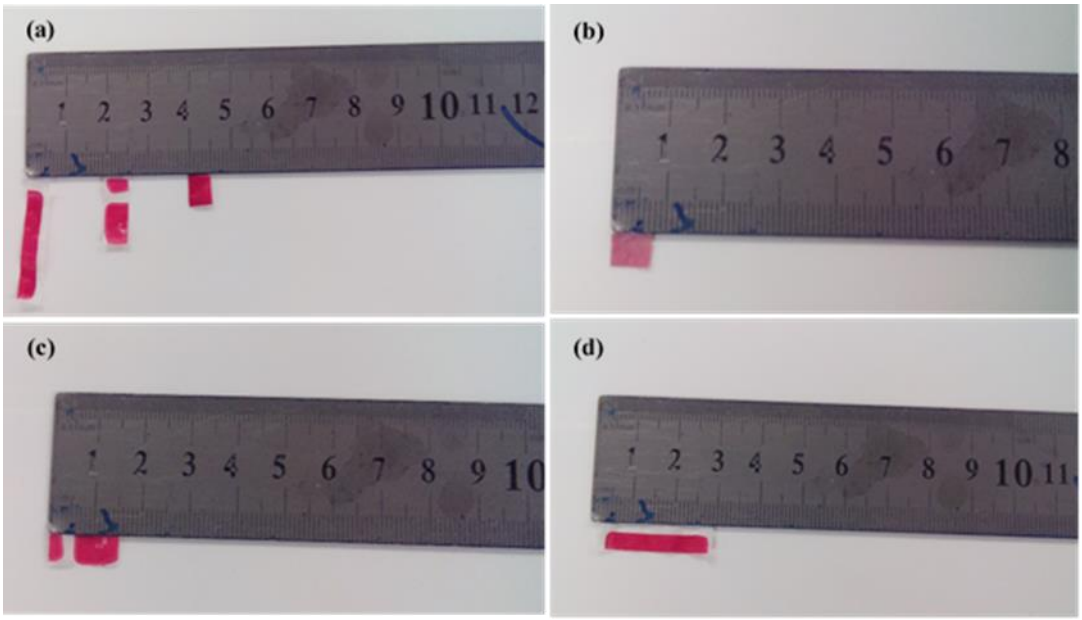

Figure 3.7: Strip parameters of prepared specimens: a) Strip width constant, W = 6 mm, b) Strip length, L1 = 7.5 mm, c) Strip length, L2 = 15 mm and d) Strip length, L3 = 30 mm

Plastic strips of various lengths were added to soil at different concentrations and randomly mixed to form a homogenous soil-plastic composite specimen. The homogeneity of the composite specimen was confirmed through visual inspection. For each experiment, a known

mass of strips and soil were accurately measured using electronic balances and carefully mixed by hand to form a composite mixture, Figure 3.8.

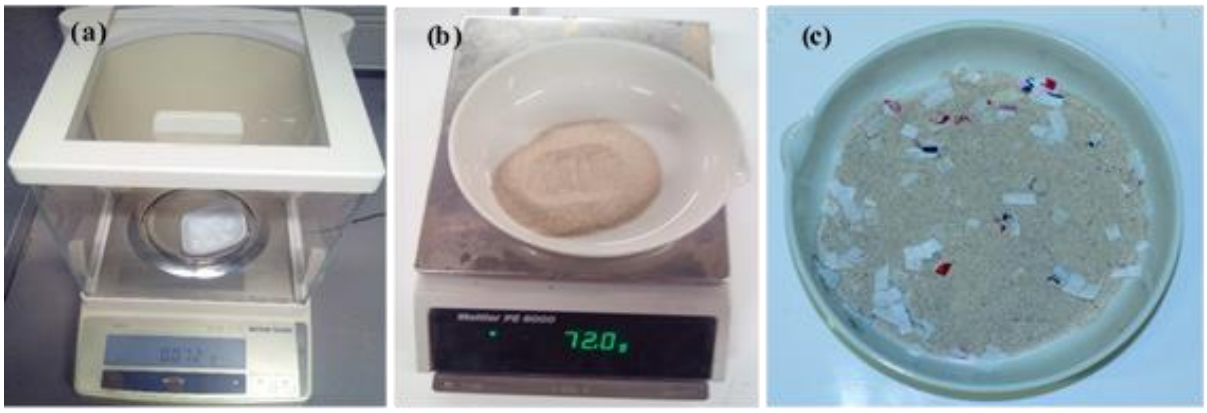

Figure 3.8: a) Weighing plastic strips for each layer on an electronic balance, b) Weighing sand for each layer on an electronic balance, and c) Randomly mixed soil-plastic matrix

Identical cylindrical specimens of size 50 mm diameter and 100 mm in height were prepared and the average-height to-average-diameter ratio kept between 2 and 2.5, and the variation of each of the height or diameter dimension from average not being more than 2 % as stipulated in ASTM D7181-11. Samples with height to diameter ratio of greater than 2.5 were discarded. The steps followed during sample preparation for the test setup are illustrated in Figure 3.9 and Figure 3.10.

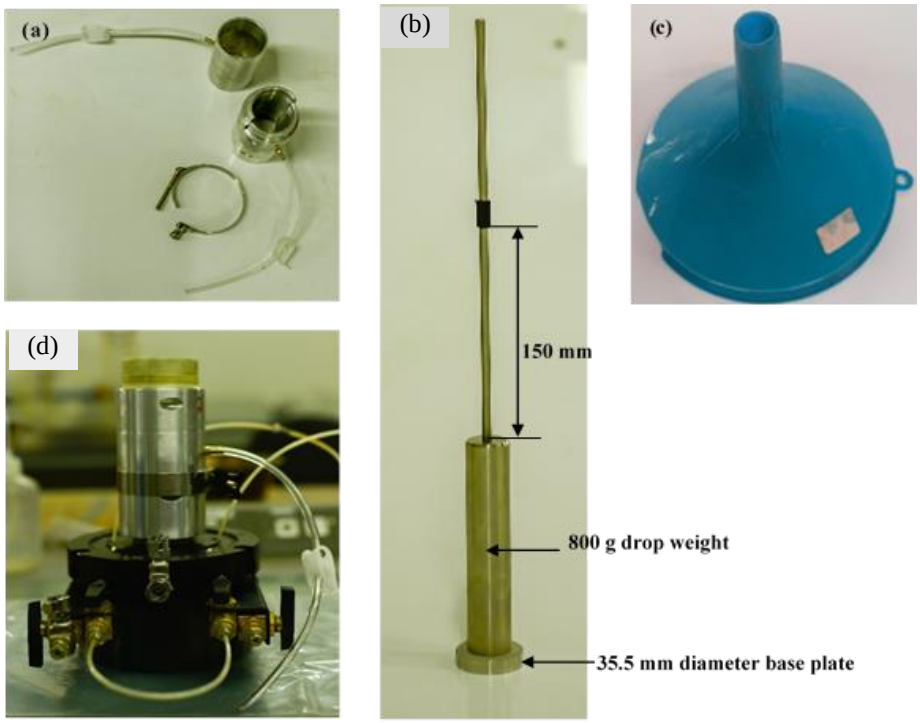

Figure 3.9: a) Split mould before assembly, b) Steel hand tamper used for compaction, c) Funnel for placing specimen into the mould, and d) Assembled split mould and membrane ready for compaction of specimen

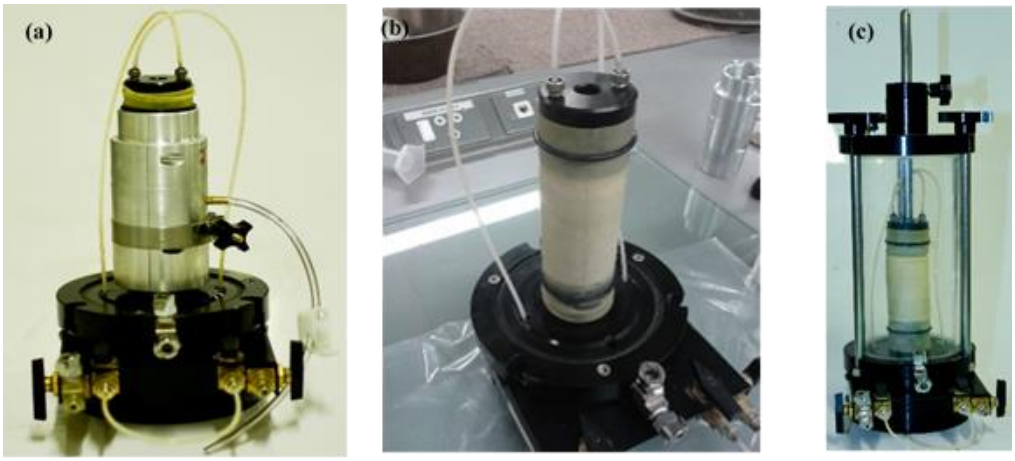

Figure 3.10: a) Prepared specimen with top platen and tubing connections, b) Prepared specimen with membrane and O-rings, and c) Specimen assembled in triaxial cell ready for testing

A 50 mm diameter latex rubber membrane was placed on the lower platen of the triaxial cell and secured using O-rings. A split mould, Figure 3.9 (a), was then placed on the bottom platen with the membrane extending up through it. The membrane was stretched firmly over the

interior surface of the split mould and over its top opening, Figure 3.9 (b). A partial vacuum was applied to the split mould to ensure the membrane was held tightly against the mould during compaction. A funnel, Figure 3.9 (c), was lowered sufficiently (approximately 3 mm from the surface of deposition) to allow for the specimen to be placed into the split mould while avoiding segregation of the composite specimen. The specimen was compacted by hand tamping in 5 layers, using a steel tamper, Figure 3.9 (d), with a 35.5 mm diameter circular base plate and weighing approximately 800 g, at a drop height of 150 mm.

Ten and twenty-one blows were applied per layer, to achieve target average dry densities of 1674 kg/m^3 and 1686 kg/m^3 (equivalent to a relative density of 52 % and 57 % respectively), in the medium dense state, for low and high compactive efforts respectively. The compactive efforts and relative densities were varied to investigate their effect on the shear behaviour of the reinforced and unreinforced soil. This was done to simulate field conditions in which the soil would be subjected to such as road construction. Furthermore, the relative densities were selected and kept constant for the two sets of tests because they were easily achieved for most of the plastic concentrations.

The compaction energy, E, and relative density, D_r, used for all tests were calculated using the equations below (Das & Sobhan, 2013).

$$E = \frac{\text{Number of blows per layer} \times \text{Number of layers} \times \text{Weight of hammer} \times \text{Height of drop of hammer}}{\text{Volume of mould}} \qquad \textbf{Equation 3.2}$$

Where; $\boldsymbol{B}$ = Number of blows per layer,

$\boldsymbol{N}$ = Number of layers,

$\boldsymbol{W}$ = Weight of hammer,

$\boldsymbol{H}$ = Height of drop hammer

$\boldsymbol{V}$ = Volume of mould.

$$D_r = \frac{\rho_{d(max)}}{\rho_d}\left[\frac{\rho_d - \rho_{d(min)}}{\rho_{d(max)} - \rho_{d(min)}}\right] \qquad \textbf{Equation 3.3}$$

Where; $\boldsymbol{\rho_{d(max)}}$ = Maximum (densest) dry density,

$\boldsymbol{\rho_d}$ = Target dry density,

$\boldsymbol{\rho_{d(min)}}$ = Minimum dry (loosest) density.

The corresponding energy for low and high compactive effort was obtained as 280 kN-m/m^3 and 589 kN-m/m^3 respectively. The compaction was also guided by the standard Proctor test described in ASTM D698-12e2 and the undercompaction process (Ladd, 1978).

During the compaction process, the top surface of each lift was scarified before compaction of the next layer. The top platen was placed and the membrane was drawn up tightly over it, O-rings were used to seal the membrane and specimen tubing connections were fixed in place as demonstrated in Figure 3.10 (a). A partial vacuum of 3 kPa was then applied to the specimen and the split mould removed, Figure 3.10 (b), in order maintain the stability of the composite specimen. The diameter and height of the specimen were then measured using a digital Vernier callipers and recorded for accurate density determination.

The triaxial cell, cover plate, and loading piston were carefully placed in position to avoid sample disturbance. The triaxial cell was then tightly fastened into position using tie rods. Figure 3.10 (c) shows the prepared test specimen placed in the triaxial cell.

3.3.4 Test procedures

The test procedures described were followed for each of the triaxial tests according to ASTM D7181-11 for consolidated drained testing conditions specified to simulate long term field conditions after construction. Consolidated drained (CD) triaxial tests were performed using confining pressures of 50 kPa, 100 kPa, 200 kPa, 300 kPa and 400 kPa to investigate the shear behaviour of the soil over the range of stresses which correspond to different stresses the soil may be subjected to in the field. The range of confining stresses was also essential in defining the shear strength envelope of the reinforced sands. A shear rate of 0.075 %/min and a maximum strain of 10 % were adopted as per recommendations in ASTM D7181-11, to allow for dissipation of pore (air) pressures during shear allowing for full drainage.

After the sample was formed, the triaxial cell was filled with tap water and then mounted onto the platen of the LoadTrac II unit ready for testing. The output tube from each flow pump unit was connected to the appropriate quick-connect coupling on the test cell. Menu options on the front panel of the LoadTrac II unit were used to position the loading piston to ensure it made contact with the load cell for the application of the load on the sample. A piece of paper was used to confirm that the loading piston and load cell were in contact. Menu options on the front panel of the FlowTrac II units were used to initialise the flow pumps to 90 % for the cell pump and 10 % for the sample pump since sand used in the study was highly porous.

Once the test set up had been completed, the software, TRIAXIAL program for processing data from triaxial tests was loaded on the computer. The test procedures followed in the software when running the test are presented in Appendix B. Data entry was then completed on the software and exported to Excel for data reduction.

3.3.5 Testing schedule

In summary, a total of 66 consolidated drained triaxial tests were carried out; 33 at low compactive and 33 at high compactive effort. For each set of triaxial tests; three repeatability tests at 100 kPa, five control tests on unreinforced sands and 25 tests on sands reinforced with plastic strips of varying length and concentration at 50 kPa, 100 kPa, 200 kPa, 300 kPa and 400 kPa confining pressures were undertaken. Table 3.4 shows a description of the codes used while Table 3.5 lists the complete testing schedule.

Table 3.4: Description of codes used for testing schedule

Code	Description
LE	Low compactive effort
HE	High compactive effort
SS	Sample of sand-sand
PS	Sample of sand-plastic
C50	Cape Flats sand at a confining pressure of 50 kPa
C100	Cape Flats sand at a confining pressure of 100 kPa
C200	Cape Flats sand at a confining pressure of 200 kPa
C300	Cape Flats sand at a confining pressure of 300 kPa
C400	Cape Flats sand at a confining pressure of 400 kPa
R100	Cape Flats sand at a confining pressure of 100 kPa for repeatability purposes
X_i	Plastic concentration: X_i1 = 0.1 %, X_i 2 = 0.2 % and X_i 3 = 0.3 %
L_i	Plastic strip length: L_i1 = 7.5 mm, L_i2 = 15 mm and L_i3 = 30 mm. W_i, Width = 6 mm

Table 3.5: Triaxial testing schedule for Cape Flats sand

Test	Materials	Parameter	Confining pressure	Test number	Test number
Sand–sand	Cape Flats sand	Repeatability	100	LE/SS/R100_1	HE/SS/R100_1
			100	LE/SS/R100_2	HE/SS/R100_2
			100	LE/SS/R100_3	HE/SS/R100_3
Sand–sand	Cape Flats sand	Control	50	LE/SS/C50	HE/SS/C50
			100	LE/SS/C100	HE/SS/C100
			200	LE/SS/C200	HE/SS/C200
			300	LE/SS/C300	HE/SS/C300
			400	LE/SS/C400	HE/SS/C400
Sand–polyethylene	Cape Flats sand–polyethylene	Strip length	50	LE/PS/X_i1/L_i1/C50	HE/PS/X_i1/L_i1/C50
			100	LE/PS/X_i1/L_i1/C100	HE/PS/X_i1/L_i1/C100
			200	LE/PS/X_i1L_i1/C200	HE/PS/X_i1L_i1/C200
			300	LE/PS/X_i1/L_i1/C300	HE/PS/X_i1/L_i1/C300
			400	LE/PS/X_i1/L_i1/C400	HE/PS/X_i1/L_i1/C400
			50	LE/PS/X_i1/L_i2/C50	HE/PS/X_i1/L_i2/C50
			100	LE/PS/X_i1/L_i2/C100	HE/PS/X_i1/L_i2/C100
			200	LE/PS/X_i1/L_i2/C200	HE/PS/X_i1/L_i2/C200
			300	LE/PS/X_i1/L_i2/C300	HE/PS/X_i1/L_i2/C300
			400	LE/PS/X_i1/L_i2/C400	HE/PS/X_i1/L_i2/C400
			50	LE/PS/X_i1/L_i3/C50	HE/PS/X_i1/L_i3/C50
			100	LE/PS/X_i1/L_i3/C100	HE/PS/X_i1/L_i3/C100
			200	LE/PS/X_i1/L_i3/C200	HE/PS/X_i1/L_i3/C200
			300	LE/PS/X_i1/L_i3/C300	HE/PS/X_i1/L_i3/C300
			400	LE/PS/X_i1/L_i3/C400	HE/PS/X_i1/L_i3/C400
	Cape Flats sand–polyethylene	Strip concentration	50	LE/SP/X_i2/L_i1/C50	HE/SP/X_i2/L_i1/C50
			100	LE/SP/X_i2/L_i1/C100	HE/SP/X_i2/L_i1/C100
			200	LE/SP/X_i2/L_i1/C200	HE/SP/X_i2/L_i1/C200
			300	LE/SP/X_i2/L_i1/C300	HE/SP/X_i2/L_i1/C300
			400	LE/SP/X_i2/L_i1/C400	HE/SP/X_i2/L_i1/C400
			50	LE/SP/X_i3/L_i1/C50	HE/SP/X_i3/L_i1/C50
			100	LE/SP/X_i3/L_i1/C100	HE/SP/X_i3/L_i1/C100
			200	LE/SP/X_i3/L_i1/C200	HE/SP/X_i3/L_i1/C200
			300	LE/SP/X_i3/L_i1/C300	HE/SP/X_i3/L_i1/C300
			400	LE/SP/X_i3/L_i1/C400	HE/SP/X_i3/L_i1/C400

3.4 Repeatability

To verify the repeatability of test results from the testing procedures and equipment, tests were carried out on different but identical specimens. Three tests were conducted on Cape Flats sand at 100 kPa confining stress, and a further three tests conducted on Cape Flats sand reinforced with 0.1 % plastic content with 7.5 mm strips at 200 kPa confining stress. All the tests were conducted in a dry state and the results obtained are presented in Chapter 4.

3.5 Quality Assurance

To ensure repeatability and reliability of all results, certain quality control measures were employed as part of all test procedures. These quality assurance measures guaranteed experimental procedures followed during testing produced repeatable and comparable results. The various aspects included:

i. New plastic strips were used for each test. The strips were also checked to eliminate geometric non-compliance and physical deformations,
ii. No sand was reused in any of the tests to avoid influencing the results since the soil fabric was likely to change during shearing,
iii. Five control and three repeatability tests each on unreinforced sand, and three repeatability tests on reinforced sand were carried out. The results from these experiments formed the basis of the assumed repeatability of the tests,
iv. All tests were conducted in compliance with standard procedures for ASTM D7181-11 for global comparability of results,
v. The drop height of the hand tamper was measured after several tests to ensure the height was consistent throughout the experimental programme,
vi. All the apparatuses and equipment used during the study were checked, cleaned and correctly calibrated before start of the testing regime, and
vii. Sand used in the study was sourced from one quarry in Cape Town for consistency in sample characteristics.

3.6 Data Processing

This section provides details of the calculations used for data reduction in excel at the end of the triaxial tests. Some of the symbols and notations used are defined below:

$\boldsymbol{\sigma_v}$ = Total vertical stress,

$\boldsymbol{\sigma'_v}$ = Effective vertical stress,

$\boldsymbol{\sigma_h}$ = Total horizontal stress,

$\boldsymbol{\sigma'_h}$ = Effective horizontal stress,

$\boldsymbol{\sigma'_1}$ = Effective major principal stress at failure,

$\boldsymbol{\sigma'_3}$ = Effective minor principal stress at failure,

$\Delta\boldsymbol{\sigma_D}$ = Deviator (axial) stress, σ_1 - σ_3,

$\boldsymbol{c'}$ = Cohesion,

$\boldsymbol{\tau_i}$ = Instantaneous shear stress,

$\boldsymbol{\sigma_i}$ = Instantaneous normal stress,

$\boldsymbol{\tau_f}$ = Shear stress at failure,

$\boldsymbol{\sigma_f}$ = Normal stress at failure,

$\boldsymbol{ABC}$ = Mohr-Coulomb failure envelope,

$\boldsymbol{DEF}, \boldsymbol{K_f}$ = Modified Mohr-Coulomb failure envelope.

A typical Mohr circle at failure used for data analysis is shown in Figure 3.11.

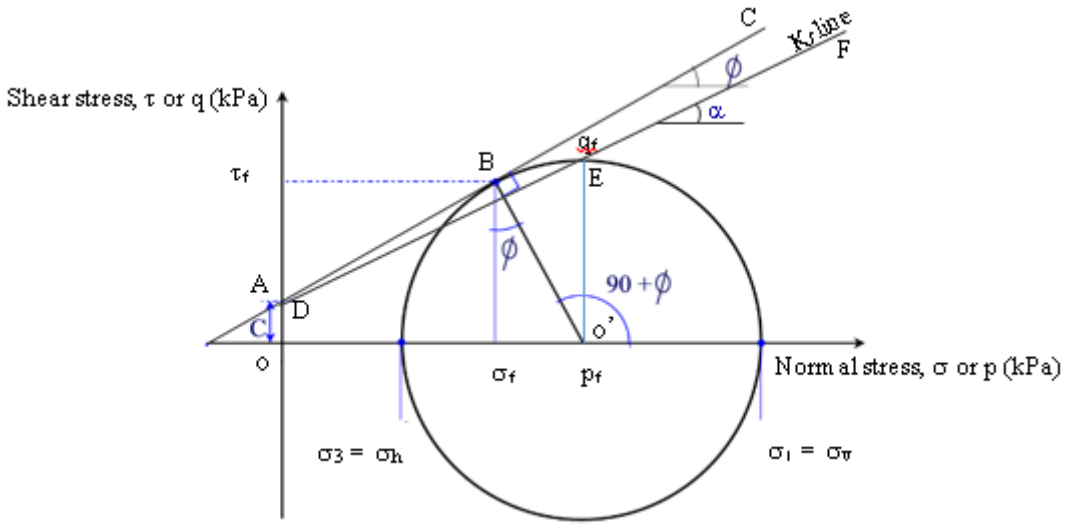

Figure 3.11: Typical Mohr circle at failure

The calculations of different shear strength parameters are shown below:

$$\boldsymbol{\tau_i = \left(\frac{\sigma'_1 - \sigma'_3}{2}\right) \sin 2\theta} \qquad \textbf{Equation 3.4}$$

$$\sigma_i = \left(\frac{\sigma'_1+\sigma'_3}{2}\right) + \left(\frac{\sigma'_1-\sigma'_3}{2}\right)\sin 2\theta \qquad \textbf{Equation 3.5}$$

Where: $\theta = \left(45^\circ + \frac{\emptyset'}{2}\right)$

$$\sigma_f = \left(\frac{\sigma'_1+\sigma'_3}{2}\right) + \left(\frac{\sigma'_1-\sigma'_3}{2}\right)\sin 2\theta \qquad \textbf{Equation 3.6}$$

$$\tau_f = \left(\frac{\sigma'_1-\sigma'_3}{2}\right)\sin 2\theta \qquad \textbf{Equation 3.7}$$

Where: $\theta = 45^\circ$ at maximum shear for failure to occur.

$$sin\phi' = \frac{\left(\frac{\sigma'_1-\sigma'_3}{2}\right)}{\left(\frac{\sigma'_1+\sigma'_3}{2}\right)} = \frac{\sigma'_1-\sigma'_3}{\sigma'_1+\sigma'_3} \qquad \textbf{Equation 3.8}$$

Thus: $\phi' = sin^{-1}\left(\frac{\sigma'_1-\sigma'_3}{\sigma'_1+\sigma'_3}\right)$

Stress-strain curves were presented from which Mohr's circles were plotted for the results obtained on the "τ-σ" coordinate axis representing the conventional Mohr-Coulomb failure envelopes.

4 RESULTS AND DISCUSSIONS

4.1 Introduction

In this chapter, all the results of the triaxial compression tests performed on Cape Flats reinforced with HDPE plastic are presented and discussed. The influence of varying strip contents and lengths, confining pressures and compactive efforts on the mechanical and shear strength behaviour of the soil are examined.

4.2 Repeatability Tests

According to ASTM E177-14, it is important to determine the repeatability of test results obtained using a standard ASTM test method and apparatus to check the consistency of the testing process. To replicate independent test results, identical test specimens were examined using the same test method, laboratory procedures, and apparatus.

In the study, two tests series were performed on unreinforced sand at low and high compactive effort (equivalent to 280 kN-m/m^3 and 589 kN-m/m^3) respectively at 100 kPa confining pressure for soil samples, and at 200 kPa for soil-plastic composite samples.

4.2.1 Unreinforced Soil Samples

Figure 4.1 and Figure 4.2 present the repeated test results on Cape Flats sand. The deviator stress (difference between the effective major principal stress, σ_1, and effective minor principal stress, σ_3) were measured from the respective repeatability tests and plotted against the corresponding vertical strains.

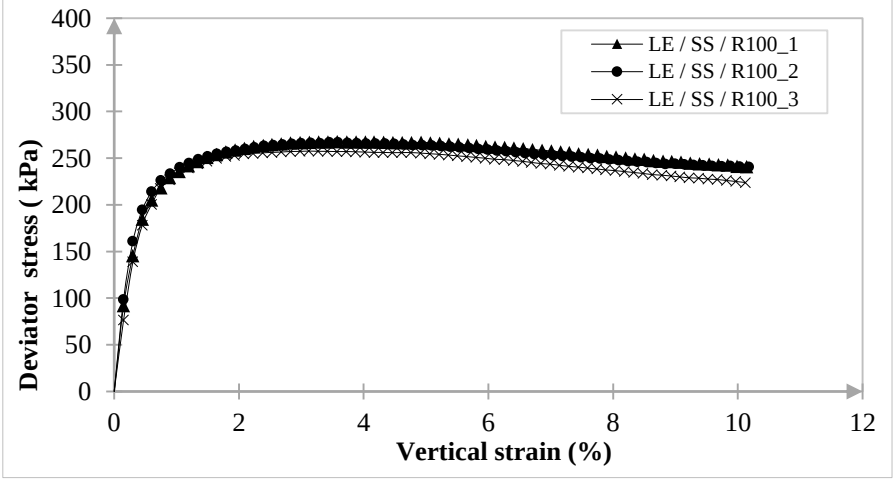

Figure 4.1: Deviator stress versus vertical strain curves at low compactive effort for soil only

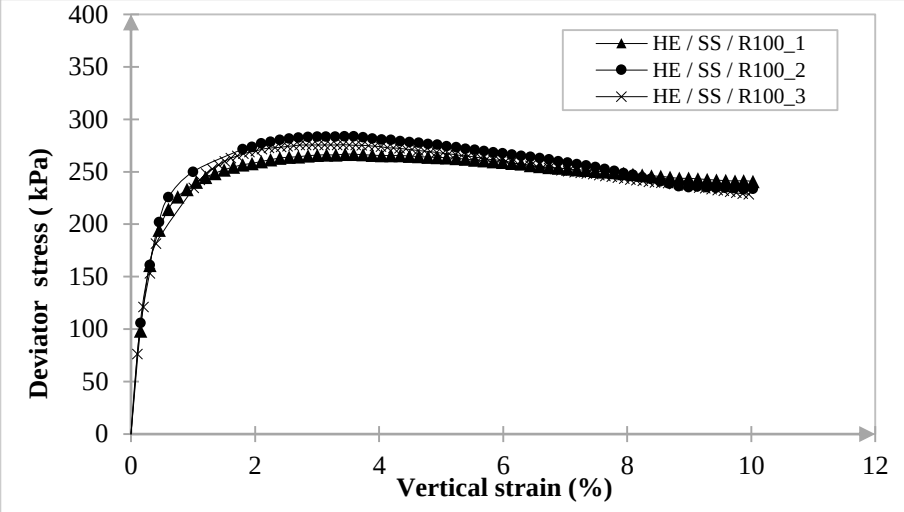

Figure 4.2: Deviator stress versus vertical strain curves at high compactive effort for soil only

From Figure 4.1 and Figure 4.2, the stress-strain response of the soil reported a similar and consistent trend in the shapes of the curves and close peak and ultimate stress values. A summary of the peak and ultimate shear stresses of each of the 6 repeated tests is shown in Table 4.1.

Table 4.1: Summary of peak and ultimate stress repeatability results on unreinforced soil

Test code	Peak stress (kPa)	Mean stress (kPa)	Deviation (%)	ultimate stress (kPa)	Mean stress (kPa)	Deviation (%)
LE/SS/R100_1	267.37	263.85	1.32	240.59	235.29	2.20
LE/SS/R100_2	266.77		1.09	240.45		2.15
LE/SS/R100_3	257.41		-2.44	224.83		-4.65
HE/SS/R100_1	266.78	275.48	-3.26	240.76	241.09	-0.13
HE/SS/R100_2	283.71		2.90	233.54		-3.23
HE/SS/R100_3	275.94		0.17	248.98		3.16

From Table 4.1, the mean peak shear stress at low and high compactive effort was 263.85 kPa and 275.48 kPa respectively. Likewise, the mean ultimate shear stress at low and high compactive effort was 235.29 kPa and 241.09 kPa respectively. The deviations from the mean peak and ultimate shear stresses were computed and found not to exceed 5 %, that is, the test results occurred within 95 % standard deviation as specified in ASTM E177. The consistency in the test results indicates that the testing procedures and equipment employed were repeatable within the laboratory setting. Based on the above results it was postulated that all the tests on unreinforced soil would be repeatable.

4.2.2 Reinforced Soil Samples

Figure 4.3 and Figure 4.4 present the deviator stress-vertical strain plots from repeatability tests on soil-plastic composites.

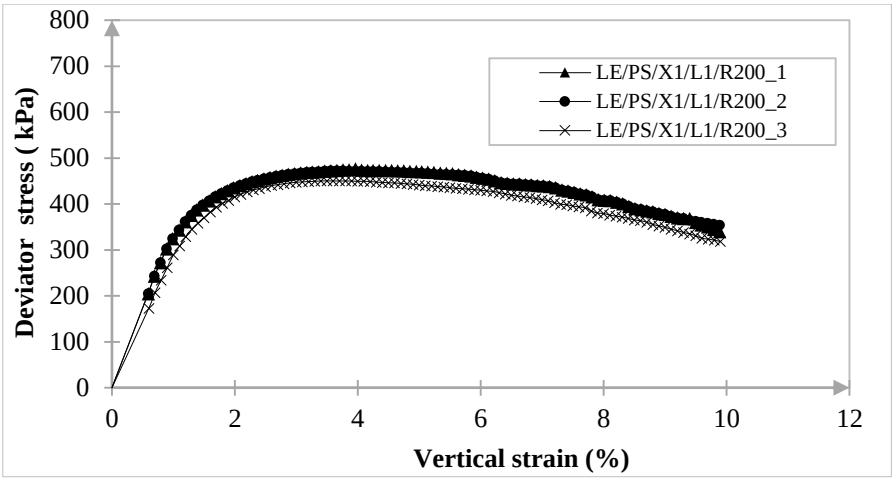

Figure 4.3: Deviator stress versus vertical strain curves at high compactive effort for soil-plastic composites

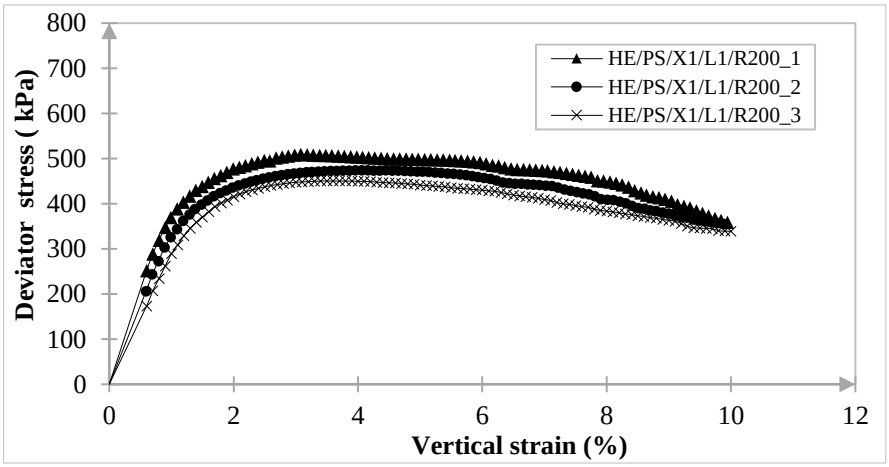

Figure 4.4: Deviator stress versus vertical strain curves at high compactive effort for soil-plastic composites

The stress-strain response of the soil showed comparable test results with close peak and ultimate shear stress values, as illustrated in Figure 4.3 and Figure 4.4. A summary of the peak and ultimate shear stresses of each of the 6 repeated tests on soil-plastic composites is shown in Table 4.2. The mean stresses and deviations from the mean are also presented.

Table 4.2: Summary of peak and ultimate stress repeatability results on reinforced soil

Test code	Peak stress (kPa)	Mean stress (kPa)	Deviation (%)	ultimate stress (kPa)	Mean stress (kPa)	Deviation (%)
LE/PS/X_i1/L_i1/R200_1	474.65	465.94	1.83	340.25	341.43	-0.35
LE/PS/X_i1/L_i1/R200_2	472.79		1.44	354.25		3.61
LE/PS/X_i1/L_i1/R200_3	450.37		-3.46	329.78		-3.53
HE/PS/X_i1/L_i1/R200_1	498.21	475.75	4.72	358.72	350.58	2.27
HE/PS/X_i1/L_i1/R200_2	473.66		-0.44	354.25		1.04
HE/PS/X_i1/L_i1/R200_3	455.37		-4.48	338.78		-3.48

From Table 4.2, the mean peak shear stress at low and high compactive effort was 465.94 kPa and 475.75 kPa respectively. In comparison, the mean ultimate shear stress at low and high compactive effort was 341.43 kPa and 350.58 kPa respectively. The deviations from the mean peak and ultimate shear stresses were calculated and found not to be greater than 5 %, that is, the test results occurred within 95 % standard deviation as specified in ASTM E177. It was anticipated that inclusion of plastics would also realise the same tendency of reliable results for all the other tests.

4.3 Triaxial Compression Test Results

The triaxial compression test results are presented and discussed in the form of deviator stress-axial strain curves and shear stress-normal stress relationships. Moreover, a practical example on slope stability analysis is presented utilising the findings of the study.

4.3.1 Deviator stress versus vertical strain relationship

Effect of plastic content on deviator stress

Figure 4.5 shows the deviator stress-axial strain relationships of unreinforced and reinforced Cape Flats sand with varying plastic content. Soil samples were reinforced with plastic strips of 7.5 mm length, concentrations of 0 %, 0.1 %, 0.2 %, and 0.3 % by dry weight of soil, and tested under confining pressures of 50 kPa, 100 kPa, 200 kPa, 300 kPa, and 400 kPa. Consequently, Figure 4.5 (a) to Figure 4.5 (e) have four curves, each representing the different plastic contents for the varied confining pressures

Generally, it can be observed from Figure 4.5 that the inclusion of plastic strips in soil increased its deviator stress. Moreover, it led to the reduction in the post-peak strength loss at 10 % strain

in the reinforced sand compared to the unreinforced sand increased. The above results were reported for all the confining stresses as shown in Figure 4.5. The results are consistent with studies conducted by previous researchers (Gray & Al-Refeai, 1986; Maher & Gray, 1990; Dutta & Rao, 2007).

The peak deviator stress improved with addition of plastic strips up to a limiting value of 0.1 % beyond which further increase in concentration resulted in reduction of the peak deviator stress, Figure 4.5. The increase in the peak deviator stress could be attributed to the greater physical interaction between the soil. The soil particles adhere and interlock tightly which results in increased frictional resistance at the soil-plastic interface. The soil is thus able to bear tensile stresses which lead to improvement in the shear strength and mechanical behaviour. Additionally, the post-peak stress of reinforced samples improved and the loss of shear strength at maximum strain tested became more limited, as observed in Figure 4.5.

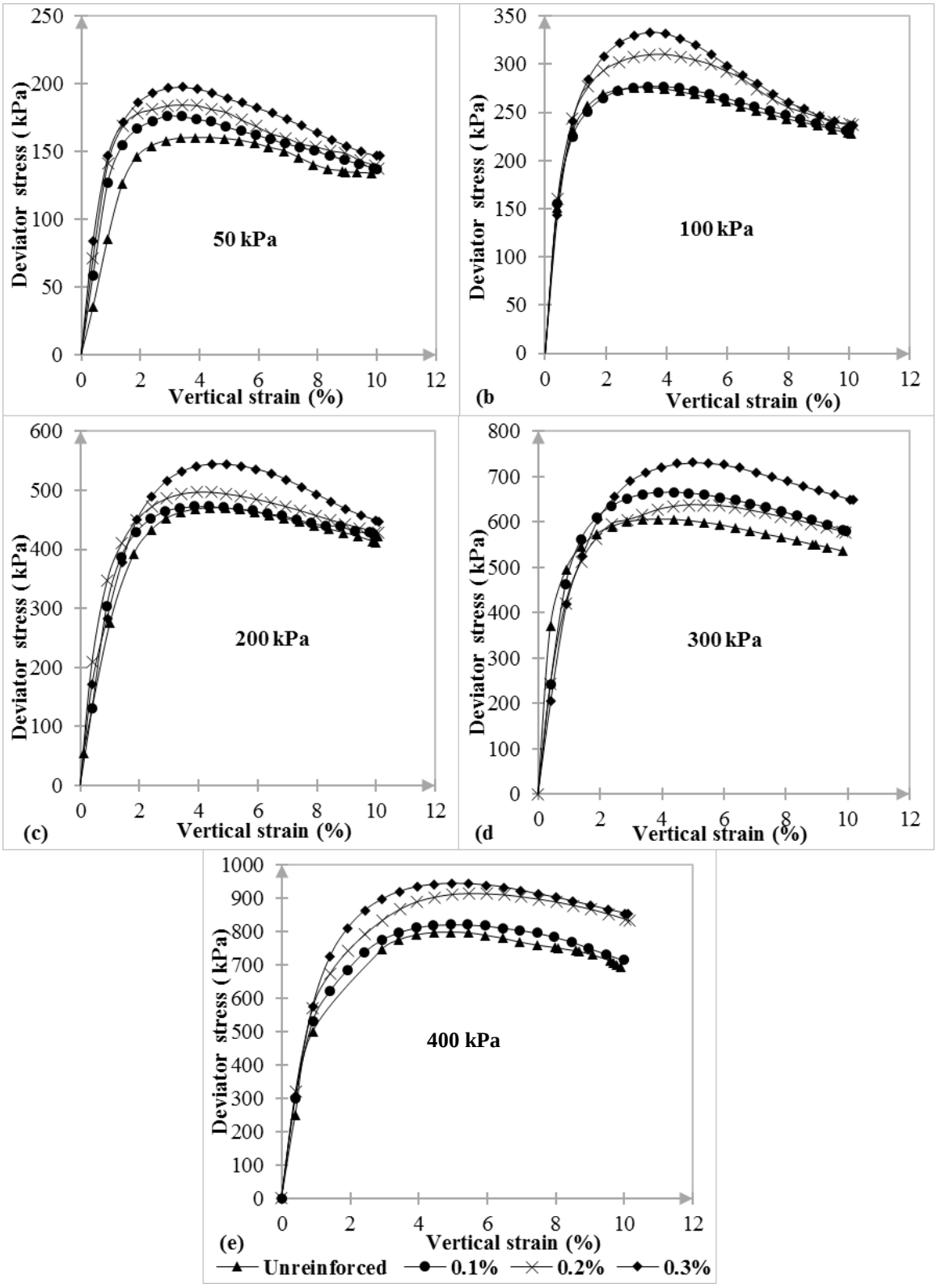

Figure 4.5: Stress-strain behaviour of the sand with varying plastic content from triaxial tests

In Figure 4.6, the peak deviator stresses measured from the different test configurations were plotted against the plastic content for confining pressures ranging from 50 kPa to 400 kPa. The plots demonstrate the enhancement in peak deviator stress with varying plastic content. The

effect was more pronounced at higher confining pressures. The greatest increase in the shear stress was reported at 0.1 % plastic content.

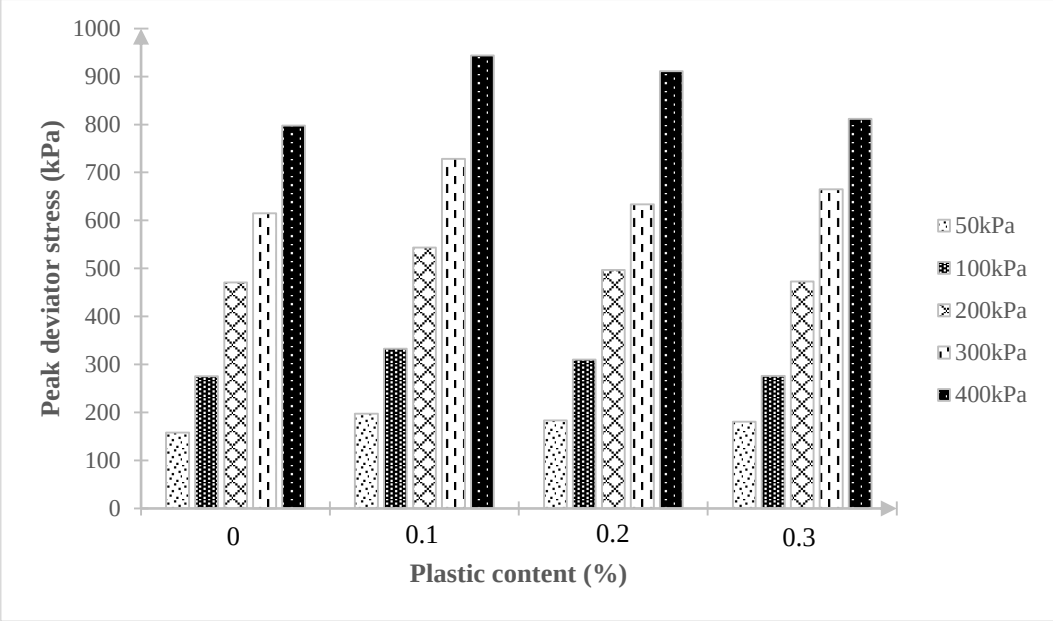

Figure 4.6: The effect of plastic content on the peak deviator stress

The percentage improvement in the peak deviator stress was shown by utilising a dimensionless parameter referred to as the peak strength ratio which is calculated by dividing the peak strength of the reinforced sample by the peak strength of the unreinforced sample. Table 4.3 shows the peak strength ratio of the triaxial specimens reinforced with plastic strip concentrations of 0.1 % to 0.3 % for tests conducted at confining stresses of 50 kPa to 400 kPa. The analysis indicates that addition of plastics at a concentration of 0.1 % realised the highest peak strength ratio for all the confining pressures. For instance, at 50 kPa confining pressure, the value ranges from 1.15 for 0.3 % plastic content to 1.25 for 0.1 % plastic content. This represents a 15 % and 25 % improvement in the peak deviator stress respectively upon insertion of HDPE strips in the soil. At 100 kPa confining stress, a peak strength ratio of 1.21 and 1.00 respectively for plastic contents of 0.1 % and 0.3 % respectively representing enhancements of 21 % upon plastic inclusion of 0.1 % concentration. For 400 kPa confining pressure peak strength ratios of 1.18 for 0.1 % concentration and 1.02 for 0.3 % plastic content were reported. This was an equivalent of 18 % upon addition of 0.1 % plastic material.

Table 4.3: Influence of confining pressure and plastic content on the peak strength ratio

Confining Pressure (kPa)	Peak strength ratio		
	Plastic content		
	0.1%	0.2%	0.3%
50	1.25	1.16	1.15
100	1.21	1.13	1.00
200	1.16	1.06	1.00
300	1.18	1.03	1.08
400	1.18	1.14	1.02

A summary of the peak deviator stresses, vertical strains and ultimate stresses for the triaxial tests conducted at varying plastic content and confining pressures are presented in Appendix C. The results demonstrate the improvement in peak and ultimate strength as well as an increase in vertical strain.

Effect of plastic strip length on deviator stress

The effect of plastic strip length on the stress-strain behaviour of Cape Flats sand is illustrated in Figure 4.7. Plastic strips of 7.5 mm, 15 mm and 30 mm length, were added to the soil specimens at a concentration of 0.1 % and tested under confining pressures of 50 kPa, 100 kPa, 200 kPa, 300 kPa, and 400 kPa. In each of the plots, Figure 4.7 (a) to Figure 4.7 (e), measurements of deviator stress were plotted against vertical strains for the different plastic strip lengths under the specified confining pressures.

As shown in Figure 4.7, specimens reinforced with plastic strips of various lengths exhibited higher peak stresses, and ultimate stresses at maximum strain of 10 %, and strains at failure compared to unreinforced specimens. Reinforced soil specimens with 15 mm long plastics reported the highest peak deviator stress for all the confining pressures. Moreover, increasing the plastic strip length resulted in reductions in the loss of the ultimate strength at a strain of 10 % of the reinforced specimens.

The improvement in the peak deviator stress may be attributed to the plastic reinforcement which resulted in greater interface resisting stresses in the composite mass. Furthermore, longer plastics are less likely to cause slippage due to the soil-plastic interaction which enable the soil to bear tensile stress. Consequently, this results in improved shear strength and mechanical behaviour of the reinforced soil. However, reinforced sand with 30 mm strips reported the lowest peak deviator stresses for all the confining stresses compared to the other lengths.

The enhancement in the peak and ultimate strength of the unreinforced and reinforced soil specimens increased linearly with the maximum value reported at lengths of 15 mm reinforcement beyond which no significant effect is observed. The greatest deviator stresses were recorded at the 400 kPa confining pressure, as illustrated in Figure 4.7. It is possible that the application of higher confining stresses resulted in greater interlock between soil particles which led to improved shear strength of the reinforced soil (Choudhary et al., 2010; Falorca & Pinto, 2011).

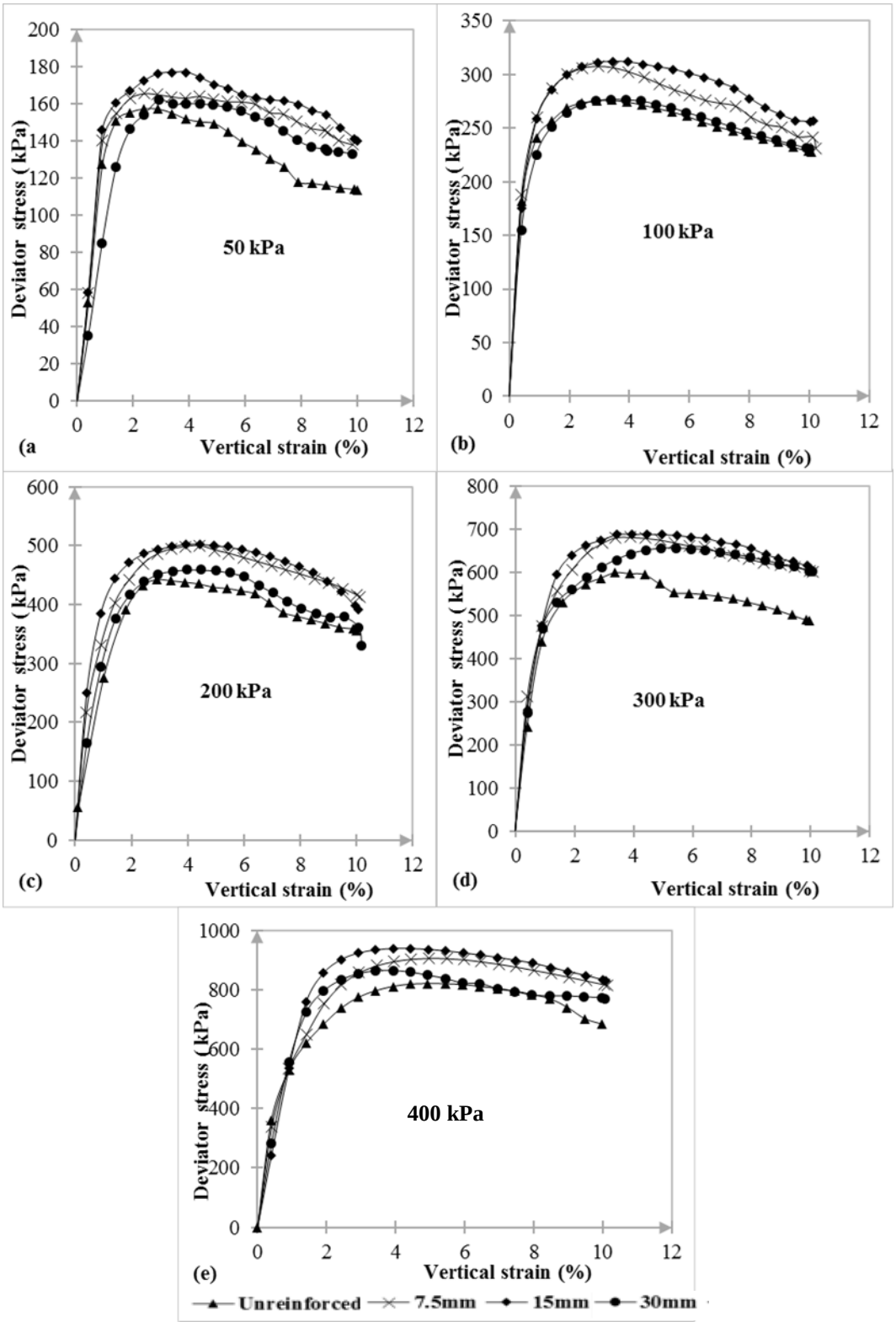

Figure 4.7: Stress-strain behaviour of the sand with varying plastic strip length from triaxial tests

The peak deviator stresses for all the soil responses were plotted for each test conducted at the varied confining stresses on specimens of 7.5 mm to 30 mm lengths, as shown in Figure 4.8. Soil samples reinforced with 15 mm plastic material reported the highest values of peak shear stress. It can also be observed that the peak deviator increased linearly with the confining stress for all testing variables.

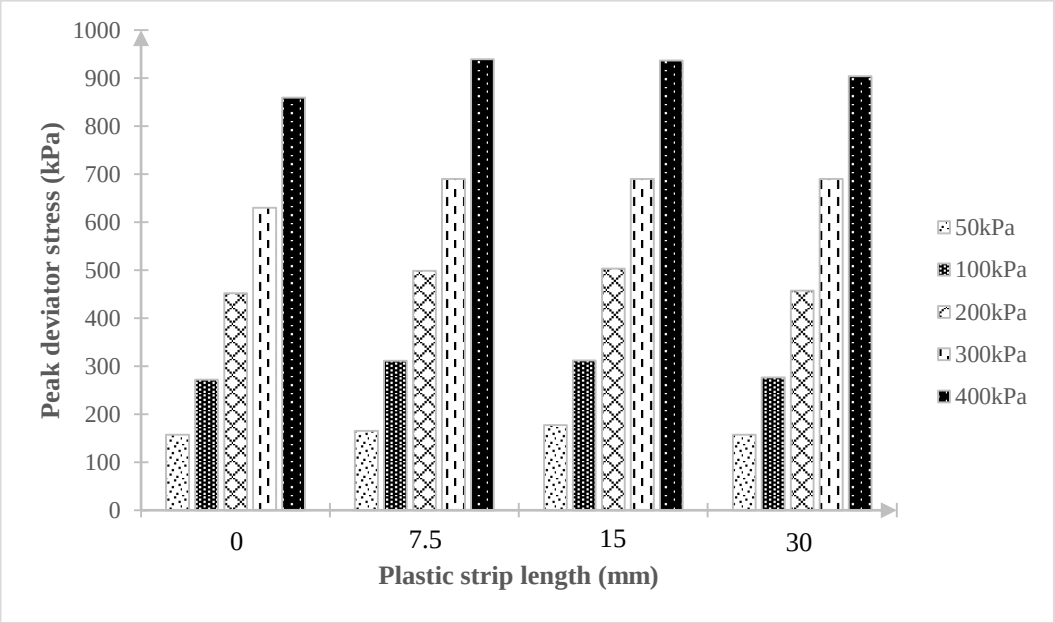

Figure 4.8: The effect of plastic strip length on the peak deviator stress

Table 4.4 illustrates the improvement in the peak strength ratio of the reinforced samples on variation of the HDPE strip length and confining stress. It can be observed that plastics of 15 mm length reported the maximum value of peak strength ratio compared to the other reinforcement lengths. Further, the relative increase in the peak strength ratio was larger at low confining pressures (50 kPa). For example, for soil specimens reinforced with 15 mm plastics, a peak strength ratio of 1.13 and 1.09 was obtained for tests conducted at 50 kPa and 400 kPa respectively. This represented a 13 % and 9 % enhancement respectively of the peak shear stress.

Upon comparison of the values of peak strength ratio due to plastic content (Table 4.3), and plastic strip length (Table 4.4), it is evident that the effect of varying concentration had a greater contribution to strengthening of the soil than the variation of the length. This could be attributed to higher interface shear stresses due to increase in plastic content, whereas increasing the strip might have led entanglement of plastic strips which led to reduction in shear stresses. The

highest peak strength ratio was obtained to be 1.25 and 1.15 from Table 4.3 and Table 4.4 respectively.

Table 4.4: Influence of confining pressure and plastic strip length on the peak strength ratio

Confining Pressure (kPa)	Peak strength ratio		
	Plastic strip length		
	7.5 mm	15 mm	30 mm
50	1.05	1.13	1.00
100	1.14	1.15	1.02
200	1.10	1.11	1.01
300	1.10	1.10	1.10
400	1.09	1.09	1.05

A summary of the triaxial compression tests conducted under varying confining pressure and plastic strip length is presented in Appendix C.

4.3.2 Shear stress-normal stress relationships of soil-plastic composites

For each triaxial test, the peak deviator stresses (or maximum shear stress) from graphs in section 4.3.1 were plotted against the respective normal stresses as shown in Figure 4.9 and Figure 4.10. The effective major principal stress, σ'_1, and effective minor principal stress, σ'_3, at failure for each confining pressure were then used to draw Mohr's circles. The best straight line fitted as a common tangent to the limiting circles corresponding to five confining pressures (50 kPa, 100 kPa, 200 kPa, 300 kPa and 400 kPa) defined the Mohr-Coulomb failure envelope. Consequently, the intercept on the vertical axis defines the apparent cohesion, *c'*, while the gradient of the line gives the internal friction angle, $\emptyset'$, of the soil.

Figure 4.9 and Figure 4.10 present the Mohr-Coulomb failure envelopes for the triaxial shear tests conducted at low and high compactive efforts (equivalent to 280 kN-m/m^3 and 589 kN-m/m^3) respectively. In each graph, a specific testing variable was varied; plastic strips of varying concentrations (0 % to 0.3 % by weight of dry soil) and length (7.5 mm to 30 mm) were added to the soil and samples compacted to average relative densities of 52 % and 57 %. Triaxial compression tests were then performed at confining stresses of 50 kPa to 400 kPa. Additionally, a maximum vertical strain of 10 % was adopted for all the tests because beyond this threshold value strain hardening was observed for trial tests conducted before the testing regime was undertaken.

The summary of triaxial shear test results from Figure 4.9 and Figure 4.10 are presented in Table 4.5 and Table 4.6 respectively. The corresponding *c'* and ∅′ values were recorded for soil and soil-plastic composites. A linear failure envelope was observed in tests on sand specimens as illustrated in Figure 4.9 (a) and Figure 4.10 (a). In comparison, triaxial compression tests on soil specimens with HDPE strip inclusions realised a bilinear failure envelope, as seen in Figure 4.9 (b) to (f), and Figure 4.10 (b) to Figure 4.10 (f). Consequently, in Table 4.5 and Table 4.6, *c'* and ∅′ parameters were reported at lower confining stress levels (50 kPa to 300 kPa), and at higher stress levels (300 kPa to 400 kPa). The critical confining stress was different for all the tests on varying plastic parameters and was observed to be in the range of 300 kPa to 400 kPa.

The results in Table 4.5 and Table 4.6 were used in the discussion on the effect of confining pressure, plastic content and plastic strip length on the shear strength parameters especially the friction angle and cohesion. Moreover, Table 4.5 and Table 4.6 were used to investigate the influence of compactive effort on the shear strength behaviour of the soil.

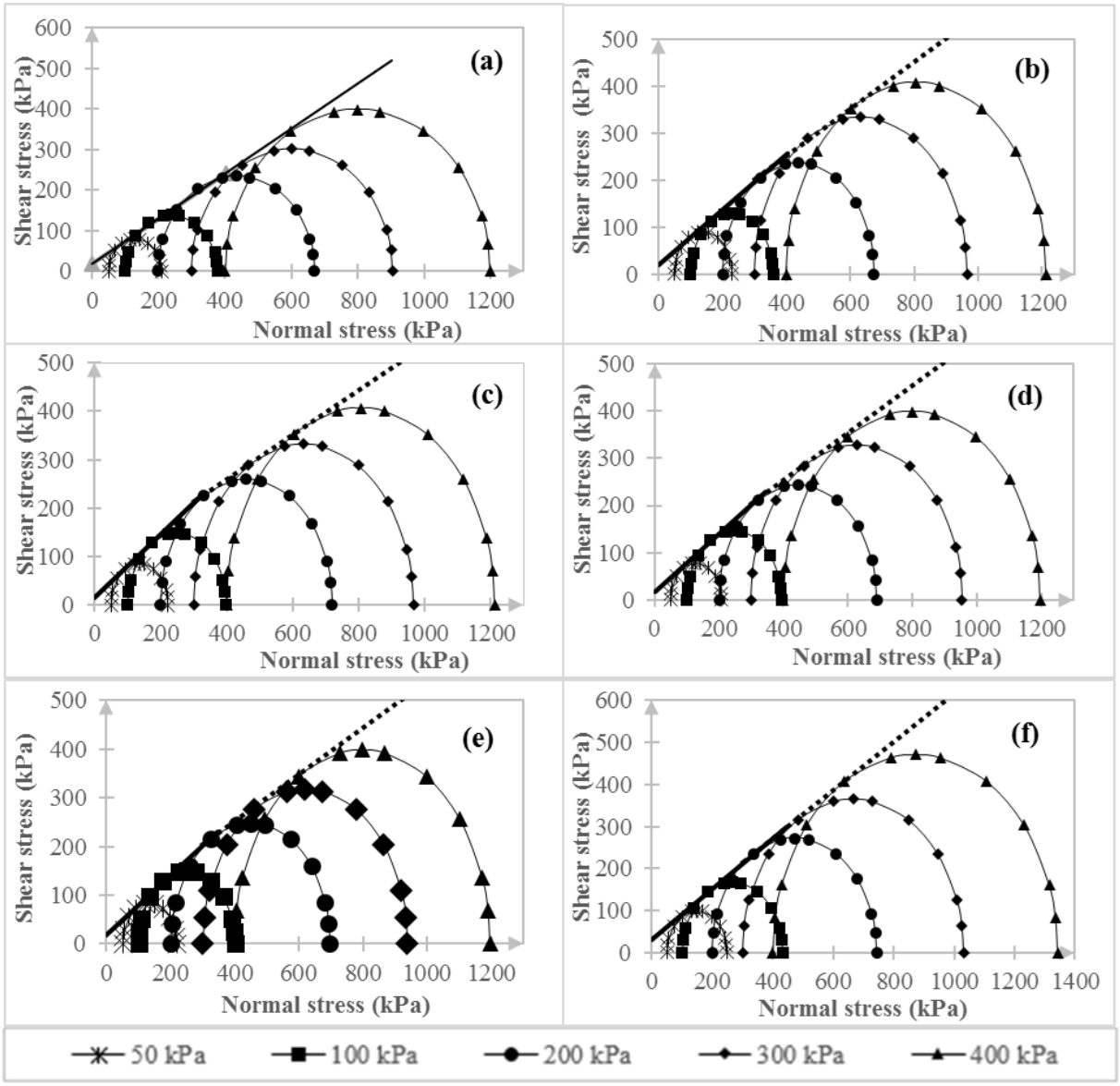

Figure 4.9: Shear strength envelopes from triaxial tests (*D_r=52%, E=280kN-m/m^3, and W_i=6 mm constant)*: a) Unreinforced soil (b) Plastic-reinforced soil (*X_i=0.1% and L_i=7.5mm),* c) Plastic-reinforced soil (*X_i =0.1% and L_i=15mm),* d) Plastic-reinforced soil (*X_i =0.1%, and L_i=3 mm),* e) Plastic-reinforced soil (*X_i =0.2% and L_i=7.5mm),* and f) Plastic-reinforced soil (*X_i =0.3% and L_i=7.5mm)*

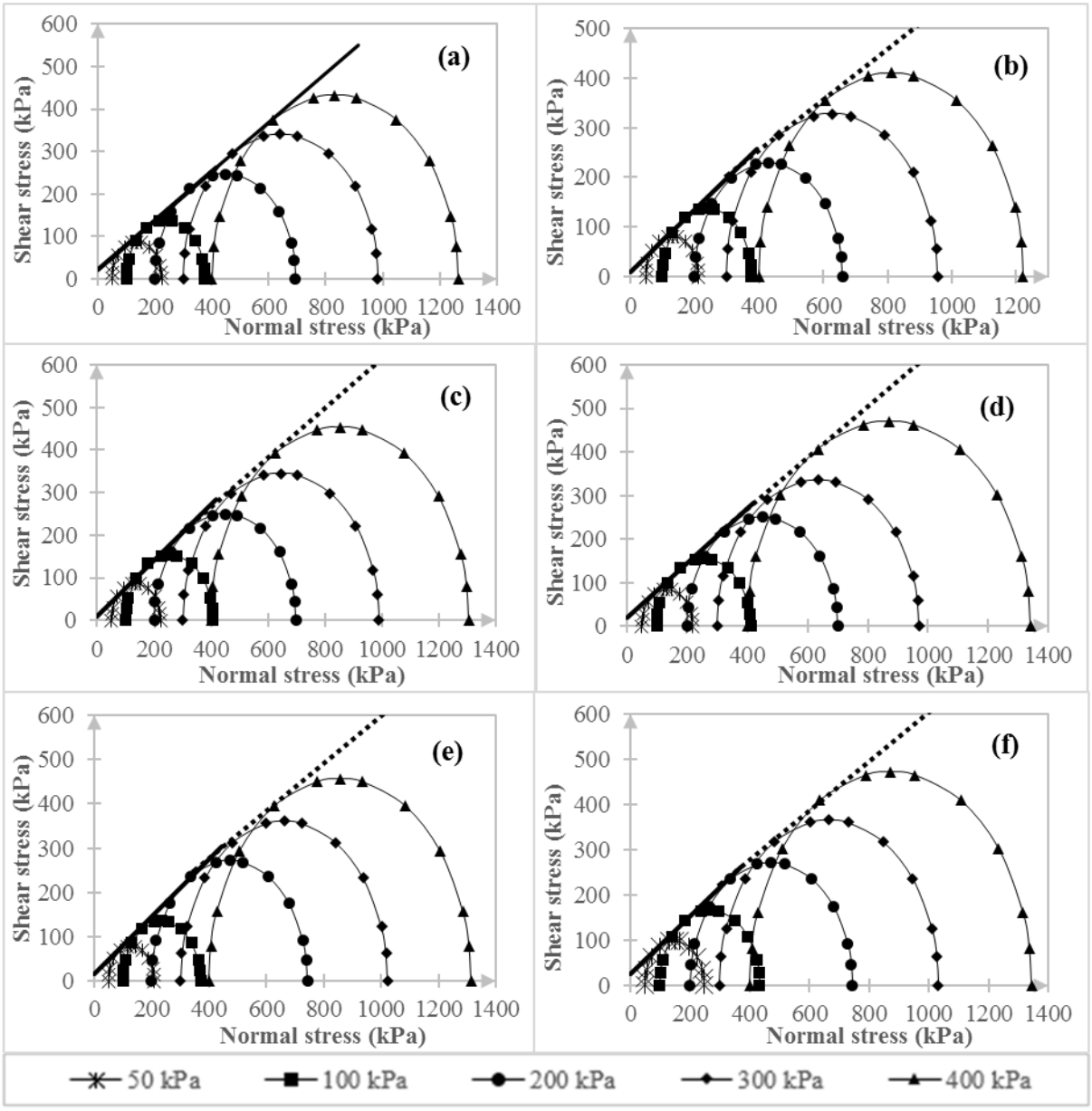

Figure 4.10: Shear strength envelopes from triaxial tests (D_r =57%, E=589kN-m/m^3 and W_i=6mm constant): a) Unreinforced soil (b) Plastic-reinforced soil (X_i=0.1% and L_i=7.5mm), c) Plastic-reinforced soil (X_i=0.1% and L_i=15mm), d) Plastic-reinforced soil (X_i=0.1%, and L_i=30mm), e) Plastic-reinforced soil (X_i=0.2% and L_i=7.5mm), and f) Plastic-reinforced soil (X_i=0.3% and L_i=7.5mm)

Table 4.5: Summary of peak shear strength results from triaxial compression tests at low compactive effort

Sample description	Applied confining pressure (kPa)	Lower stress level		Higher stress level	
		Friction angle, ∅′ (deg)	Apparent cohesion, c’ (kPa)	Friction angle, ∅′ (deg)	Apparent cohesion, c’ (kPa)
Unreinforced soil (D_r=52%)	50	∅′=29.0 and c’=19.0 (Linear failure envelope)			
	100				
	200				
	300				
	400				
Soil-plastic composite (D_r=52%, X_i=0.1%, W_i=6mm, and L_i=7.5mm)	50	30.5	19.5	26.5	52.5
	100				
	200				
	300				
	400				
Soil-plastic composite (D_r=52%, X_i=0.1%, W_i=6 mm, and L_i =15mm)	50	33.0	15.0	24.8	75.4
	100				
	200				
	300				
	400				
Soil-plastic composite (D_r=52%, X_i=0.1%, W_i=6 mm, and L_i=30mm)	50	31.5	17.0	26.6	52.6
	100				
	200				
	300				
	400				
Soil-plastic composite (D_r=52%, X_i=0.2%, W_i=6 mm, and L_i=7.5mm)	50	31.3	18.5	25.7	60.5
	100				
	200				
	300				
	400				
Soil-plastic composite (D_r=52%, X_i=0.3%, W_i=6 mm, and L_i=7.5mm)	50	31.1	30.8	29.9	42.6
	100				
	200				
	300				
	400				

Table 4.6: Summary of peak shear strength results from triaxial compression tests at high compactive effort

Sample description	Applied confining pressure (kPa)	Lower stress level		Higher stress level	
		Friction angle, ∅′ (deg)	Apparent cohesion, c’ (kPa)	Friction angle, ∅′ (deg)	Apparent cohesion, c’ (kPa)
Unreinforced soil (D_r=57%)	50	∅′=30.0 and c’=21.5 (Linear failure envelope)			
	100				
	200				
	300				
	400				
Soil-plastic composite (D_r=57%, X_i=0.1%, W_i=6mm, and L_i=7.5mm)	50	31.9	10.0	27.1	49.7
	100				
	200				
	300				
	400				
Soil-plastic composite (D_r=57%, X_i=0.1%, W_i=6 mm, and L_i =15mm)	50	33.2	9.0	30.1	33.8
	100				
	200				
	300				
	400				
Soil-plastic composite (D_r=57%, X_i=0.1%, W_i=6 mm, and L_i=30mm)	50	32.1	18.5	30.5	33.1
	100				
	200				
	300				
	400				
Soil-plastic composite (D_r=57%, X_i=0.2%, W_i=6 mm, and L_i=7.5mm)	50	32.9	16.0	28.4	59.1
	100				
	200				
	300				
	400				
Soil-plastic composite (D_r=57%, X_i=0.3%, W_i=6 mm, and L_i=7.5mm)	50	32.1	24.3	28.7	59.1
	100				
	200				
	300				
	400				

Effect of confining pressure

The effect of vertical confining stress is illustrated from the Mohr-Colomb failure envelopes in Figure 4.9, and from the shear strength parameters (c', $\emptyset'$) presented in Table 4.5. The envelopes are comparable to results reported by previous researchers (Maher & Gray, 1990; Benson & Khire, 1994; Consoli et al., 2002).

Based on the results, it can be observed that there exists a critical confining stress at which the failure envelope ceases to be linear for soil-plastic composites. Below this threshold stress, shear strength failure was governed by plastic slippage while beyond this confining pressure, failure was governed by the tensile strength or pull-out of the plastic strips (Gray & Ohashi, 1983; Gray & Al-Refeai, 1986; Maher & Gray, 1990; Benson & Khire, 1994). Maher & Gray (1990) indicate that the critical confining stress is influenced by the specific soil-plastic parameters including; plastic strip length, angular shape and gradation of Cape Flats sand. However, relatively no influence is attributed to the strip contents. This explains the clear deviation from the linear relationship in Figure 4.9 (b), Figure 4.9 (c) and Figure 4.9 (d) on varying the plastic strip length. However, variation of the plastic content as observed in Figure 4.9 (d) and Figure 4.9 (e) resulted in steeper slopes of the curve at higher stresses compared to varying the strip length. Moreover, the bilinear relationship is attributed to the angular shape of the sand (Maher & Gray, 1990).

The critical confining pressure was found to be in the range of 300 kPa to 400 kPa as observed in Figure 4.9, and it improved with increasing plastic strip length which is consistent with test results reported from previous research (Gray & Ohashi, 1983; Maher & Gray, 1990; Consoli et al., 2002).

In the case of unreinforced soil, a linear failure envelope was observed, as shown in Figure 4.9 (a). From the graph, the strength parameters obtained were c' = 19.0 kPa and $\emptyset' = 29.0^{o}$. Likewise, the bilinear shear strength values for the soil reinforced with optimum plastic strip length were obtained as c' = 15.0 kPa and $\emptyset' = 33.0^{o}$ at lower stress levels and c' = 75.4 kPa and $\emptyset' = 24.8^{o}$ at higher stress levels. The large cohesion value for unreinforced dry sand could probably be due to sample preparation techniques (Della et al., 2015), and the interlocking of sand grains on increasing the confining stress. It can be observed that an increase in the confining stress resulted in an increase in the apparent cohesion and reduction in the friction angle of the soil beyond the critical stress level. For all results, an increase in the frictional resistance angle at lower confining stresses was observed upon addition of plastic material.

Furthermore, the failure envelope for reinforced sand at normal stresses greater than the critical confining stress was almost parallel to that of the unreinforced sand, as observed in previous studies (e.g., Maher & Gray, 1990).

Effect of plastic content on strength parameters

In Figure 4.11, the results of the peak friction angle and cohesion in relation to the plastic concentration are presented. According to the results, the peak friction angle increases linearly to the reinforcement up to a limiting content at higher concentrations. A 0.2 % strip concentration added to the soil increased the angle of internal friction from 29^{o} to 31.3^{o} representing an enhancement of 8 %. In contrast, the cohesion remained approximately constant up to a concentration of 0.2 % beyond which it improved significantly. The soil-plastic composite had a cohesion component of 30.8 kPa compared 19 kPa for the unreinforced soil. This is equivalent to a 62 % increase. It is evident the inclusion of the plastic material had a significant influence on the strength parameters of the soil-plastic composite.

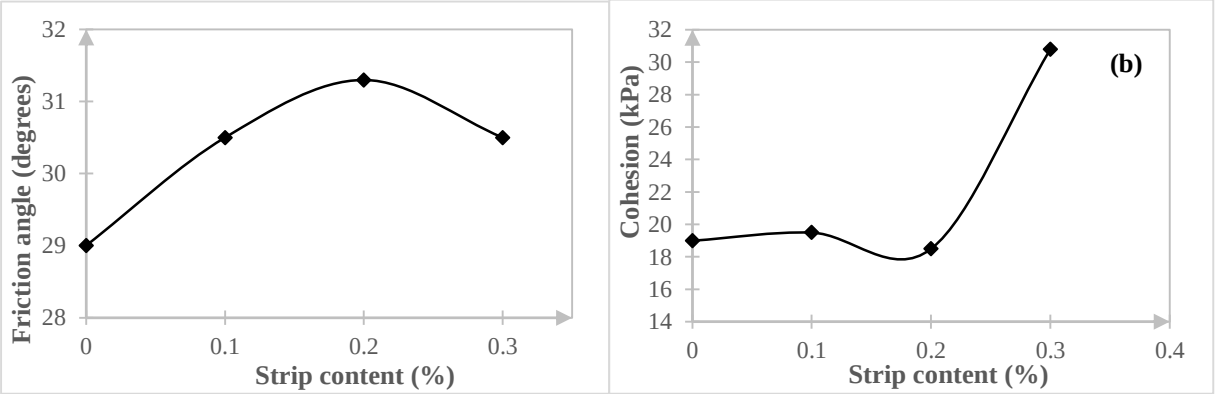

Figure 4.11: Variation of friction angle and cohesion with plastic strip content

Effect of plastic strip length on peak strength parameters

Figure 4.12 presents the relationship between the plastic strip length and peak strength parameters. Increasing the strip length with the width kept constant at 6 mm from 0 mm to 15 mm caused an increase in the internal soil friction angle from 29^{o} to 33^{o}. This represents approximately 14 % improvement. The cohesion values reported mixed results compared to inclusion of plastic material at different amounts. The cohesion reduced from 19 kPa to 17 kPa on varying the length from 0 mm to 30 mm.

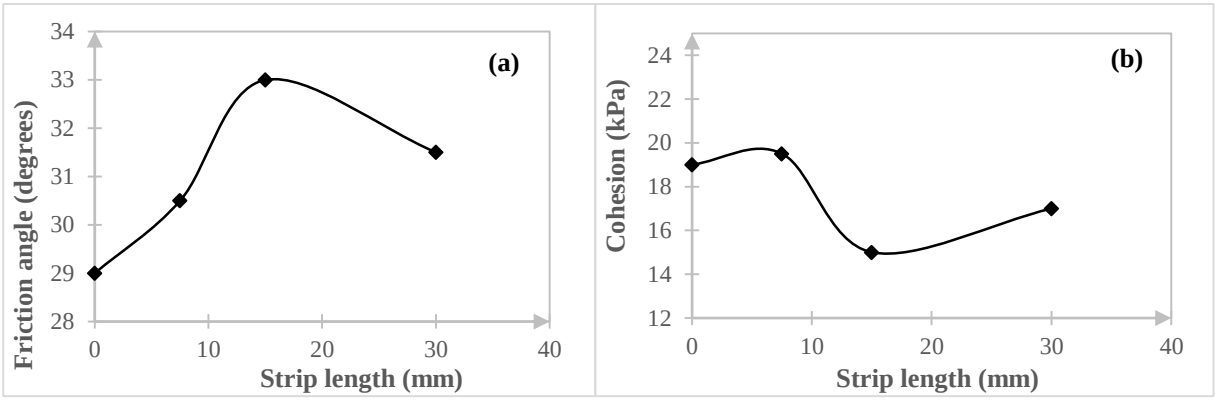

Figure 4.12: Variation of friction angle and cohesion with plastic strip length

Effect of compactive effort on peak friction angle and apparent cohesion

The effect of compactive effort on peak friction angle with varying plastic parameters is shown in Figure 4.13.

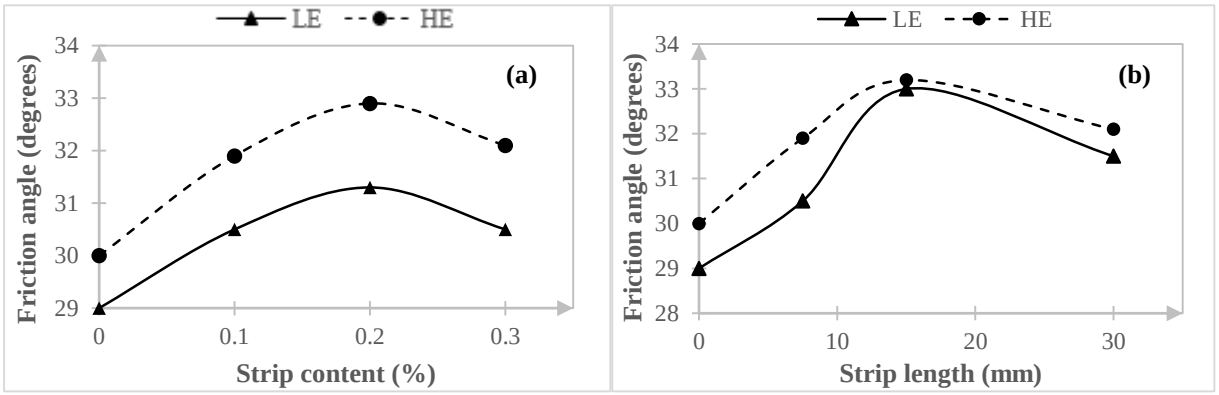

Figure 4.13: Variation of plastic parameters with friction angle at different compactive efforts

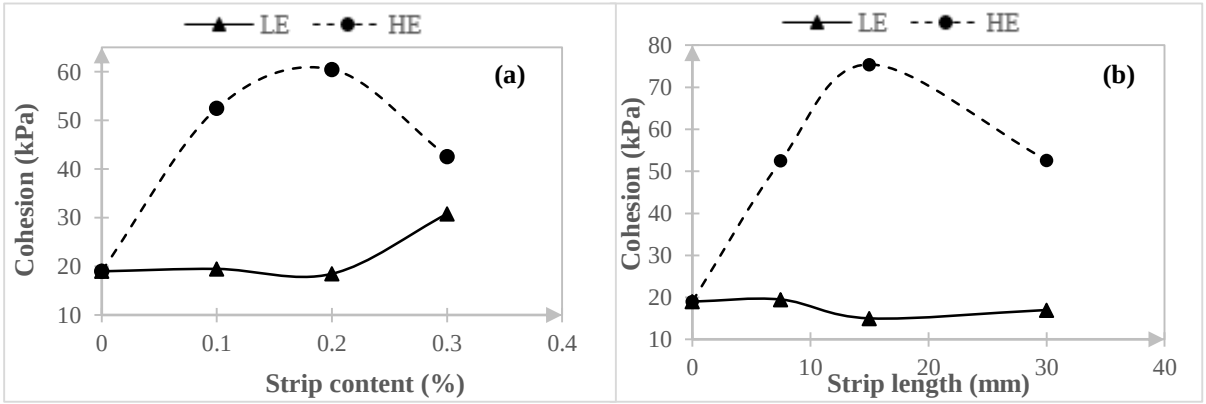

Figure 4.14: Variation of plastic parameters with cohesion at different compactive efforts

The effect of compaction density on the friction angle on varying plastic content and length is presented in Figure 4.13 presents the influence of compactive effort on the cohesion at different plastic contents. It can be observed that the friction angle of the reinforced soil improved on varying the strip concentration from 0 % to 0.3 % and increasing the compactive energy from a low compactive effort, LE, of 280 kN-m/m^3 (D_r =*52%*), to a high compactive effort, HE, of 589 kN-m/m^3 (D_r =*57%*), as illustrated in Figure 4.13 (a). The soil friction angle increased from 31.3 ^{o} to 32.9 ^{o} corresponding to 5 %. In contrast, on varying the strip length and compactive effort, no significant improvement in the friction angle was reported. The soil internal friction angle enhanced from 33.0 ^{o}, to 33.2 ^{o}, as shown in Figure 4.13 (b). This is equivalent to approximately 1 %. It is probable the soil was strengthened due to denser packing of the soil-plastic composite as the compaction density was increased. The reinforcing action was greater on varying HDPE content as compared to varying the strip length.

Figure 4.14 illustrates the impact of variation of compactive effort on the apparent cohesion at different plastic contents and lengths. Increasing the plastic concentration from 0.1 % to 0.3 % and on varying the compactive effort from 280 kN-m/m^3 (D_r =*52%) to* 589 kN-m/m^3 (D_r =*57%*), realised a significant increase in the apparent cohesion, Figure 4.14 (a). The cohesion value at higher compactive effort increased from 19.0 kPa to 60.5 kPa, representing 218 %. Likewise, the same trend was observed on variation of the length Figure 4.14 (b). An increase in the strip length from 7.5 mm to 30 mm led to an improvement in the apparent cohesion from 19.0 kPa to 75.4 kPa, equivalent to 297 % increase. In spite of the enhancement in the apparent cohesion values, caution is usually taken in applying them for design purposes.

The compaction density also affected the failure mode of the triaxial specimens. Triaxial specimens tested under confining pressures of 50 kPa to 200 kPa and a relative density of 52 %, exhibited a planar shear failure plane predicted by the Mohr-Coulomb failure criterion. The failed sample was inclined at an angle $\theta = (45^o + \frac{\emptyset'}{2})$ where $\emptyset'$ is the peak internal friction angle of the soil, Figure 4.15.

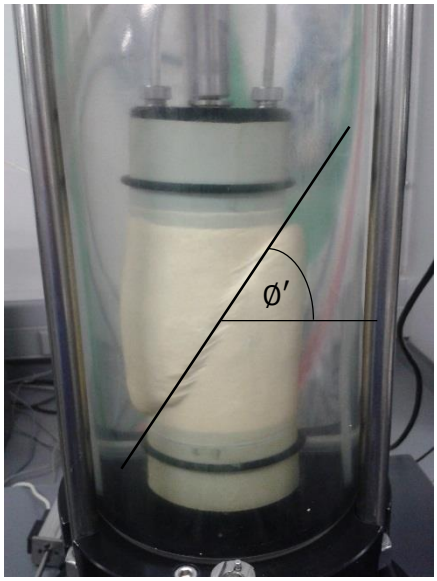

Figure 4.15: Failure by shear of triaxial test specimen at low compactive effort

In contrast, triaxial test samples tested at confining pressures of 300 kPa to 400 kPa and a relative density of 57 %, showed a bulging failure of the specimens. This can be observed in Figure 4.16.

Figure 4.16: Failure by bulging of a triaxial test specimen at high compactive effort

4.4 Practical Applications

Currently, there is a debate among researchers and industry players on the selection of peak versus residual shear strength parameters of the backfill that should be adopted in the design of earth reinforced structures. To this end, Zornberg & Leshchinsky (2001) presented a review of

international design criteria for geosynthetic-reinforced structures that can be applied to soil-plastic composites, Table 4.7.

Table 4.7: Summarised guidelines on selection of soil shear strength characteristics for earth reinforced structures design (Adapted from Zornberg & Leshchinsky, 2001)

Design Method/Agency	Shear strength parameter
Jewell's method	Residual
Leshchinsky and Boedeker's method	Residual
Queensland Department of Transport, Australia	Residual
New South Wells, Australia	Residual
Bureau National Sols-Routes, France	Residual
Federal Highway Administration (FHWA), AASHTO, USA	Peak
National Concrete Masonry Association	Peak
Canadian Geotechnical Society	Peak
German Society of Soil Mechanics and Geotechnical Engineering	Peak
Geotechnical Engineering Office, Hong Kong	Peak
Public Works Research Center, Japan	Peak
British Standards, United Kingdom	Peak
Leshchinsky's hybrid method	Hybrid

Proponents of the use of residual parameters attribute it to the potential for gradual development of progressive failure (Zornberg, 2002). Moreover, a hybrid approach has been proposed in which both peak and residual parameters are utilised (Leshchinsky, 2001). Lastly, as it can be seen in Table 4.7, most countries are still inclined towards use of peak strength parameters in their design guidelines for reinforced soil structures.

Consequently, a basic design example of a soil-plastic reinforced structure is presented, and limit equilibrium slope stability analyses carried out using Rocscience Slide Modeler software. In the illustration and to avoid repetition, peak strength parameters of the unreinforced, and reinforced soil with optimum plastic content were utilised in the design. However, the same design concept applies to all other soil-plastic composites with different test variables. The parameters were selected from tests conducted in the range of confining pressures (50 kPa to 200 kPa) that simulate practical loading conditions in geotechnical engineering construction on rural roads (Chandra et al., 2008).

4.4.1 Analysis of embankment model using Slide Modeler software

Slide Modeler is a 2D limit equilibrium package used for slope stability analysis of all types of soil and rock slopes, embankments, dams and retaining structures in geotechnical engineering. The software also has capabilities to carry out seismic analysis, probabilistic analysis, finite element groundwater seepage analysis, multi-scenario modelling, and support design. It is user-friendly and allows CAD files to be imported for creation and editing of models with complex geometries. Additionally, the software is one of the most widely used around the world for various geotechnical analyses (Hammah et al., 2004; Hammah, 2005).

Several analysis options exist but in the design example, Bishop's simplified method was adopted for both static and dynamic analysis. The method is widely used for analysis of slopes because of its simplicity and basis on limit equilibrium of static forces. Additionally, the choice was based on comparative studies that have shown the factors of safety computed from advanced methods such as Spencer and Morgenstern-Price are similar to those obtained by the Bishop's simplified method (Fredlund & Krahn, 1977), and the variation in values has been found to be less than 5 % (Yu et al., 1998).

In the method, the slope is divided into slices and an iterative approach is needed to determine the critical failure plane with the least global factor of safety. The factor of safety is calculated using the equation below.

$$\boldsymbol{F} = \frac{1}{\Sigma\,(\boldsymbol{W}\sin\alpha)}\sum\left[\{\boldsymbol{c'b} + (\boldsymbol{W}-\boldsymbol{ub})\tan\emptyset'\}\frac{\sec\alpha}{1+(\tan\alpha\tan\emptyset')/\boldsymbol{F}}\right] \qquad \textbf{Equation 4.1}$$

Where $\boldsymbol{F}$ = Factor of safety of the slope,

$\boldsymbol{W}$ = Self-weight of the slice (kN/m),

$\boldsymbol{\alpha}$ = Angle the normal force makes with centre of each slice (degrees),

$\boldsymbol{c'}$ = Cohesion (kN/m^2),

$\boldsymbol{b}$ = Slice width (m),

$\boldsymbol{u}$ = Pore water pressure force (kN/m), and

$\emptyset'$ = Effective angle of internal friction of the soil (degrees).

In seismic analysis, various approaches exist but a pseudo-static method was used because it is recommended in most national design manuals and standards (Baker et al., 2006). The pseudo-

static approach was first introduced by Terzaghi (1950) for use in geotechnical earthquake engineering applications. It is a simple technique because dynamic loads are computed from the already determined static forces. That is, seismic load coefficients are multiplied by the slice weight to obtain the driving forces, as given by:

$$\textit{Seismic force} = \textit{Seismic load coefficient} \times \textit{slice self weight} \qquad \textbf{Equation 4.2}$$

Once the critical failure surface was obtained, the factor of safety was computed by dividing the resisting forces; numerator, by the disturbing forces; denominator, to obtain the overall factor of the slope against external stability, that is, safe against failure due to sliding, overturning and bearing capacity. The various output options available were used for viewing and report generation of different types (e.g. query slip slices data, global factor of safety).

4.4.2 Design example

A proposed embankment is 5 m high with a horizontal crest 8 m long is to be constructed on a rural road with low volume traffic. Cape Flats sand, a free-draining granular fill material, and 0.2 % polyethylene plastic strips will be utilised. The embankment fill has a slope of 2H: 1V and the existing founding conditions are deemed adequate for construction. The ground water table is well below the foundation soil layer, and therefore the influence of pore water pressures was neglected. A static surcharge load of 10 kPa to represent the anticipated vehicular loading was adopted for analysis in both case 1 and case 2. Design case 1 involved static slope stability analysis while design case 2 involved dynamic slope stability analysis. Furthermore, vertical and horizontal seismic coefficients of 0.15 were assumed for dynamic analysis in scenario 2 based on previous research (Terzaghi, 1950; Melo & Sharma, 2004; Baker et al., 2006).

The soil properties of the backfill and underlying foundation materials are summarised in Table 4.8. Reinforced soil with plastic content of 0.2 % was used in the design example for demonstration purposes. Consequently, slope stability analysis of soils reinforced with the different plastic parameters would follow the same procedure. These were obtained from classification and triaxial tests in the laboratory. The selection of peak strength parameters at either lower or higher confining stress levels depends on the anticipated stress levels in the field. In the current design problem, a road subjected to low traffic loading was used. Consequently, the strength values of the linear portion of Mohr-Coulomb failure envelope were chosen.

The embankment was analysed, and the factors of safety of the unreinforced slope compared to that of reinforced soil. The apparent cohesion for the unreinforced sand was assumed to be zero even though a value was obtained from triaxial tests. This is due to the fact that the cohesion value is usualy ignored in the design of reinforced soil structures if the backfill material is cohesionless (Christopher et al., 1990). The software does not have an option for inclusion of plastic strips as a reinforcement material, therefore the soil peak strength properties were used to differentiate the soil models.

Table 4.8: Summary of selected soil properties

Material	Dry unit weight, γ_d (kN/m^3)	Cohesion, c' (kPa)	Friction angle, ∅′ (degrees)
Unreinforced Cape Flats sand	18.0	0	30.0
Reinforced Cape Flats sand	17.8	16	32.9
Foundation material (silty clay)	19.1	15	20.0

The soil models used in the slope stability analysis are shown in Figure 4.17 and Figure 4.18. Each model was analysed under static and seismic loading cases. All the dimensions indicated are in metres.

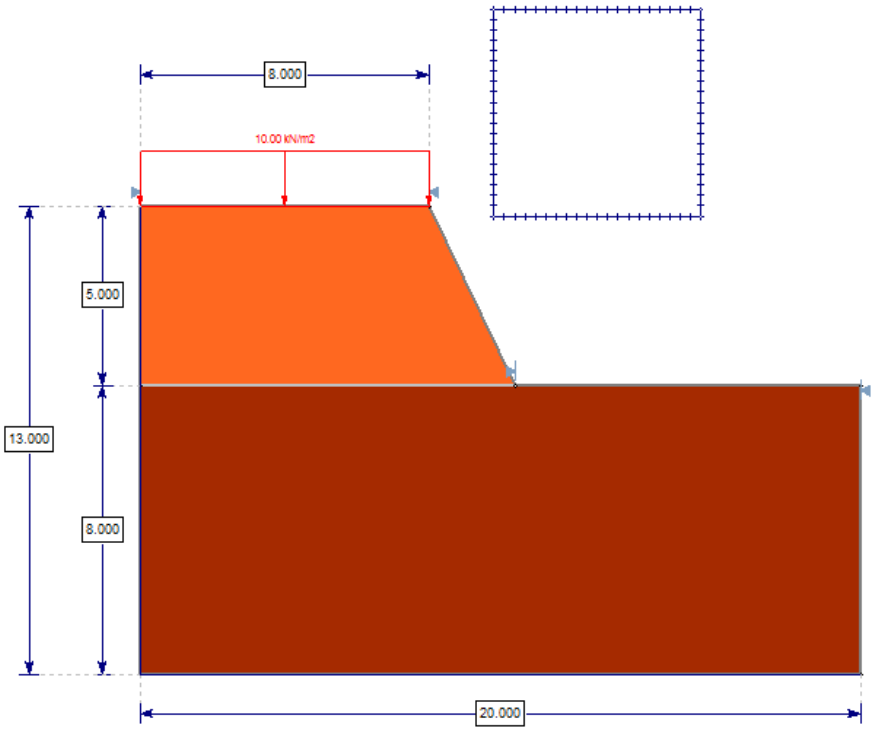

Figure 4.17: Embankment model created using Slide Modeler software for soil-plastic fill

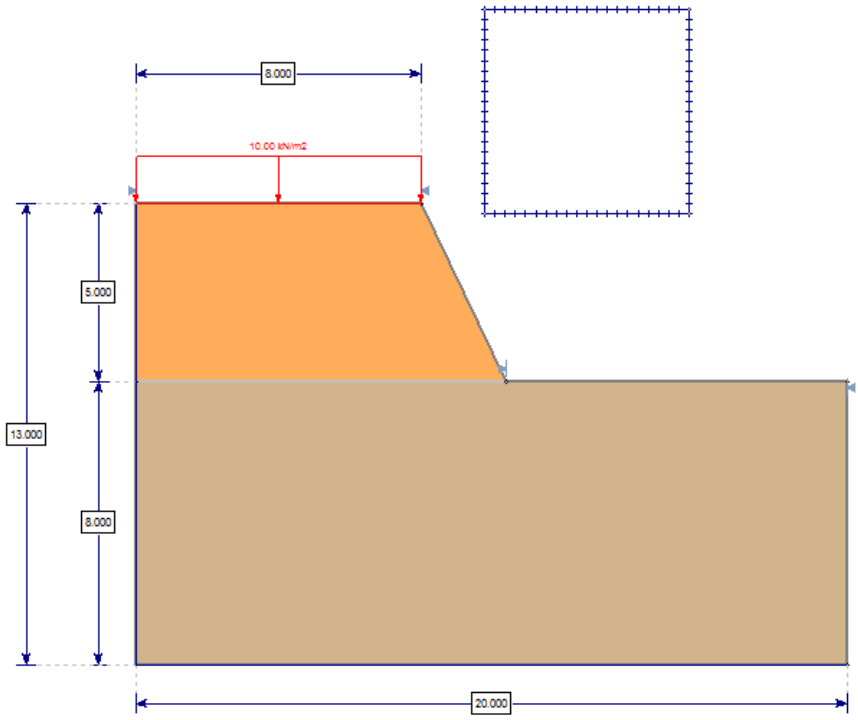

Figure 4.18: Embankment model created using Slide Modeler software for reinforced fill

Design solution 1: Static analysis

Figure 4.19 shows the global minimum slip surface obtained from the software after analysis of the slope with Cape Flats sand as the backfill material. A factor of safety of 0.369 was obtained. In contrast, the use of shear strength parameters of the soil-plastic composites in the model realised a factor of safety of 1.548, as shown in Figure 4.20. Detailed outputs from the software are attached in Appendix C.

The factor of safety obtained is greater than 1.25 (SAICE, 1989), and is thus safe in the long term or drained condition. The Federal Highways The addition of plastic material in the sand soil increased the external stability of the embankment.

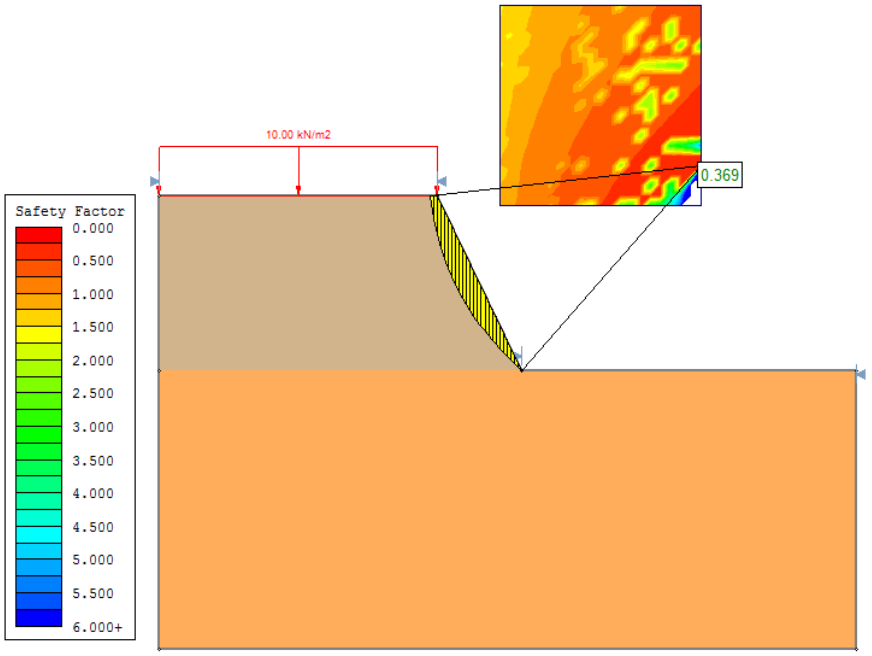

Figure 4.19: Global minimum slip surface for unreinforced backfill under static load

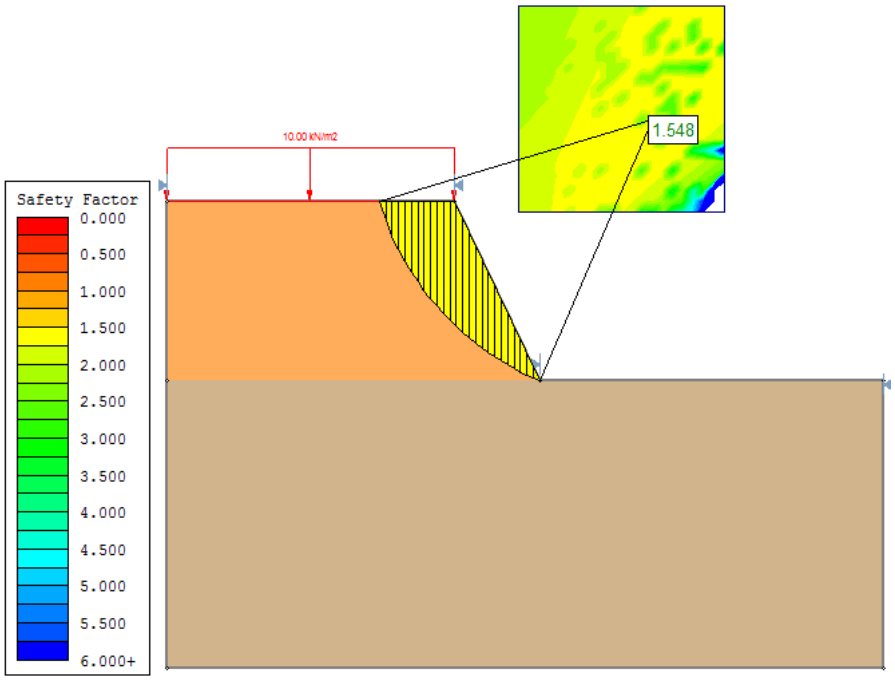

Figure 4.20: Global minimum slip surface for reinforced backfill under static load

Design solution 2: Seismic analysis

The results of the dynamic loading condition are presented in Figure 4.21 and Figure 4.22, whereby overall factors of 0.269 and 1.267 were obtained for soil and soil-composite samples respectively. Detailed design parameters and results are attached in appendix C.

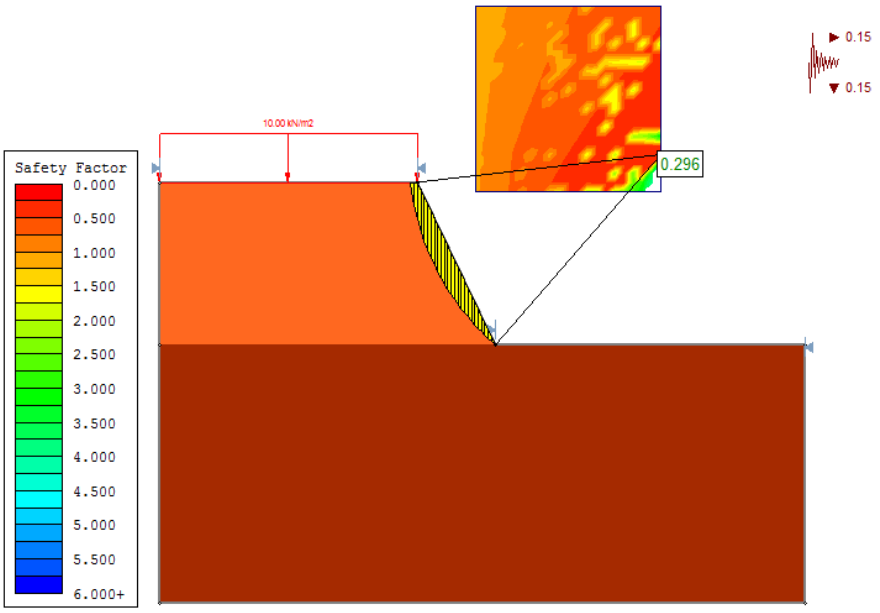

Figure 4.21: Global minimum slip surface for unreinforced backfill under dynamic load

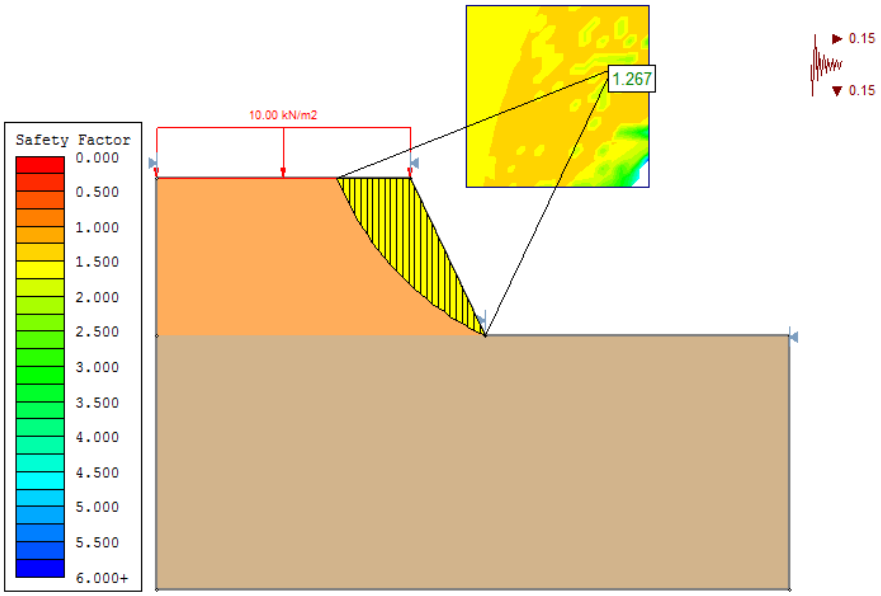

Figure 4.22: Global minimum slip surface for reinforced backfill under dynamic load

The stability of the slope is safe against failure since the value obtained is more than 1.25 (SAICE, 1989). The design outcomes indicate that the insertion of polyethylene plastic in sand resulted in a significant improvement in the stabilisation of the road embankment. Further to this, the safety factors obtained are lower than those obtained in static analysis which could be attributed the nature of application of the load in the different models.

For both design scenarios, an unreinforced sand could not be used for the chosen embankment geometry because the slope is unstable with factors of safety of less than 1 whereas with reinforced sand the chosen geometry meets the design requirements. Design option 2 would be recommended for adoption in the construction phase since it is the worst case scenario. The probability of destruction of property and loss of life during the design of the embankment would be minimised.

5 CONCLUSIONS AND RECOMMENDATIONS

Triaxial compression tests were conducted on dry Cape Flats sand with random inclusions of HDPE plastic strips at different concentrations and lengths. Moreover, different compactive efforts and confining pressures were used in the study. These test parameters were systematically varied to examine their influence on the stress-strain response and shear strength characteristics of the soil-plastic composites. The main findings of this research are summarised below and recommendations for future research are also proposed.

5.1 Conclusions

The following main conclusions were drawn from the results of this research:

1. The addition of plastic strips in soil increased its deviator stress. Additionally, the post-peak strength (or ultimate strength) loss was limited in the reinforced soil.
2. A linear failure envelope was observed in tests on unreinforced samples while a bilinear failure envelope was observed in soil-plastic composites. The bilinear relationship was influenced mainly by the plastic strip length, plastic content and the range of confining pressures used in the study.
3. There exists a critical confining stress below which failure is governed by plastic slippage while above this threshold value failure is governed by plastic breakage or pull-out strength. The failure envelope for soil-plastic composites was nearly parallel to that of the unreinforced soil.
4. An increase in the plastic content and strip length, and compactive effort resulted in a significant improvement in the friction angle of the soil-plastic composites. However, the enhancement approached a limiting value beyond which no a decrease in the friction angle was observed. The greatest enhancement in friction angle was reported at a strip length of 15 mm and plastic content of 0.2 % respectively.
5. An embankment model with 0.2 % plastic reinforcement was created using Slide Modeler software and factors of safety of the unreinforced and reinforced slopes determined under static and seismic loading. A significant improvement in the safety factor was realised due to the use of soil-plastic composites as a lightweight fill material.
6. The use of plastic strips in soil reinforcement has proved to be an efficient technique in altering the engineering properties of Cape Flats sand. Consequently, the method should be considered for possible practical application in geotechnical engineering projects.

7. The use of plastic strips in sand for soil reinforcement provides a sustainable way of reducing plastic wastes destined for landfills.

5.2 Recommendations

The following are the recommendations for future research:

1. Further research should be conducted over a wide range of plastic content and strip length in order to investigate the optimum values for design. Moreover, the effect of varying strip width, perforations, and textured strips should be investigated in order to better understand the shear behaviour of plastic reinforced soil.
2. The triaxial specimens used in this study and the results obtained from these tests may not be representative of field conditions due to the size of samples used. The test samples were utilized for comparative studies. Subsequently, additional research using large scale tests and field tests should be conducted on soil-plastic composites to eliminate scale effects, and simulate field conditions. Therefore, large scale direct shear and triaxial tests should be conducted on soil-plastic composites prepared at the same density to evaluate the shear behaviour of the reinforced soil.
3. The study investigated the improvement in strength of reinforced soil using laboratory tests. Further research into the durability and long term behaviour (creep) should be conducted through field scale tests.
4. A comparison of finite element slope stability analysis with conventional limit equilibrium approach of the soil-plastic composites should be explored.
5. Additional research should be conducted to investigate the behaviour of soil-plastic composites under cyclic loading.

REFERENCES

ASTM International. 2009. *Standard test methods for particle-size distribution (gradation) of soils using siieve analysis*. (ASTM D6913-04). West Conshohocken, PA: ASTM International. http://dx.doi.org/10.1520/D6913-04R09E01.

ASTM International. 2010. *Standard test methods for laboratory determination of water (moisture) content of soil and rock by mass.* (ASTM D2216-10). West Conshohocken, PA: ASTM International. http://dx.doi.org/10.1520/D2216-10.

ASTM International. 2011. *Standard test methods for consolidated drained triaxial compression test for soils.* (ASTM D7181-11) West Conshohocken, PA: ASTM International. http://dx.doi.org/10.1520/D7181-11.

ASTM International. 2012. *Standard test methods for laboratory compaction characteristics of soil using standard effort (12 400 ft-lbf/ft^3 (600 kN-m/m^3)).* (ASTM D698-12e2) West Conshohocken, PA: ASTM International. http://dx.doi.org/10.1520/D0698-12E02.

ASTM International. 2014. *Standard test methods for specific gravity of soil solids by water pycnometer*. (ASTM D854-14). West Conshohocken, PA: ASTM International. http://dx.doi.org/10.1520/D0854-14.

ASTM International. 2014. *Standard practice for use of the terms precision and bias in ASTM test methods.* (ASTM E177-14). West Conshohocken, PA: ASTM International. http://dx.doi.org/10.1520/E0177-14.

ASTM International. 2015. *Standard terminology for geosynthetics*. (ASTM D4439-15a). West Conshohocken, PA: ASTM International. https://doi.org/10.1520/D4439-15A.

ASTM International. 2016. *Standard test methods for maximum index density and unit weight of soils using a vibratory table.* (ASTM D4253-16). West Conshohocken, PA: ASTM International. http://dx.doi.org/10.1520/D4253-16.

ASTM International. 2016. *Standard test methods for minimum index density and unit weight of soils and calculation of relative density*. (ASTM D4254-16). West Conshohocken, PA: ASTM International. http://dx.doi.org/10.1520/D4254-16.

Azapagic, A., Emsley, A. & Hamerton, I. 2003. *Polymers: the environment and sustainable development.* John Wiley & Sons.

Babu, G.S. & Chouksey, S.K. 2011. Stress–strain response of plastic waste mixed soil. *Waste Management.* 31(3):481-488.

Babu, S., Chouksey, S., Anoosha, G. & Manjari, K.G. 2010. Strength and compressibility response of plastic waste mixed soil. *Indian Geotechnical Conference-2010.*

Baker, R., Shukha, R., Operstein, V. & Frydman, S. 2006. Stability charts for pseudo-static slope stability analysis. *Soil Dynamics and Earthquake Engineering.* 26(9):813-823.

Benson, C.H. & Khire, M.V. 1994. Reinforcing sand with strips of reclaimed high-density polyethylene. *Journal of Geotechnical Engineering.* 120(5):838-855.

Bishop, A.W. & Bjerrum, L.1960. The relevance of the triaxial test to the solution of stability problems. *Proceedings, Research Conference on Shear Strength of Cohesive Soils, ASCE.* 437-501.

Chandra, S., Viladkar, M. & Nagrale, P.P. 2008. Mechanistic approach for fiber-reinforced flexible pavements. *Journal of Transportation Engineering.* 134(1):15-23.

Chebet, F. & Kalumba, D. 2014. Laboratory Investigation On Re-Using Polyethylene (Plastic) Bag Waste Material for Soil Reinforcement in Geotechnical Engineering. *International Journal on Civil Engineering & Urban Planning (IJCEUP).* 1(1):33-49.

Choudhary, A., Jha, J. & Gill, K. 2010. A study on CBR behavior of waste plastic strip reinforced soil. *Emirates Journal for Engineering Research.* 15(1):51-57.

Christopher, B.R., Gill, S.A., Giroud, J., Juran, I., Mitchell, J.K., Schlosser, F. & Dunnicliff, J. 1990. *Reinforced soil structures volume I. Design and construction guidelines.* (FHWA-RD-89-043). Virginia: FHWA.

Consoli, N.C., Heineck, K.S., Casagrande, M.D.T. & Coop, M.R. 2007. Shear strength behavior of fiber-reinforced sand considering triaxial tests under distinct stress paths. *Journal of Geotechnical and Geoenvironmental Engineering.* 133(11):1466-1469.

Consoli, N.C., Montardo, J.P., Prietto, P.D.M. & Pasa, G.S. 2002. Engineering behavior of a sand reinforced with plastic waste. *Journal of Geotechnical and Geoenvironmental Engineering.* 128(6):462-472.

Craig, R.F. & Knappett, J.A. 2012. *Craig's Soil Mechanics.* 8th ed. London and New York: Spon Press.

Das, B.M. & Sobhan, K. 2013. *Principles of Geotechnical Engineering, SI Edition.* 8th ed. Delhi, India: Cengage Learning.

Della, N., Belkhatir, M., Canou, J. & Dupla, J.C.2015. Saturation and sample reconstitution effects on the mechanical behavior of Chlef sand in northern Algeria-an experimental study. *Proceedings of the 16th African Regional Conference on Soil Mechanics and Geotechnical Engineering.* 27th - 30th April, 2015. M. Bouassida, M. Khemakhem & S.E. Haffoudhi, Eds. 116.

Dikgang, J., Leiman, A. & Visser, M. 2012. Analysis of the plastic-bag levy in South Africa. *Resources, Conservation and Recycling.* 66(0):59-65. DOI:http://dx.doi.org/10.1016/j.resconrec.2012.06.009.

Dutta, R.K. & Rao, G.V. 2007. Regression models for predicting the behavior of sand reinforced with waste plastic. *Turkish Journal of Engineering and Environmental Sciences.* 31(2):119-126.

EPA. 1990. *Report to Congress: Methods to manage and control plastic wastes.* (EPA/530-SW-89-051). Washington D.C.: US Government Printing Office.

Falorca, I. & Pinto, M. 2011. Effect of short, randomly distributed polypropylene microfibres on shear strength behaviour of soils. *Geosynthetics International.* 18(1):2-11.

Fluet, J. 1985. *Geotextile testing and the design engineer.* Los Angeles: ASTM.

Foose, G.J., Benson, C.H. & Bosscher, P.J. 1996. Sand reinforced with shredded waste tires. *Journal of Geotechnical Engineering.* 122(9):760-767.

Fredlund, D. & Krahn, J. 1977. Comparison of slope stability methods of analysis. *Canadian Geotechnical Journal.* 14(3):429-439.

Freilich, B.J., Li, C. & Zornberg, G.2010. Effective shear strength of fiber-reinforced clays. *9th International Conference on Geosynthetics, Brazil.* 1997-2000.

Ghiassian, H., Poorebrahim, G. & Gray, D.H. 2004. Soil reinforcement with recycled carpet wastes. *Waste Management & Research.* 22(2):108-114. DOI:10.1177/0734242X04043938.

Gray, D.H. & Al-Refeai, T. 1986. Behavior of fabric-versus fiber-reinforced sand. *Journal of Geotechnical Engineering.* 112(8):804-820.

Gray, D.H. & Ohashi, H. 1983. Mechanics of fiber reinforcement in sand. *Journal of Geotechnical Engineering.* 109(3):335-353.

Gurung, N. 2001. 1-D analytical solution for extensible and inextensible soil/rock reinforcement in pull-out tests. *Geotextiles and Geomembranes.* 19(4):195-212.

Hammah, R.2005. A comparison of finite element slope stability analysis with conventional limit-equilibrium investigation. *Proceedings of the 58th Canadian Geotechnical and 6th Joint IAH-CNC and CGS Groundwater Specialty Conferences–GeoSask 2005.* Citeseer.

Hammah, R.E., Curran, J.H., Yacoub, T. & Corkum, B.2004. Stability analysis of rock slopes using the finite element method. *Proceedings of the ISRM Regional Symposium EUROCK.* Citeseer.

Hataf, N. & Rahimi, M. 2006. Experimental investigation of bearing capacity of sand reinforced with randomly distributed tire shreds. *Construction and Building Materials.* 20(10):910-916.

Hejazi, S.M., Sheikhzadeh, M., Abtahi, S.M. & Zadhoush, A. 2012. A simple review of soil reinforcement by using natural and synthetic fibers. *Construction and Building Materials.* 30:100-116. DOI:http://dx.doi.org/10.1016/j.conbuildmat.2011.11.045.

Ibraim, E. & Fourmont, S.2007. Behaviour of sand reinforced with fibres. *Geotechnical Symposium on Soil Stress-Strain Behavior: Measurement, Modeling and Analysis, Roma, March 16 & 17, 2006.* H.I. Ling, L. Callisto, D. Leshchinsky & J. Koseki, Eds. Netherlands: Springer. 807-818.

Ingold, T.S. & Miller, K.S. 1983. Drained axisymmetric loading of reinforced clay. *Journal of Geotechnical Engineering.* 109(7):883-898.

Kalumba, D. 1998. Effect of Grading and Grain Size on the Friction Characteristics of a Sand/geotextile Inteface. MSc. Thesis. University of Cape Town.

Karani, P. & Jewasikiewitz, S.M. 2007. Waste management and sustainable development in South Africa. *Environment, Development and Sustainability.* 9(2):163-185.

Koerner, R.M. 2012. *Designing with geosynthetics.* 6th ed. USA: Xlibris Corporation.

Ladd, R. 1978. Preparing test specimens using undercompaction. *Geotechnical Testing Journal.* 1(1):16-23.

Leshchinsky, D. 2001. Design dilemma: Use peak or residual strength of soil. *Geotextiles and Geomembranes.* 19(2):111-125.

Maher, M.H. & Gray, D.H. 1990. Static response of sands reinforced with randomly distributed fibers. *Journal of Geotechnical Engineering.* 116(11):1661-1677.

Manceau, S., Macdiarmid, C. & Renewables, S. 2012. Chapter 73: Design of soil reinforced slopes and structures. *ICE Manual of Geotechnical Engineering: Geotechnical Design, Construction and Verification.* 2:1093-1107.

Marandi, S.M., Bagheripour, M.H., Rahgozar, R. & Zare, H. 2008. Strength and ductility of randomly distributed palm fibers reinforced silty-sand soils. *American Journal of Applied Sciences.* 5(3):209-220.

McGown, A., Andrawes, K.Z. & Al-Hasani, M.M. 1978. Effect of inclusion properties on the behaviour of sand. *Geotechnique.* 28(3):327-346.

Melo, C. & Sharma, S.2004. Seismic coefficients for pseudostatic slope analysis. *13th World Conference on Earthquake Engineering, Vancouver, BC, Canada, Paper.*

Michalowski, R.L. & Cermák, J. 2003. Triaxial compression of sand reinforced with fibers. *Journal of Geotechnical and Geoenvironmental Engineering.* 129(2):125-136.

Michalowski, R.L. & Zhao, A. 1996. Failure of fiber-reinforced granular soils. *Journal of Geotechnical Engineering.* 122(3):226-234.

Mirafi 2010. *Geosynthetics for soil reinforcement.* Available: http://www.tencate.com/pt/lam/Images/bro_soilrein_tcm31-10830.pdf [2015, March 13].

Miraftab, M. & Lickfold, A. 2008. Utilization of carpet waste in reinforcement of substandard soils. *Journal of Industrial Textiles.* 38(2):167-174.

Mishra, P., Jha Ajachi, R., Satrawala, M. & Amin, H. 2013. Experimental study on waste recycled product (WRP) and waste plastic strips (WPS) as pavement sub-base material. *International Journal of Scientific & Technology Research.* 2(12):258-262.

Mitchell, J.K. & Villet, W.C. 1987. *Reinforcement of earth slopes and embankments.* (290). Washington, D.C.: National Cooperative Highway Research Program.

Mughtar, A.P. 2009. Utilizing consumer polyethylene bags to reinforce soil. BSc Thesis. University of Cape Town.

Mustapha, A.M. 2008. Bamboo as soil reinforcement: A laboratory trial. *Leonardo Journal of Sciences.* (13):69-77.

Nahman, A. 2010. Extended producer responsibility for packaging waste in South Africa: Current approaches and lessons learned. *Resources, Conservation and Recycling.* 54(3):155-162. DOI:http://dx.doi.org/10.1016/j.resconrec.2009.07.006.

Neopaney, M., Ugyen, K.W., Tenzin, S. & Chamberlin, K.S. 2012. Stabilization of soil by using plastic wastes. *International Journal of Emerging Trends in Engineering and Development ISSN.* :2249-6149.

Nguyen, M., Yang, K., Lee, S., Wu, C. & Tsai, M. 2013. Behavior of nonwoven-geotextile-reinforced sand and mobilization of reinforcement strain under triaxial compression. *Geosynthetics International.* 20(3):207-225.

Nicholson, P.G. 2014. *Soil Improvement and Ground Modification Methods.* New York: Butterworth-Heinemann.

Nicholson, P.G. 2015. *Soil improvement and ground modification methods.* Boston: Butterworth-Heinemann. DOI:http://dx.doi.org.ezproxy.uct.ac.za/10.1016/B978-0-12-408076-8.09988-X.

Plastics SA. 2011. *The plastic identification code.* Available: https://www.capetown.gov.za/en/Solidwaste2/Documents/The_Plastics_Identification_Code.pdf [2015, April 14].

Pokharel, G. 1995. Deformation and ultimate load of reinforced soil structures, theory and experiment. PhD Thesis. Department of civil engineering, Nagoya University, Japan.

Ranjan, G., Vasan, R. & Charan, H. 1996. Probabilistic analysis of randomly distributed fiber-reinforced soil. *Journal of Geotechnical Engineering.* 122(6):419-426.

Rao, G. & Dutta, R.2004. Ground improvement with plastic waste. *Proceeding, 5th International Conference on Ground Improvement Technique: 22-23 March 2004. Kuala Lumpur, Malaysia.* 321-328.

SAICE 1989. *Code of Practice on Lateral Support in Surface Excavations.* Johannesburg: Geotechnical Division, South African Institution of Civil Engineering.

Sarsby, R.W. 2007. Use of 'Limited Life Geotextiles'(LLGs) for basal reinforcement of embankments built on soft clay. *Geotextiles and Geomembranes.* 25(4):302-310.

South Africa. 2014. *National Environmental Management: Waste Amendment Act, 2014.* (37714). Pretoria, South Africa: Government printer.

SouthAfrica.info. 2003. *Plastic bags: think thicker!* Available: http://www.southafrica.info/services/consumer/plasticbags.htm#.VSzhevmUdzU [2015, April 14].

Terzaghi, K. 1950. Mechanisms of landslides, engineering geology (Berkley) volume. *Geological Society of America.*

Vidal, H. 1969. *The principle of Reinforced Earth .* (282). Washington D.C.: Highway Research Record.

Waldron, L. 1977. The shear resistance of root-permeated homogeneous and stratified soil. *Soil Science Society of America Journal.* 41(5):843-849.

Williamson, C. 2012. Investigation into the use of perforated high density polyethylene shopping bag waste as a soil reinforcement. Honors Thesis. University of Cape Town.

Yetimoglu, T., Inanir, M. & Inanir, O.E. 2005. A study on bearing capacity of randomly distributed fiber-reinforced sand fills overlying soft clay. *Geotextiles and Geomembranes.* 23(2):174-183.

Yetimoglu, T. & Salbas, O. 2003. A study on shear strength of sands reinforced with randomly distributed discrete fibers. *Geotextiles and Geomembranes.* 21(2):103-110.

Yoon, S., Prezzi, M., Siddiki, N.Z. & Kim, B. 2006. Construction of a test embankment using a sand–tire shred mixture as fill material. *Waste Management.* 26(9):1033-1044.

Yoon, Y.W., Cheon, S.H. & Kang, D.S. 2004. Bearing capacity and settlement of tire-reinforced sands. *Geotextiles and Geomembranes.* 22(5):439-453.

Yu, H., Salgado, R., Sloan, S. & Kim, J. 1998. Limit analysis versus limit equilibrium for slope stability. *Journal of Geotechnical and Geoenvironmental Engineering.* 124(1):1-11.

Zornberg, J. 2002. Discrete framework for limit equilibrium analysis of fibre-reinforced soil. *Géotechnique.* 52(8):593-604.

Zornberg, J. & Leshchinsky, D. 2001. Comparison of international design criteria for geosynthetic-reinforced soil structures. *Geosynthetics and Earth Reinforcement.* :106-117.

APPENDICES

A CLASSIFICATION TESTS

A.1 Calculations for specific gravity for Cape Flats sand

SPECIFIC GRAVITY DATA SHEET		
Pycnometer bottle no.	4	6
W_P = Mass of empty, clean pycnometer (g)	33.354	35.357
W_{PS} = Mass of empty pycnometer + dry soil (g)	45.421	45.422
W_B = Mass of pycnometer +dry soil+ water (g)	93.553	90.114
W_A = Mass of pycnometer +water (g)	85.279	83.869
W_{PS}-W_P	12.067	10.065
W_A-W_B	8.274	6.245
Specific gravity (G_s)	2.65	2.63
Average specific gravity	**2.64**	

A.2 Calculations for loosest density for Cape Flats sand

LOOSEST DENSITY DATA SHEET		
Sample number	1	2
Volume of mould (m^3)	0.00283	0.00283
Mass of empty mould (kg)	3.035	3.035
Mass of mould + sand (kg)	7.435	7.405
Mass of sand (kg)	4.400	4.370
Density (kg/m^3)	1557	1546
Average loosest density (kg/m^3)	**1552**	

A.3 Calculations for densest density for Cape Flats sand

DENSEST DENSITY DATA SHEET		
Sample number	3	4
Volume of mould (m^3)	0.00241	0.00242
Mass of empty mould (kg)	3.035	3.035
Mass of mould + sand (kg)	7.390	7.385
Mass of sand (kg)	4.355	4.350
Density (kg/m^3)	1805	1800
Average densest density (kg/m^3)	**1803**	

A.4 Sample calculation for relative density for Cape Flats sand

RELATIVE DENSITY DATA SHEET	
Diameter of sample (mm)	51.28
Radius of sample (m)	0.02564
Height of sample (m)	0.10344
Volume of sample (m^3)	0.00021
Mass of sand (kg)	0.36
Dry density of compacted soil	1685
Densest density (kg/m^3)	1803
Loosest density (kg/m^3)	1552
Relative density (%)	**57**

B Test Procedures

B.1 Triaxial shear test

i. A template file was loaded from the File menu of the software for each triaxial test.

ii. All the necessary information was entered; project, testing parameters and test standards. The parameters controlled initialisation, saturation, consolidation and shearing stage during testing. A shear rate of 0.075 %/min, confining pressures of 50 kPa, 100 kPa, 200 kPa, 300 kPa and 400 kPa and maximum strain of 10 % were specified.

iii. The System Monitor and the Calibration Summary windows were opened to zero loads, displacements and pressures. This was done by copying the System Monitor offset values to the Calibration Summary.

iv. The Run menu was pulled down and "Start" clicked. A folder and file name were chosen and the test file saved.

v. A dialog box appeared to initialise pumps. "No" was clicked since the initialisation of the pumps had been done manually.

vi. When prompted to position platen, "No" option was selected since the platen had been positioned before start of test. The piston lock was unlocked and "Ok" clicked in the Unlock Piston window.

B.1.1 Initialisation and saturation phases

i. The initialisation phase was then allowed to run for 2 minutes. All tests were conducted in unsaturated conditions and thus all test parameters for saturation had been zeroed to skip the phase. The tap controlling supply of water to the specimen was also closed.

ii. At the end of the 2 minutes, the Run menu was pulled down and "next phase" selected.

B.1.2 Consolidation phase

i. The consolidation phase was allowed to run for 5 minutes. Allowing the consolidation phase to run for longer durations in unsaturated conditions did not yield any differences in results since the specimen is mainly made up of sand samples.

ii. After 5 minutes, the Run menu was pulled down and "next phase" selected.

B.1.3 Shearing phase

i. The shear phase commenced automatically and the test was able to run to completion with no need for further intervention. Each experiment was set to a maximum strain of 10 % and strength at maximum shear recorded.

B.1.4 Monitoring a test

i. The View menu was opened to examine the current progress of the test. The display options were either “Test monitor” or “Test Graph.”

B.1.5 Specimen removal

i. At end of each triaxial test, piston lock was tightened and coupler that held the cell piston to the load cell was loosened.

ii. The platen was lowered and all tubing connections removed. The sheared specimen was then removed and discarded in a bucket.

B.2 Calibration data

MENU	ITEM	PARAMETERS				
1. System	1. A/D Channel	4				
	2. Units	Metric (or English if you prefer)				
2. Network	1. Node ID	65 (Can be changed to any value between 20 and 256.)				
3. A/D	1. Channel 1	1. Type	2. Excitation	3. Polarity	4. Range	
		Force	7.5 V	Bipolar	20 mV	
		5. Factor*	6. Offset	7. Low. Lim.	8. Up. Lim.	
		$3x10^{-4}$ kN/cnt	32767 cnt	0 cnt	65535 cnt	
		9. Advanced				
		1. Mode	2. Rate	3. Filter	4 Chop	5. Fast
		Diff.	400	Enabled	Enabled	Enabled
	2. Channel 2	1. Type	2. Excitation	3. Polarity	4. Range	
		Displacement	5 V	Unipolar	2560 mV	
		5. Factor*	6. Offset	7. Low. Lim.	8. Up. Lim.	
		$1.5x10^{-3}$ mm/cnt	32768 cnt	0 cnt	65535 cnt	
		9. Advanced				
		1. Mode	2. Rate	3. Filter	4 Chop	5. Fast
		Diff.	200	Enabled	Enabled	Enabled
	3. Channel 3**	1. Type	2. Excitation	3. Polarity	4. Range	
		Pressure	12 V	Bipolar	160 mV	
		5. Factor*	6. Offset	7. Low. Lim.	8. Up. Lim.	
		$5.6x10^{-2}$ kPa/cnt	32768 cnt	0 cnt	65535 cnt	
		9. Advanced				
		1. Mode	2. Rate	3. Filter	4 Chop	5. Fast
		Diff.	200	Enabled	Enabled	Enabled
4. PID	1. P-Gain	2. I-Gain	3. D-Gain	4. V-Offset		
	2 steps/sec/cnt	0.1 steps/sec/cnt	0 steps/sec/cnt	0 steps/sec		
	5. I-Limit	6. V-Limit	7. Dither Ampl.	8. Dither Freq.		
	1024 steps/sec	32768 steps/sec	0 steps/sec	0 Hz		
	9. Advanced					
	1. Filter	2. FB Channel	3. Anti-Windup	4. Derivative FB		
	256 Hz	Channel 0	Reset	De/dt		
5. Motor	1. Frequency	16384 Hz				
	2. Acceleration	40960 steps/sec/sec				
	3. Step Capacity	1432234				
	4. Step factor	$5.3x10^{-5}$ mm/step ($2.0x10^{-6}$ in/step) (Approximately)				

C Summary of Triaxial Compression Test Results

C.1 Variation of Peak Deviator Stress with Plastic Strip Length

Plastic content in reinforced soil (%)	Confining pressure (kPa)	Peak deviator stress (kPa)	Vertical Strain at failure (%)	Ultimate deviator stress (kPa)
0	50	157.9	2.88	133.8
0.1		197.5	2.91	147.1
0.2		183.8	2.91	147.1
0.3		181.0	3.43	137.5
0	100	275.3	2.90	230.6
0.1		332.9	3.40	236.7
0.2		310.0	3.44	236.7
0.3		276.4	3.45	236.7
0	200	470.8	3.36	412.9
0.1		543.8	3.86	449.2
0.2		496.8	3.93	449.2
0.3		473.0	4.44	428.6
0	300	614.9	3.37	535.5
0.1		728.5	3.88	650.2
0.2		633.8	4.36	577.7
0.3		664.9	4.48	577.7
0	400	797.4	3.43	684.4
0.1		943.6	3.93	854.4
0.2		911.0	4.47	854.4
0.3		811.6	4.97	684.41

C.2 Variation of Peak Deviator Stress with Plastic Content

Plastic strip lengths in reinforced soil (mm)	Confining pressure (kPa)	Peak deviator stress (kPa)	Vertical strain (%)	Ultimate deviator stress (kPa)
0	50	157.0	2.90	113.3
7.5		164.9	2.88	140.9
15		176.9	3.40	140.9
30		157.0	2.90	132.8
0	100	271.7	2.40	231.2
7.5		310.9	2.94	241.5
15		311.9	3.45	256.1
30		276.4	3.40	231.2
0	200	451.7	2.95	361.5
7.5		498.7	3.44	413.8
15		503.2	3.94	397.9
30		457.0	3.46	361.5
0	300	629.6	3.42	488.71
7.5		689.7	3.94	610.9
15		690.2	4.45	616.1
30		690.2	4.45	610.9
0	400	859.6	4.43	684.16
7.5		939.5	4.44	833.8
15		936.5	4.95	833.8
30		904.3	4.46	770.8

D Slope Stability Analysis Output from Slide Modeler Software

D.1 Static Analysis

D.1.1 Embankment with unreinforced sand backfill

Slide Analysis Information

Slope Stability Analysis of Embankment

Project Summary

File Name: Embankment model_Sand
Slide Modeler Version: 6.009
Project Title: Slope Stability Analysis of Embankment
Author: Paul Wanyama (WNYPAU001)

General Settings

Units of Measurement: Metric Units
Time Units: days
Permeability Units: meters/second
Failure Direction: Left to Right
Data Output: Standard
Maximum Material Properties: 20
Maximum Support Properties: 20

Analysis Options

Analysis Methods Used

Bishop simplified

Number of slices: 25
Tolerance: 0.005
Maximum number of iterations: 50
Check malpha < 0.2: Yes
Initial trial value of FS: 1
Steffensen Iteration: Yes

Groundwater Analysis

Groundwater Method: Water Surfaces
Pore Fluid Unit Weight: 9.81 kN/m3
Advanced Groundwater Method: None

Random Numbers

Pseudo-random Seed: 10116
Random Number Generation Method: Park and Miller v.3

Surface Options

Surface Type: Circular
Search Method: Grid Search
Radius Increment: 10
Composite Surfaces: Disabled
Reverse Curvature: Create Tension Crack
Minimum Elevation: Not Defined

Minimum Depth: Not Defined

Loading

1 Distributed Load present

Distributed Load 1

Distribution: Constant
Magnitude [kN/m2]: 10
Orientation: Normal to boundary

Material Properties

Property	Silty clay	Fill
Color		
Strength Type	Mohr-Coulomb	Mohr-Coulomb
Unit Weight [kN/m3]	19.1	18
Cohesion [kPa]	15	0
Friction Angle [deg]	20	30
Water Surface	None	None
Ru Value	0	0

Global Minimums

Method: bishop simplified

FS: 0.369437
Center: 15.541, 5.868
Radius: 7.803
Left Slip Surface Endpoint: 7.786, 5.000
Right Slip Surface Endpoint: 10.395, 0.002
Resisting Moment=117.927 kN-m
Driving Moment=319.208 kN-m

Slice Data

Global Minimum Query (bishop simplified) - Safety Factor: 0.369437

Slice Number	Width [m]	Weight [kN]	Base Material	Base Cohesion [kPa]	Base Friction Angle [degrees]	Shear Stress [kPa]	Shear Strength [kPa]	Base Normal Stress [kPa]	Pore Pressure [kPa]	Effective Normal Stress [kPa]
1	0.104334	0.627838	Fill	0	30	2.28705	0.844922	1.46345	0	1.46345
2	0.104334	1.67832	Fill	0	30	5.29793	1.95725	3.39007	0	3.39007
3	0.104334	2.25484	Fill	0	30	5.42433	2.00395	3.47093	0	3.47093
4	0.104334	2.47465	Fill	0	30	6.63715	2.45201	4.24699	0	4.24699
5	0.104334	2.6108	Fill	0	30	7.74373	2.86082	4.95509	0	4.95509
6	0.104334	2.68815	Fill	0	30	8.65317	3.1968	5.53703	0	5.53703
7	0.104334	2.72082	Fill	0	30	9.38506	3.46719	6.00536	0	6.00536
8	0.104334	2.71793	Fill	0	30	9.95415	3.67743	6.36948	0	6.36948
9	0.104334	2.68577	Fill	0	30	10.3718	3.83174	6.63676	0	6.63676
10	0.104334	2.62888	Fill	0	30	10.6473	3.93349	6.81299	0	6.81299
11	0.104334	2.55072	Fill	0	30	10.7878	3.98541	6.90291	0	6.90291

12	0.104334	2.45394	Fill	0	30	10.7996	3.98976	6.91046	0	6.91046
13	0.104334	2.34068	Fill	0	30	10.6876	3.94841	6.83884	0	6.83884
14	0.104334	2.21266	Fill	0	30	10.4563	3.86294	6.69079	0	6.69079
15	0.104334	2.07128	Fill	0	30	10.1091	3.73466	6.46864	0	6.46864
16	0.104334	1.91774	Fill	0	30	9.64901	3.5647	6.17426	0	6.17426
17	0.104334	1.75305	Fill	0	30	9.07865	3.35399	5.80928	0	5.80928
18	0.104334	1.57807	Fill	0	30	8.40013	3.10332	5.3751	0	5.3751
19	0.104334	1.39353	Fill	0	30	7.61518	2.81333	4.87283	0	4.87283
20	0.104334	1.20008	Fill	0	30	6.72529	2.48457	4.3034	0	4.3034
21	0.104334	0.998291	Fill	0	30	5.73159	2.11746	3.66756	0	3.66756
22	0.104334	0.788663	Fill	0	30	4.63505	1.71236	2.96589	0	2.96589
23	0.104334	0.57164	Fill	0	30	3.43634	1.26951	2.19885	0	2.19885
24	0.104334	0.347618	Fill	0	30	2.1359	0.789079	1.36672	0	1.36672
25	0.104334	0.116952	Fill	0	30	0.734039	0.271181	0.469699	0	0.469699

Query 1 (bishop simplified) - Safety Factor: 0.369437

Slice Number	Width [m]	Weight [kN]	Base Material	Base Cohesion [kPa]	Base Friction Angle [degrees]	Shear Stress [kPa]	Shear Strength [kPa]	Base Normal Stress [kPa]	Pore Pressure [kPa]	Effective Normal Stress [kPa]
1	0.104334	0.627838	Fill	0	30	2.28705	0.844922	1.46345	0	1.46345
2	0.104334	1.67832	Fill	0	30	5.29793	1.95725	3.39007	0	3.39007
3	0.104334	2.25484	Fill	0	30	5.42433	2.00395	3.47093	0	3.47093
4	0.104334	2.47465	Fill	0	30	6.63715	2.45201	4.24699	0	4.24699
5	0.104334	2.6108	Fill	0	30	7.74373	2.86082	4.95509	0	4.95509
6	0.104334	2.68815	Fill	0	30	8.65317	3.1968	5.53703	0	5.53703
7	0.104334	2.72082	Fill	0	30	9.38506	3.46719	6.00536	0	6.00536
8	0.104334	2.71793	Fill	0	30	9.95415	3.67743	6.36948	0	6.36948
9	0.104334	2.68577	Fill	0	30	10.3718	3.83174	6.63676	0	6.63676
10	0.104334	2.62888	Fill	0	30	10.6473	3.93349	6.81299	0	6.81299
11	0.104334	2.55072	Fill	0	30	10.7878	3.98541	6.90291	0	6.90291
12	0.104334	2.45394	Fill	0	30	10.7996	3.98976	6.91046	0	6.91046
13	0.104334	2.34068	Fill	0	30	10.6876	3.94841	6.83884	0	6.83884
14	0.104334	2.21266	Fill	0	30	10.4563	3.86294	6.69079	0	6.69079
15	0.104334	2.07128	Fill	0	30	10.1091	3.73466	6.46864	0	6.46864
16	0.104334	1.91774	Fill	0	30	9.64901	3.5647	6.17426	0	6.17426
17	0.104334	1.75305	Fill	0	30	9.07865	3.35399	5.80928	0	5.80928
18	0.104334	1.57807	Fill	0	30	8.40013	3.10332	5.3751	0	5.3751
19	0.104334	1.39353	Fill	0	30	7.61518	2.81333	4.87283	0	4.87283
20	0.104334	1.20008	Fill	0	30	6.72529	2.48457	4.3034	0	4.3034
21	0.104334	0.998291	Fill	0	30	5.73159	2.11746	3.66756	0	3.66756
22	0.104334	0.788663	Fill	0	30	4.63505	1.71236	2.96589	0	2.96589
23	0.104334	0.57164	Fill	0	30	3.43634	1.26951	2.19885	0	2.19885
24	0.104334	0.347618	Fill	0	30	2.1359	0.789079	1.36672	0	1.36672
25	0.104334	0.116952	Fill	0	30	0.734039	0.271181	0.469699	0	0.469699

Interslice Data

Global Minimum Query (bishop simplified) - Safety Factor: 0.369437

Slice Number	X coordinate [m]	Y coordinate - Bottom [m]	Interslice Normal Force [kN]	Interslice Shear Force [kN]	Interslice Force Angle [degrees]
1	7.78623	5	0	0	0

2	7.89056	4.33138	0.741532	0	0
3	7.9949	3.88128	1.7185	0	0
4	8.09923	3.52043	2.40899	0	0
5	8.20357	3.2122	3.03042	0	0
6	8.3079	2.93991	3.57733	0	0
7	8.41224	2.6943	4.04074	0	0
8	8.51657	2.46958	4.41788	0	0
9	8.62091	2.26185	4.70971	0	0
10	8.72524	2.06832	4.91957	0	0
11	8.82957	1.88691	5.0524	0	0
12	8.93391	1.71603	5.11425	0	0
13	9.03824	1.55444	5.11202	0	0
14	9.14258	1.40112	5.05321	0	0
15	9.24691	1.25526	4.94583	0	0
16	9.35125	1.11616	4.79827	0	0
17	9.45558	0.98324	4.61922	0	0
18	9.55992	0.856018	4.41768	0	0
19	9.66425	0.734067	4.20287	0	0
20	9.76858	0.617019	3.98424	0	0
21	9.87292	0.504553	3.77144	0	0
22	9.97725	0.396388	3.57431	0	0
23	10.0816	0.292271	3.40289	0	0
24	10.1859	0.191981	3.26738	0	0
25	10.2903	0.0953187	3.1782	0	0
26	10.3946	0.00210388	0	0	0

Query 1 (bishop simplified) - Safety Factor: 0.369437

Slice Number	X coordinate [m]	Y coordinate - Bottom [m]	Interslice Normal Force [kN]	Interslice Shear Force [kN]	Interslice Force Angle [degrees]
1	7.78623	5	0	0	0
2	7.89056	4.33138	0.741532	0	0
3	7.9949	3.88128	1.7185	0	0
4	8.09923	3.52043	2.40899	0	0
5	8.20357	3.2122	3.03042	0	0
6	8.3079	2.93991	3.57733	0	0
7	8.41224	2.6943	4.04074	0	0
8	8.51657	2.46958	4.41788	0	0
9	8.62091	2.26185	4.70971	0	0
10	8.72524	2.06832	4.91957	0	0
11	8.82957	1.88691	5.0524	0	0
12	8.93391	1.71603	5.11425	0	0
13	9.03824	1.55444	5.11202	0	0
14	9.14258	1.40112	5.05321	0	0
15	9.24691	1.25526	4.94583	0	0
16	9.35125	1.11616	4.79827	0	0
17	9.45558	0.98324	4.61922	0	0
18	9.55992	0.856018	4.41768	0	0
19	9.66425	0.734067	4.20287	0	0
20	9.76858	0.617019	3.98424	0	0
21	9.87292	0.504553	3.77144	0	0
22	9.97725	0.396388	3.57431	0	0
23	10.0816	0.292271	3.40289	0	0
24	10.1859	0.191981	3.26738	0	0

25	10.2903	0.0953187	3.1782	0	0
26	10.3946	0.00210388	0	0	0

List Of Coordinates

Line Load

X	Y
8	5
0	5

External Boundary

X	Y
0	5
0	0
0	-8
20	-8
20	0
10.3956	0
8	5

Material Boundary

X	Y
0	0
10.3956	0

D.1.2 Embankment with reinforced backfill

Slide Analysis Information

Slope Stability Analysis of Embankment

Project Summary

File Name: Embankment model_Sand_Plastic
Slide Modeler Version: 6.009
Project Title: Slope Stability Analysis of Embankment
Author: Paul Wanyama (WNYPAU001)

General Settings

Units of Measurement: Metric Units
Time Units: days
Permeability Units: meters/second
Failure Direction: Left to Right
Data Output: Standard
Maximum Material Properties: 20
Maximum Support Properties: 20

Analysis Options

Analysis Methods Used

Bishop simplified

Number of slices: 25
Tolerance: 0.005
Maximum number of iterations: 50
Check malpha < 0.2: Yes
Initial trial value of FS: 1
Steffensen Iteration: Yes

Groundwater Analysis

Groundwater Method: Water Surfaces
Pore Fluid Unit Weight: 9.81 kN/m3
Advanced Groundwater Method: None

Random Numbers

Pseudo-random Seed: 10116
Random Number Generation Method: Park and Miller v.3

Surface Options

Surface Type: Circular
Search Method: Grid Search
Radius Increment: 10
Composite Surfaces: Disabled
Reverse Curvature: Create Tension Crack
Minimum Elevation: Not Defined

Minimum Depth: Not Defined

Loading

1 Distributed Load present

Distributed Load 1

Distribution: Constant
Magnitude [kN/m2]: 10
Orientation: Normal to boundary

Material Properties

Property	Silty clay	Fill
Color		
Strength Type	Mohr-Coulomb	Mohr-Coulomb
Unit Weight [kN/m3]	19.1	17.8
Cohesion [kPa]	15	16
Friction Angle [deg]	20	32.9
Water Surface	None	None
Ru Value	0	0

Global Minimums

Method: bishop simplified

FS: 1.548080
Center: 13.531, 7.304
Radius: 7.948
Left Slip Surface Endpoint: 5.924, 5.000
Right Slip Surface Endpoint: 10.396, 0.000
Resisting Moment=1502.14 kN-m
Driving Moment=970.326 kN-m

Slice Data

Global Minimum Query (bishop simplified) - Safety Factor: 1.54808

Slice Number	Width [m]	Weight [kN]	Base Material	Base Cohesion [kPa]	Base Friction Angle [degrees]	Shear Stress [kPa]	Shear Strength [kPa]	Base Normal Stress [kPa]	Pore Pressure [kPa]	Effective Normal Stress [kPa]
1	0.178864	0.8343	Fill	16	32.9	7.40129	11.4578	-7.02119	0	-7.02119
2	0.178864	2.35521	Fill	16	32.9	9.97027	15.4348	-0.873704	0	-0.873704
3	0.178864	3.63361	Fill	16	32.9	12.3113	19.0588	4.72821	0	4.72821
4	0.178864	4.74914	Fill	16	32.9	14.4801	22.4163	9.91816	0	9.91816
5	0.178864	5.74436	Fill	16	32.9	16.5107	25.5598	14.7772	0	14.7772
6	0.178864	6.64535	Fill	16	32.9	18.4259	28.5247	19.3602	0	19.3602
7	0.178864	7.46948	Fill	16	32.9	20.2422	31.3365	23.7066	0	23.7066
8	0.178864	8.22907	Fill	16	32.9	21.972	34.0144	27.8461	0	27.8461
9	0.178864	8.93322	Fill	16	32.9	23.6251	36.5735	31.8018	0	31.8018
10	0.178864	9.58888	Fill	16	32.9	25.2091	39.0257	35.5923	0	35.5923
11	0.178864	10.2015	Fill	16	32.9	26.7303	41.3807	39.2327	0	39.2327

12	0.178864	10.6835	Fill	16	32.9	26.8737	41.6026	39.5756	0	39.5756
13	0.178864	10.2526	Fill	16	32.9	24.7899	38.3767	34.5891	0	34.5891
14	0.178864	9.57083	Fill	16	32.9	24.0303	37.2008	32.7715	0	32.7715
15	0.178864	8.85949	Fill	16	32.9	23.1644	35.8604	30.6995	0	30.6995
16	0.178864	8.12066	Fill	16	32.9	22.1984	34.3649	28.3878	0	28.3878
17	0.178864	7.35615	Fill	16	32.9	21.1373	32.7223	25.8487	0	25.8487
18	0.178864	6.56752	Fill	16	32.9	19.9857	30.9394	23.0928	0	23.0928
19	0.178864	5.75614	Fill	16	32.9	18.7471	29.022	20.129	0	20.129
20	0.178864	4.92321	Fill	16	32.9	17.4249	26.9751	16.9649	0	16.9649
21	0.178864	4.06976	Fill	16	32.9	16.0217	24.8028	13.6071	0	13.6071
22	0.178864	3.19672	Fill	16	32.9	14.5398	22.5087	10.061	0	10.061
23	0.178864	2.30492	Fill	16	32.9	12.9812	20.0959	6.3313	0	6.3313
24	0.178864	1.39509	Fill	16	32.9	11.3475	17.5669	2.42199	0	2.42199
25	0.178864	0.467875	Fill	16	32.9	9.64012	14.9237	-1.66375	0	-1.66375

Query 1 (bishop simplified) - Safety Factor: 1.54808

Slice Number	Width [m]	Weight [kN]	Base Material	Base Cohesion [kPa]	Base Friction Angle [degrees]	Shear Stress [kPa]	Shear Strength [kPa]	Base Normal Stress [kPa]	Pore Pressure [kPa]	Effective Normal Stress [kPa]
1	0.178864	0.8343	Fill	16	32.9	7.40129	11.4578	-7.02119	0	-7.02119
2	0.178864	2.35521	Fill	16	32.9	9.97027	15.4348	-0.873704	0	-0.873704
3	0.178864	3.63361	Fill	16	32.9	12.3113	19.0588	4.72821	0	4.72821
4	0.178864	4.74914	Fill	16	32.9	14.4801	22.4163	9.91816	0	9.91816
5	0.178864	5.74436	Fill	16	32.9	16.5107	25.5598	14.7772	0	14.7772
6	0.178864	6.64535	Fill	16	32.9	18.4259	28.5247	19.3602	0	19.3602
7	0.178864	7.46948	Fill	16	32.9	20.2422	31.3365	23.7066	0	23.7066
8	0.178864	8.22907	Fill	16	32.9	21.972	34.0144	27.8461	0	27.8461
9	0.178864	8.93322	Fill	16	32.9	23.6251	36.5735	31.8018	0	31.8018
10	0.178864	9.58888	Fill	16	32.9	25.2091	39.0257	35.5923	0	35.5923
11	0.178864	10.2015	Fill	16	32.9	26.7303	41.3807	39.2327	0	39.2327
12	0.178864	10.6835	Fill	16	32.9	26.8737	41.6026	39.5756	0	39.5756
13	0.178864	10.2526	Fill	16	32.9	24.7899	38.3767	34.5891	0	34.5891
14	0.178864	9.57083	Fill	16	32.9	24.0303	37.2008	32.7715	0	32.7715
15	0.178864	8.85949	Fill	16	32.9	23.1644	35.8604	30.6995	0	30.6995
16	0.178864	8.12066	Fill	16	32.9	22.1984	34.3649	28.3878	0	28.3878
17	0.178864	7.35615	Fill	16	32.9	21.1373	32.7223	25.8487	0	25.8487
18	0.178864	6.56752	Fill	16	32.9	19.9857	30.9394	23.0928	0	23.0928
19	0.178864	5.75614	Fill	16	32.9	18.7471	29.022	20.129	0	20.129
20	0.178864	4.92321	Fill	16	32.9	17.4249	26.9751	16.9649	0	16.9649
21	0.178864	4.06976	Fill	16	32.9	16.0217	24.8028	13.6071	0	13.6071
22	0.178864	3.19672	Fill	16	32.9	14.5398	22.5087	10.061	0	10.061
23	0.178864	2.30492	Fill	16	32.9	12.9812	20.0959	6.3313	0	6.3313
24	0.178864	1.39509	Fill	16	32.9	11.3475	17.5669	2.42199	0	2.42199
25	0.178864	0.467875	Fill	16	32.9	9.64012	14.9237	-1.66375	0	-1.66375

Interslice Data

Global Minimum Query (bishop simplified) - Safety Factor: 1.54808

Slice Number	X coordinate [m]	Y coordinate - Bottom [m]	Interslice Normal Force [kN]	Interslice Shear Force [kN]	Interslice Force Angle [degrees]
1	5.92399	5	0	0	0

2	6.10286	4.47591	-5.00352	0	0
3	6.28172	4.04459	-7.16361	0	0
4	6.46058	3.67284	-7.60782	0	0
5	6.63945	3.34383	-6.93456	0	0
6	6.81831	3.04765	-5.51087	0	0
7	6.99718	2.77785	-3.58297	0	0
8	7.17604	2.52995	-1.32646	0	0
9	7.35491	2.30069	1.12769	0	0
10	7.53377	2.08761	3.67834	0	0
11	7.71263	1.88881	6.24529	0	0
12	7.8915	1.70277	8.76348	0	0
13	8.07036	1.52824	10.8639	0	0
14	8.24923	1.36423	12.1033	0	0
15	8.42809	1.20986	12.864	0	0
16	8.60696	1.06444	13.1853	0	0
17	8.78582	0.927349	13.1068	0	0
18	8.96468	0.798058	12.6682	0	0
19	9.14355	0.676113	11.9097	0	0
20	9.32241	0.561115	10.8715	0	0
21	9.50128	0.452713	9.59399	0	0
22	9.68014	0.3506	8.11788	0	0
23	9.85901	0.254503	6.48419	0	0
24	10.0379	0.164177	4.73431	0	0
25	10.2167	0.0794074	2.91006	0	0
26	10.3956	0	0	0	0

Query 1 (bishop simplified) - Safety Factor: 1.54808

Slice Number	X coordinate [m]	Y coordinate - Bottom [m]	Interslice Normal Force [kN]	Interslice Shear Force [kN]	Interslice Force Angle [degrees]
1	5.92399	5	0	0	0
2	6.10286	4.47591	-5.00352	0	0
3	6.28172	4.04459	-7.16361	0	0
4	6.46058	3.67284	-7.60782	0	0
5	6.63945	3.34383	-6.93456	0	0
6	6.81831	3.04765	-5.51087	0	0
7	6.99718	2.77785	-3.58297	0	0
8	7.17604	2.52995	-1.32646	0	0
9	7.35491	2.30069	1.12769	0	0
10	7.53377	2.08761	3.67834	0	0
11	7.71263	1.88881	6.24529	0	0
12	7.8915	1.70277	8.76348	0	0
13	8.07036	1.52824	10.8639	0	0
14	8.24923	1.36423	12.1033	0	0
15	8.42809	1.20986	12.864	0	0
16	8.60696	1.06444	13.1853	0	0
17	8.78582	0.927349	13.1068	0	0
18	8.96468	0.798058	12.6682	0	0
19	9.14355	0.676113	11.9097	0	0
20	9.32241	0.561115	10.8715	0	0
21	9.50128	0.452713	9.59399	0	0
22	9.68014	0.3506	8.11788	0	0
23	9.85901	0.254503	6.48419	0	0
24	10.0379	0.164177	4.73431	0	0

25	10.2167	0.0794074	2.91006	0	0
26	10.3956	0	0	0	0

List Of Coordinates

Line Load

X	Y
8	5
0	5

External Boundary

X	Y
0	5
0	0
0	-8
20	-8
20	0
10.3956	0
8	5

Material Boundary

X	Y
0	0
10.3956	0

D.2 Seismic Analysis

D.2.1 Embankment with unreinforced sand backfill

Slide Analysis Information

Slope Stability Analysis of Embankment

Project Summary

File Name: Embankment model_Sand_Seismic
Slide Modeler Version: 6.009
Project Title: Slope Stability Analysis of Embankment
Author: Paul Wanyama (WNYPAU001)

General Settings

Units of Measurement: Metric Units
Time Units: days
Permeability Units: meters/second
Failure Direction: Left to Right
Data Output: Standard
Maximum Material Properties: 20
Maximum Support Properties: 20

Analysis Options

Analysis Methods Used

Bishop simplified

Number of slices: 25
Tolerance: 0.005
Maximum number of iterations: 50
Check malpha< 0.2: Yes
Initial trial value of FS: 1
Steffensen Iteration: Yes

Groundwater Analysis

Groundwater Method: Water Surfaces
Pore Fluid Unit Weight: 9.81 kN/m3
Advanced Groundwater Method: None

Random Numbers

Pseudo-random Seed: 10116
Random Number Generation Method: Park and Miller v.3

Surface Options

Surface Type: Circular
Search Method: Grid Search
Radius Increment: 10
Composite Surfaces: Disabled
Reverse Curvature: Create Tension Crack
Minimum Elevation: Not Defined
Minimum Depth: Not Defined

Loading

Seismic Load Coefficient (Horizontal): 0.15
Seismic Load Coefficient (Vertical): 0.15
1 Distributed Load present

Distributed Load 1

Distribution: Constant
Magnitude [kN/m2]: 10
Orientation: Normal to boundary

Material Properties

Property	Silty clay	Fill
Color		
Strength Type	Mohr-Coulomb	Mohr-Coulomb
Unit Weight [kN/m3]	19.1	18
Cohesion [kPa]	15	0
Friction Angle [deg]	20	30
Water Surface	None	None
Ru Value	0	0

Global Minimums

Method: bishop simplified

FS: 0.296387
Center: 15.541, 5.868
Radius: 7.803
Left Slip Surface Endpoint: 7.786, 5.000
Right Slip Surface Endpoint: 10.395, 0.002
Resisting Moment=114.673 kN-m
Driving Moment=386.904 kN-m

Slice Data

Global Minimum Query (bishop simplified) - Safety Factor 0.296387

Slice Number	Width [m]	Weight [kN]	Base Material	Base Cohesion [kPa]	Base Friction Angle [degrees]	Shear Stress [kPa]	Shear Strength [kPa]	Base Normal Stress [kPa]	Pore Pressure [kPa]	Effective Normal Stress [kPa]
1	0.104334	0.627838	Fill	0	30	2.47549	0.733704	1.27081	0	1.27081
2	0.104334	1.67832	Fill	0	30	5.97584	1.77116	3.06773	0	3.06773
3	0.104334	2.25484	Fill	0	30	6.45639	1.91359	3.31442	0	3.31442
4	0.104334	2.47465	Fill	0	30	7.95757	2.35852	4.08508	0	4.08508
5	0.104334	2.6108	Fill	0	30	9.3195	2.76218	4.78424	0	4.78424
6	0.104334	2.68815	Fill	0	30	10.4493	3.09703	5.36424	0	5.36424
7	0.104334	2.72082	Fill	0	30	11.3682	3.36939	5.83596	0	5.83596
8	0.104334	2.71793	Fill	0	30	12.0922	3.58396	6.20761	0	6.20761
9	0.104334	2.68577	Fill	0	30	12.6335	3.74441	6.48554	0	6.48554
10	0.104334	2.62888	Fill	0	30	13.0021	3.85365	6.67471	0	6.67471
11	0.104334	2.55072	Fill	0	30	13.2058	3.91402	6.77929	0	6.77929
12	0.104334	2.45394	Fill	0	30	13.2511	3.92744	6.80253	0	6.80253
13	0.104334	2.34068	Fill	0	30	13.1433	3.8955	6.74723	0	6.74723
14	0.104334	2.21266	Fill	0	30	12.8868	3.81949	6.61557	0	6.61557
15	0.104334	2.07128	Fill	0	30	12.4854	3.7005	6.40946	0	6.40946
16	0.104334	1.91774	Fill	0	30	11.9419	3.53941	6.13047	0	6.13047
17	0.104334	1.75305	Fill	0	30	11.2588	3.33695	5.77976	0	5.77976

18	0.104334	1.57807	Fill	0	30	10.438	3.09369	5.35843	0	5.35843
19	0.104334	1.39353	Fill	0	30	9.48115	2.81009	4.86722	0	4.86722
20	0.104334	1.20008	Fill	0	30	8.38934	2.48649	4.30674	0	4.30674
21	0.104334	0.998291	Fill	0	30	7.1634	2.12314	3.67739	0	3.67739
22	0.104334	0.788663	Fill	0	30	5.80386	1.72019	2.97946	0	2.97946
23	0.104334	0.57164	Fill	0	30	4.31088	1.27769	2.21303	0	2.21303
24	0.104334	0.347618	Fill	0	30	2.68447	0.795642	1.37809	0	1.37809
25	0.104334	0.116952	Fill	0	30	0.924268	0.273941	0.474479	0	0.474479

Query 1 (bishop simplified) - Safety Factor 0.296387

Slice Number	Width [m]	Weight [kN]	Base Material	Base Cohesion [kPa]	Base Friction Angle [degrees]	Shear Stress [kPa]	Shear Strength [kPa]	Base Normal Stress [kPa]	Pore Pressure [kPa]	Effective Normal Stress [kPa]
1	0.104334	0.627838	Fill	0	30	2.47549	0.733704	1.27081	0	1.27081
2	0.104334	1.67832	Fill	0	30	5.97584	1.77116	3.06773	0	3.06773
3	0.104334	2.25484	Fill	0	30	6.45639	1.91359	3.31442	0	3.31442
4	0.104334	2.47465	Fill	0	30	7.95757	2.35852	4.08508	0	4.08508
5	0.104334	2.6108	Fill	0	30	9.3195	2.76218	4.78424	0	4.78424
6	0.104334	2.68815	Fill	0	30	10.4493	3.09703	5.36424	0	5.36424
7	0.104334	2.72082	Fill	0	30	11.3682	3.36939	5.83596	0	5.83596
8	0.104334	2.71793	Fill	0	30	12.0922	3.58396	6.20761	0	6.20761
9	0.104334	2.68577	Fill	0	30	12.6335	3.74441	6.48554	0	6.48554
10	0.104334	2.62888	Fill	0	30	13.0021	3.85365	6.67471	0	6.67471
11	0.104334	2.55072	Fill	0	30	13.2058	3.91402	6.77929	0	6.77929
12	0.104334	2.45394	Fill	0	30	13.2511	3.92744	6.80253	0	6.80253
13	0.104334	2.34068	Fill	0	30	13.1433	3.8955	6.74723	0	6.74723
14	0.104334	2.21266	Fill	0	30	12.8868	3.81949	6.61557	0	6.61557
15	0.104334	2.07128	Fill	0	30	12.4854	3.7005	6.40946	0	6.40946
16	0.104334	1.91774	Fill	0	30	11.9419	3.53941	6.13047	0	6.13047
17	0.104334	1.75305	Fill	0	30	11.2588	3.33695	5.77976	0	5.77976
18	0.104334	1.57807	Fill	0	30	10.438	3.09369	5.35843	0	5.35843
19	0.104334	1.39353	Fill	0	30	9.48115	2.81009	4.86722	0	4.86722
20	0.104334	1.20008	Fill	0	30	8.38934	2.48649	4.30674	0	4.30674
21	0.104334	0.998291	Fill	0	30	7.1634	2.12314	3.67739	0	3.67739
22	0.104334	0.788663	Fill	0	30	5.80386	1.72019	2.97946	0	2.97946
23	0.104334	0.57164	Fill	0	30	4.31088	1.27769	2.21303	0	2.21303
24	0.104334	0.347618	Fill	0	30	2.68447	0.795642	1.37809	0	1.37809
25	0.104334	0.116952	Fill	0	30	0.924268	0.273941	0.474479	0	0.474479

Interslice Data

Global Minimum Query (bishop simplified) - Safety Factor 0.296387

Slice Number	X coordinate [m]	Y coordinate - Bottom [m]	Interslice Normal Force [kN]	Interslice Shear Force [kN]	Interslice Force Angle [degrees]
1	7.78623	5	0	0	0
2	7.89056	4.33138	0.689077	0	0
3	7.9949	3.88128	1.70657	0	0
4	8.09923	3.52043	2.5763	0	0
5	8.20357	3.2122	3.38765	0	0
6	8.3079	2.93991	4.12276	0	0
7	8.41224	2.6943	4.768	0	0
8	8.51657	2.46958	5.3175	0	0
9	8.62091	2.26185	5.77015	0	0
10	8.72524	2.06832	6.12791	0	0
11	8.82957	1.88691	6.39489	0	0
12	8.93391	1.71603	6.57673	0	0

13	9.03824	1.55444	6.68021	0	0
14	9.14258	1.40112	6.71302	0	0
15	9.24691	1.25526	6.68355	0	0
16	9.35125	1.11616	6.60078	0	0
17	9.45558	0.98324	6.47418	0	0
18	9.55992	0.856018	6.31366	0	0
19	9.66425	0.734067	6.12953	0	0
20	9.76858	0.617019	5.93242	0	0
21	9.87292	0.504553	5.73334	0	0
22	9.97725	0.396388	5.54357	0	0
23	10.0816	0.292271	5.37472	0	0
24	10.1859	0.191981	5.23872	0	0
25	10.2903	0.0953187	5.14778	0	0
26	10.3946	0.00210388	0	0	0

Query 1 (bishop simplified) - Safety Factor 0.296387

Slice Number	X coordinate [m]	Y coordinate - Bottom [m]	Interslice Normal Force [kN]	Interslice Shear Force [kN]	Interslice Force Angle [degrees]
1	7.78623	5	0	0	0
2	7.89056	4.33138	0.689077	0	0
3	7.9949	3.88128	1.70657	0	0
4	8.09923	3.52043	2.5763	0	0
5	8.20357	3.2122	3.38765	0	0
6	8.3079	2.93991	4.12276	0	0
7	8.41224	2.6943	4.768	0	0
8	8.51657	2.46958	5.3175	0	0
9	8.62091	2.26185	5.77015	0	0
10	8.72524	2.06832	6.12791	0	0
11	8.82957	1.88691	6.39489	0	0
12	8.93391	1.71603	6.57673	0	0
13	9.03824	1.55444	6.68021	0	0
14	9.14258	1.40112	6.71302	0	0
15	9.24691	1.25526	6.68355	0	0
16	9.35125	1.11616	6.60078	0	0
17	9.45558	0.98324	6.47418	0	0
18	9.55992	0.856018	6.31366	0	0
19	9.66425	0.734067	6.12953	0	0
20	9.76858	0.617019	5.93242	0	0
21	9.87292	0.504553	5.73334	0	0
22	9.97725	0.396388	5.54357	0	0
23	10.0816	0.292271	5.37472	0	0
24	10.1859	0.191981	5.23872	0	0
25	10.2903	0.0953187	5.14778	0	0
26	10.3946	0.00210388	0	0	0

List Of Coordinates

Line Load

X	Y
8	5
0	5

External Boundary

X	Y
0	5
0	0
0	-8
20	-8
20	0
10.3956	0
8	5

Material Boundary

X	Y
0	0
10.3956	0

D.2.2 Embankment with reinforced backfill

Slide Analysis Information

Slope Stability Analysis of Embankment

Project Summary

File Name: Embankment model_Sand_Plastic_Seismic
Slide Modeler Version: 6.009
Project Title: Slope Stability Analysis of Embankment
Author: Paul Wanyama (WNYPAU001)

General Settings

Units of Measurement: Metric Units
Time Units: days
Permeability Units: meters/second
Failure Direction: Left to Right
Data Output: Standard
Maximum Material Properties: 20
Maximum Support Properties: 20

Analysis Options

Analysis Methods Used

Bishop simplified

Number of slices: 25
Tolerance: 0.005
Maximum number of iterations: 50
Check malpha< 0.2: Yes
Initial trial value of FS: 1
Steffensen Iteration: Yes

Groundwater Analysis

Groundwater Method: Water Surfaces
Pore Fluid Unit Weight: 9.81 kN/m3
Advanced Groundwater Method: None

Random Numbers

Pseudo-random Seed: 10116
Random Number Generation Method: Park and Miller v.3

Surface Options

Surface Type: Circular
Search Method: Grid Search
Radius Increment: 10
Composite Surfaces: Disabled
Reverse Curvature: Create Tension Crack
Minimum Elevation: Not Defined
Minimum Depth: Not Defined

Loading

Seismic Load Coefficient (Horizontal): 0.15
Seismic Load Coefficient (Vertical): 0.15
1 Distributed Load present

Distributed Load 1

Distribution: Constant
Magnitude [kN/m2]: 10
Orientation: Normal to boundary

Material Properties

Property	Silty clay	Fill
Color		
Strength Type	Mohr-Coulomb	Mohr-Coulomb
Unit Weight [kN/m3]	19.1	17.8
Cohesion [kPa]	15	16
Friction Angle [deg]	20	32.9
Water Surface	None	None
Ru Value	0	0

Global Minimums

Method: bishop simplified

FS: 1.267300
Center: 14.393, 8.452
Radius: 9.350
Left Slip Surface Endpoint: 5.704, 5.000
Right Slip Surface Endpoint: 10.396, 0.000
Resisting Moment=1835.18 kN-m
Driving Moment=1448.1 kN-m

Slice Data

Global Minimum Query (bishop simplified) - Safety Factor 1.2673

Slice Number	Width [m]	Weight [kN]	Base Material	Base Cohesion [kPa]	Base Friction Angle [degrees]	Shear Stress [kPa]	Shear Strength [kPa]	Base Normal Stress [kPa]	Pore Pressure [kPa]	Effective Normal Stress [kPa]
1	0.187682	0.733824	Fill	16	32.9	9.13272	11.5739	-6.8417	0	-6.8417
2	0.187682	2.11291	Fill	16	32.9	11.8799	15.0554	-1.46017	0	-1.46017
3	0.187682	3.33708	Fill	16	32.9	14.5126	18.3919	3.69727	0	3.69727
4	0.187682	4.44256	Fill	16	32.9	17.0414	21.5966	8.651	0	8.651
5	0.187682	5.45279	Fill	16	32.9	19.4756	24.6815	13.4195	0	13.4195
6	0.187682	6.38401	Fill	16	32.9	21.8235	27.6569	18.0188	0	18.0188
7	0.187682	7.24807	Fill	16	32.9	24.0921	30.5319	22.4628	0	22.4628
8	0.187682	8.05391	Fill	16	32.9	26.2874	33.314	26.7634	0	26.7634
9	0.187682	8.80847	Fill	16	32.9	28.4147	36.0099	30.9306	0	30.9306
10	0.187682	9.51729	Fill	16	32.9	30.4785	38.6254	34.9735	0	34.9735
11	0.187682	10.1849	Fill	16	32.9	32.4827	41.1653	38.8998	0	38.8998
12	0.187682	10.8149	Fill	16	32.9	34.4308	43.6342	42.716	0	42.716
13	0.187682	11.0284	Fill	16	32.9	32.8609	41.6446	39.6405	0	39.6405
14	0.187682	10.3199	Fill	16	32.9	31.0607	39.3632	36.114	0	36.114
15	0.187682	9.54549	Fill	16	32.9	29.8642	37.8469	33.7701	0	33.7701
16	0.187682	8.74341	Fill	16	32.9	28.5365	36.1643	31.1693	0	31.1693
17	0.187682	7.91536	Fill	16	32.9	27.0831	34.3224	28.3222	0	28.3222

18	0.187682	7.06282	Fill	16	32.9	25.5086	32.3271	25.2379	0	25.2379
19	0.187682	6.18709	Fill	16	32.9	23.8172	30.1836	21.9245	0	21.9245
20	0.187682	5.28931	Fill	16	32.9	22.0123	27.8962	18.3888	0	18.3888
21	0.187682	4.3705	Fill	16	32.9	20.0968	25.4687	14.6364	0	14.6364
22	0.187682	3.43157	Fill	16	32.9	18.0733	22.9044	10.6725	0	10.6725
23	0.187682	2.47332	Fill	16	32.9	15.944	20.2058	6.50119	0	6.50119
24	0.187682	1.49651	Fill	16	32.9	13.7105	17.3754	2.12598	0	2.12598
25	0.187682	0.501769	Fill	16	32.9	11.3745	14.4149	-2.45023	0	-2.45023

Query 1 (bishop simplified) - Safety Factor 1.2673

Slice Number	Width [m]	Weight [kN]	Base Material	Base Cohesion [kPa]	Base Friction Angle [degrees]	Shear Stress [kPa]	Shear Strength [kPa]	Base Normal Stress [kPa]	Pore Pressure [kPa]	Effective Normal Stress [kPa]
1	0.187682	0.733824	Fill	16	32.9	9.13272	11.5739	-6.8417	0	-6.8417
2	0.187682	2.11291	Fill	16	32.9	11.8799	15.0554	-1.46017	0	-1.46017
3	0.187682	3.33708	Fill	16	32.9	14.5126	18.3919	3.69727	0	3.69727
4	0.187682	4.44256	Fill	16	32.9	17.0414	21.5966	8.651	0	8.651
5	0.187682	5.45279	Fill	16	32.9	19.4756	24.6815	13.4195	0	13.4195
6	0.187682	6.38401	Fill	16	32.9	21.8235	27.6569	18.0188	0	18.0188
7	0.187682	7.24807	Fill	16	32.9	24.0921	30.5319	22.4628	0	22.4628
8	0.187682	8.05391	Fill	16	32.9	26.2874	33.314	26.7634	0	26.7634
9	0.187682	8.80847	Fill	16	32.9	28.4147	36.0099	30.9306	0	30.9306
10	0.187682	9.51729	Fill	16	32.9	30.4785	38.6254	34.9735	0	34.9735
11	0.187682	10.1849	Fill	16	32.9	32.4827	41.1653	38.8998	0	38.8998
12	0.187682	10.8149	Fill	16	32.9	34.4308	43.6342	42.716	0	42.716
13	0.187682	11.0284	Fill	16	32.9	32.8609	41.6446	39.6405	0	39.6405
14	0.187682	10.3199	Fill	16	32.9	31.0607	39.3632	36.114	0	36.114
15	0.187682	9.54549	Fill	16	32.9	29.8642	37.8469	33.7701	0	33.7701
16	0.187682	8.74341	Fill	16	32.9	28.5365	36.1643	31.1693	0	31.1693
17	0.187682	7.91536	Fill	16	32.9	27.0831	34.3224	28.3222	0	28.3222
18	0.187682	7.06282	Fill	16	32.9	25.5086	32.3271	25.2379	0	25.2379
19	0.187682	6.18709	Fill	16	32.9	23.8172	30.1836	21.9245	0	21.9245
20	0.187682	5.28931	Fill	16	32.9	22.0123	27.8962	18.3888	0	18.3888
21	0.187682	4.3705	Fill	16	32.9	20.0968	25.4687	14.6364	0	14.6364
22	0.187682	3.43157	Fill	16	32.9	18.0733	22.9044	10.6725	0	10.6725
23	0.187682	2.47332	Fill	16	32.9	15.944	20.2058	6.50119	0	6.50119
24	0.187682	1.49651	Fill	16	32.9	13.7105	17.3754	2.12598	0	2.12598
25	0.187682	0.501769	Fill	16	32.9	11.3745	14.4149	-2.45023	0	-2.45023

Interslice Data

Global Minimum Query (bishop simplified) - Safety Factor 1.2673

Slice Number	X coordinate [m]	Y coordinate - Bottom [m]	Interslice Normal Force [kN]	Interslice Shear Force [kN]	Interslice Force Angle [degrees]
1	5.70355	5	0	0	0
2	5.89123	4.56068	-4.6065	0	0
3	6.07891	4.17438	-7.07916	0	0
4	6.2666	3.8278	-8.01594	0	0
5	6.45428	3.51257	-7.81494	0	0
6	6.64196	3.22301	-6.7598	0	0
7	6.82964	2.95507	-5.06256	0	0
8	7.01732	2.70572	-2.88761	0	0
9	7.20501	2.47264	-0.366062	0	0
10	7.39269	2.25399	2.3951	0	0
11	7.58037	2.04829	5.30694	0	0
12	7.76805	1.85434	8.29433	0	0

13	7.95573	1.67111	11.293	0	0
14	8.14342	1.49778	13.6624	0	0
15	8.3311	1.3336	15.3206	0	0
16	8.51878	1.17797	16.4135	0	0
17	8.70646	1.03034	16.9805	0	0
18	8.89414	0.890252	17.0619	0	0
19	9.08182	0.757285	16.6984	0	0
20	9.26951	0.631081	15.9316	0	0
21	9.45719	0.511315	14.8036	0	0
22	9.64487	0.397701	13.3572	0	0
23	9.83255	0.289981	11.6358	0	0
24	10.0202	0.187926	9.68339	0	0
25	10.2079	0.0913283	7.54475	0	0
26	10.3956	0	0	0	0

Query 1 (bishop simplified) - Safety Factor 1.2673

Slice Number	X coordinate [m]	Y coordinate - Bottom [m]	Interslice Normal Force [kN]	Interslice Shear Force [kN]	Interslice Force Angle [degrees]
1	5.70355	5	0	0	0
2	5.89123	4.56068	-4.6065	0	0
3	6.07891	4.17438	-7.07916	0	0
4	6.2666	3.8278	-8.01594	0	0
5	6.45428	3.51257	-7.81494	0	0
6	6.64196	3.22301	-6.7598	0	0
7	6.82964	2.95507	-5.06256	0	0
8	7.01732	2.70572	-2.88761	0	0
9	7.20501	2.47264	-0.366062	0	0
10	7.39269	2.25399	2.3951	0	0
11	7.58037	2.04829	5.30694	0	0
12	7.76805	1.85434	8.29433	0	0
13	7.95573	1.67111	11.293	0	0
14	8.14342	1.49778	13.6624	0	0
15	8.3311	1.3336	15.3206	0	0
16	8.51878	1.17797	16.4135	0	0
17	8.70646	1.03034	16.9805	0	0
18	8.89414	0.890252	17.0619	0	0
19	9.08182	0.757285	16.6984	0	0
20	9.26951	0.631081	15.9316	0	0
21	9.45719	0.511315	14.8036	0	0
22	9.64487	0.397701	13.3572	0	0
23	9.83255	0.289981	11.6358	0	0
24	10.0202	0.187926	9.68339	0	0
25	10.2079	0.0913283	7.54475	0	0
26	10.3956	0	0	0	0

List Of Coordinates

Line Load

X	Y
8	5
0	5

External Boundary

X	Y
0	5
0	0
0	-8
20	-8
20	0
10.3956	0
8	5

Material Boundary

X	Y
0	0
10.3956	0

EBE Faculty: Assessment of Ethics in Research Projects (Rev2)

Any person planning to undertake research in the Faculty of Engineering and the Built Environment at the University of Cape Town is required to complete this form before collecting or analysing data. When completed it should be submitted to the supervisor (where applicable) and from there to the Head of Department. If any of the questions below have been answered YES, and the applicant is NOT a fourth year student, the Head should forward this form for approval by the Faculty EIR committee: submit to Ms Zulpha Geyer (Zulpha.Geyer@uct.ac.za; Chem Eng Building, Ph 021 650 4791).
NB: A copy of this signed form must be included with the thesis/dissertation/report when it is submitted for examination

This form must only be completed once the most recent revision EBE EiR Handbook has been read.

Name of Principal Researcher/Student: Paul Wanyama Department: Civil

Preferred email address of the applicant: WNYPAU001@myuct.ac.za

If a Student: Degree: MSc Civil (Geotechnical) Eng. Supervisor: Dr Denis Kalumba

If a Research Contract indicate source of funding/sponsorship: N/A

Research Project Title:
Experimental investigation on engineering behaviour of HDPE-reinforced sand under triaxial compression

Overview of ethics issues in your research project:

Question 1: Is there a possibility that your research could cause harm to a third party (i.e. a person not involved in your project)?	YES	NO √
Question 2: Is your research making use of human subjects as sources of data? If your answer is YES, please complete Addendum 2.	YES	NO √
Question 3: Does your research involve the participation of or provision of services to communities? If your answer is YES, please complete Addendum 3.	YES	NO √
Question 4: If your research is sponsored, is there any potential for conflicts of interest? If your answer is YES, please complete Addendum 4.	YES	NO √

If you have answered YES to any of the above questions, please append a copy of your research proposal, as well as any interview schedules or questionnaires (Addendum 1) and please complete further addenda as appropriate. Ensure that you refer to the EiR Handbook to assist you in completing the documentation requirements for this form.

I hereby undertake to carry out my research in such a way that

- there is no apparent legal objection to the nature or the method of research; and
- the research will not compromise staff or students or the other responsibilities of the University;
- the stated objective will be achieved, and the findings will have a high degree of validity;
- limitations and alternative interpretations will be considered;
- the findings could be subject to peer review and publicly available; and
- I will comply with the conventions of copyright and avoid any practice that would constitute plagiarism.

Signed by:

	Full name and signature	Date
Principal Researcher/Student:	Paul Wanyama Signed	11/08/2016

This application is approved by:

Supervisor (if applicable):	Dr Denis Kalumba Signed	11/08/2016
HOD (or delegated nominee): *Final authority for all assessments with NO to all questions and for all undergraduate research.*	M Vandecasteele Signed	
Chair : Faculty EIR Committee For applicants other than undergraduate students who have answered YES to any of the above questions.		